Technische Universität München

III. Medizinische Klinik und Poliklinik
Klinikum rechts der Isar

IMiDs mediate their anti-myeloma activity via destabilization of the CD147/MCT1 complex

Michael Eric Heider

Vollständiger Abdruck der von der Fakultät für Medizin der Technischen Universität München zur Erlangung des akademischen Grades eines

Doktors der Medizin

genehmigten Dissertation.

Vorsitzender: Prof. Dr. Ernst J. Rummeny

Prüfer der Dissertation:
1. Prof. Dr. Florian Bassermann
2. Prof. Dr. Christian Peschel
3. Prof. Dr. Angela Krackhardt

Die Dissertation wurde am 07.11.2016 bei der Technischen Universität München eingereicht und durch die Fakultät für Medizin am 03.01.2018 angenommen.

Index

Abbreviations

AIDS ..... acquired immunodeficiency syndrome
APS ..... ammonium persulfate
ARPPA ..... acidic ribosomal phosphoprotein P0
ASCT ..... autologous stemm cell transplantation
ATP ..... adenosine triphosphate
BES ..... N,N-Bis(2-hydroxyethyl)taurine
BMSC ..... bone marrow stromal cell
bp ..... base pairs
BRD4 ..... bromodomain-containing protein 4
BSA ..... bovine serum albumin
$CaCl_2$ ..... calcium chloride
$CaPO_4$ ..... calcium phosphate
cDNA ..... complimentary deoxyribonucleic acid
CD147 ..... cluster of differentiation 147
CHC ..... α-cyano-4-hydroxy cinnamate
CK1α ..... casein kinase 1α
COX2 ..... cyclooxygenase 2
CRBN ..... cereblon
CRL4 ..... cullin4-RING E3 ubiquitin ligase
CUL1 ..... cullin 1
CUL4 ..... cullin 4
d ..... day(s)
DCAF ..... DDB1-CUL4-associated factor
DDB1 ..... damaged DNA binding protein 1
del(5q) ..... deletion of q-arm on chromosome 5
DLBCL ..... diffuse large B-cell lymphoma
DMEM ..... Dulbecco's Modified Eagle's Medium
DMSO ..... dimethyl sulfoxide
DNA ..... deoxyribonucleic acid
dNTP ..... deoxynucleoside triphosphate mix
DTT ..... Dithiotheritol
EDTA ..... Ethylenediaminetetraacetic acid
EMMPRIN ..... extracellular matrix metalloproteinase inducer
ELISA ..... enzyme-linked immunosorbent assay
EtBr ..... ethidium bromide
FACS ..... fluorescence activated cell sorting
FBS ..... fetal bovine serum
FDA ..... Food and Drug Administration

FSC ..... forward scatter
fw ..... forward
G2P ..... glycerol 2-phosphate disodium salt pentahydrate
GLUT1 ..... glucose transporter 1
h ..... hour(s)
H_2O_2 ..... hydrogen peroxide
HD ..... high dose
HPLC ..... high performance liquid chromatography
HUVEC ..... human umbilical vein endothelial cell
IMiDs ..... immunomodulatory drugs
IKZF1 ..... Ikaros family zinc finger protein 1, Ikaros
IKZF3 ..... Ikaros family zinc finger protein 3, Aiolos
IRF4 ..... interferon-regulatory factor 4
ISS ..... international staging system
kb ..... kilo basepairs
kDa ..... kilo Dalton
LDH ..... lactate dehydrogenase
MCT ..... monocarboxylate transporter
MDS ..... myelodysplastic syndrome
MGUS ..... monoclonal gammopathy of undetermined significance
min ..... minute(s)
MM ..... multiple myeloma
MMP7 ..... matrix metalloproteinase 7
mRNA ..... messenger ribonucleic acid
NaF ..... sodium fluoride
NaCl ..... sodium chloride
NaVa ..... sodium orthovanadate
NF-κB ..... nuclear factor 'kappa-light-chain-enhancer' of activated B-cells
NP40 ..... Nonident P40
PBS ..... phosphate buffered saline
PCR ..... polymerase chain reaction
qPCR ..... quantitative polymerase chain reaction
PDH ..... pyruvate dehydrogenase
PDK1 ..... pyruvate dehydrogenase kinase 1
PIN ..... peptidylprolyl isomerase inhibitor
PMSF ..... phenylmethylsulfonylfluoride
puro ..... puromycin
RGS ..... regulator of G-protein signaling
RNA ..... ribonucleic acid
RNAi ..... RNA-interference

ROC1 ..... ring finger protein 1
RPMI ..... Roswell Parc Memorial Institute
RT ..... room temperature
RT-PCR ..... reverse transcription polymerase chain reaction
rv ..... reverse
s ..... second(s)
SD ..... standard deviation
SDS ..... sodium dodecyl sulfate
SDS-PAGE ..... sodium dodecyl sulfate polyacrylamide gel-electrophoresis
shRNA ..... small hairpin ribonucleic acid
siRNA ..... small interfering ribonucleic acid
SLC ..... solute carrier
SMM ..... smouldering multiple myeloma
SSC ..... sideward scatter
TBE ..... tris borate EDTA
TEMED ..... tetramethylethylenediamine
TIMP ..... tissue inhibitor of metalloproteinases
TLCK ..... tosyl-L-lysyl-chloromethyl-ketone
TNFα ..... tumor necrosis factor α
TPCK ..... tosyl-phenylalanyl-chloromethyl-ketone
TRC ..... the RNA-consortium
TRIS ..... tris(hydroxymethyl)aminomethane
UV ..... ultra-violett
VEGF ..... vascular endothelial growth factor
WB ..... wash buffer

1 Introduction

1.1 Multiple Myeloma

1.1.1 Epidemiology, classification and disease characterization

Multiple myeloma (MM), a B-cell malignancy also known as Kahler's disease, is considered to be the second most common hematologic malignancy, accounting for roughly 10-15% thereof, and is responsible for 15-20% of deaths caused by hematological cancer (D. Smith, 2013). It is estimated that approximately 3000 women and 3800 men will be diagnosed with MM in Germany in 2016. MM is a disease of the elderly; only 2% of patients are aged below 45 years at time of diagnosis. In 2012, the median age at diagnosis was 73 years in Germany. MM occurs more often in men than in women and is also more frequent in Afro-Caribbeans than in Caucasians or Asians (2015). Apart from age and gender, environmental risk factors or hereditary genetic components have remained unclear and controversial (Becker, 2011; D. Smith, 2013). Despite recent advances in therapy, including the introduction of various new drugs, mortality rates remain high with a 5-year-overall survival of only 45-48%. Up to now, MM remains incurable (Robert-Koch-Institut, 2015).

1.1.2 Disease characterization and diagnostic criteria

The pathology behind MM lies in the uncontrolled proliferation of monoclonal plasma cells, terminally differentiated B-cells, which are responsible for the production of antibodies. These malignant plasma cells accumulate in the bone marrow and produce dysfunctional monoclonal immunoglobulins (typically Ig-G or Ig-A) or free immunoglobulin light chains (κ- and λ-), often referred to as paraproteins or M-proteins. These proteins can precipitate and thereby impair tissue and organ function (Palumbo, 2011; D. Smith, 2013). High levels of free light chains lead to the formation of precipitates in kidney tubules, causing tubulo-interstitial inflammation, and subsequently a form of acute kidney injury termed cast nephropathy. Of note, some MM patients do not secrete any monoclonal protein and are therefore called non-secretors (D. Smith, 2013). Infiltration of the bone marrow by neoplastic plasma cells, combined with renal impairment and abnormal iron utilization, results in insufficient erythropoiesis, which, together with hemolysis, causes anemia (Birgegard, 2006). Malignant MM cells strongly interact with the bone marrow microenvironment via secretion of different cytokines, thereby activating bone-resorbing osteoclasts and inhibiting bone-forming osteoblasts. This results in the development of osteolytic bone lesions (Oranger, 2013). The above-mentioned

symptoms of tissue and organ impairment can be summarized by the acronym CRAB as presented in Table 1.

C – Hypercalcaemia: Ca^{2+}-concentration > 2.75 mmol/l
R – Renal insufficiency: Creatinine concentration > 2 mg/dl
A – Anemia: Hemoglobin < 10 g/dl
B – Bone lesions: Lytic bone lesions with compression fractures
Other: Symptomatic hyperviscosity, amyloidosis, recurrent bacterial infections

Table 1: CRAB-criteria of tissue/organ impairment. Adapted from (Raab, 2009)

M-proteins can be detected in the serum and urine, monoclonality can be verified by immunofixation and bone marrow infiltration can be assessed by morphological examination and flow cytometry of bone marrow aspirates. Low-dose computer tomography scans are used to detect myeloma-related bone lesions (Possinger, 2015). The Durie-Salmon classification of tumor burden and disease stage, in use since 1975, takes the extent of bone lesions, hemoglobin levels, serum calcium levels and M-protein levels in serum and urine into account (Durie, 1975). The International Staging System (ISS) is an improved simple prognostic system and has been applied broadly since 2005. It includes only two parameters, serum $beta_2$-microglobulin and serum albumin (Greipp, 2005). A newly revised version of the ISS now includes LDH-levels and chromosomal abnormalities for better risk assessment (Palumbo, 2015).

MM is frequently preceded by an asymptomatic monoclonal gammopathy of undetermined significance (MGUS) and asymptomatic or smouldering myeloma (SMM). The International Myeloma Working Group has defined three criteria, which help to classify these stages of monoclonal gammopathy: plasma cell bone marrow infiltration, M-protein in serum/urine and organ or tissue impairment (see Table 2).

	MGUS	Asymptomatic myeloma	MM
M-protein in serum	< 30mg/dl and	> 30mg/dl and/or	> 30mg/dl and/or
Plasma cell bone marrow infiltration	< 10%	> 10%	> 10% or solitary plasmocytoma
Organ/Tissue impairment	No	No	Yes

Table 1: International Myeloma Working Group criteria for diagnosis of MGUS, asymptomatic myeloma and symptomatic MM. Adapted from (Possinger, 2015).

MGUS und SMM are diseases characterized by elevated M-protein and increased bone marrow plasma cell content, without myeloma related organ or tissue impairment (2003). Patients with MGUS or SMM have an annual risk of progression to symptomatic MM of 1% and 10%, respectively (Bird, 2009; Bird, 2011). Extramedullary plasmocytoma is a plasma cell tumor found outside the bone marrow, with frequent localization in the upper respiratory tract. Another rare form of monoclonal plasma cell disorder is plasma cell leukemia, which is defined by more

than 2.0 x 10^9 /l absolute plasma cell count and > 20% plasma cells in the peripheral blood differential white cell count (Kyle, 2003).

1.1.3 Treatment

MM needs to be treated as soon as organ or tissue impairment (CRAB-criteria) occur (Possinger, 2015). Dramatic advances in therapeutic strategies within the last decades have improved survival rates not only in the young and fit, but also in elderly patients (S. K. Kumar, 2014b). Most of the first-line therapy regimens, including alkylating agents and steroids, resulted in poor survival rates. First advances were achieved by high-dose (HD) melphalan therapy combined with autologous stem cell transplantation (ASCT). The subsequent introduction of novel therapeutic agents, such as proteasome inhibitors like bortezomib (Velcade) or immunomodulatory drugs (IMiDs) like thalidomide (Thalomid) and lenalidomide (Revlimid) have led to striking improvements in the overall survival of patients with MM (S. K. Kumar, 2008). Recent reports demonstrate that the increased use of ASCT and the inclusion of new therapeutic agents improve overall survival, progression-free survival and post-relapse survival (Costa, 2013). Several patient-specific risk factors need to be determined before deciding on which treatment to pursue. Apart from the above-mentioned ISS-assessment, age, comorbidities, complications, lactate-dehydrogenase (LDH) levels, proliferation rate, cytogenetic aberrations and the presence of plasma cell leukemia or extramedullary disease need to be taken into consideration. HD chemotherapy followed by ASCT is the current European standard for patients under the age of 65-70 and low comorbidity. This high-dose melphalan-based therapy is preceded by a two- or three-drug induction therapy, including at least one novel agent. ASCT can be followed by a short consolidation therapy and or maintenance therapy with thalidomide, lenalidomide or bortezomib. However, both consolidation and maintenance therapies are still under clinical investigation and wait to be approved for routine settings (Engelhardt, 2014; Ludwig, 2014). Of note, several reports show a beneficial role for lenalidomide maintenance after ASCT (Attal, 2012; Palumbo, 2014). Patients, who are not eligible for ASCT receive induction therapies, most commonly based on melphalan combined with prednisone and either an IMiD or a proteasome inhibitor. Several studies support the strategy of continuous maintenance treatment, again involving one of the novel agents (Moreau, 2015).

1.1.4 Cytogenetics

On the molecular level, neoplastic plasma cells are characterized by several genetic changes. One main alteration, present in 50-60% of tumors, is a translocation including the immunoglobulin heavy chain locus (14q32) and one of the following loci: 11q13, 4p16, 16q23, 6p21. Other tumor cells display hyperdiploid chromosome content as a sign of chromosome instability (Fonseca, 2004).

Cytogenetics have important implications for the prognosis of MM. Several cytogenetic abnormalities, like t(4;14), t(14;16), t(14;20), 1q gains and 17p deletions have been associated with a poor outcome (Bergsagel, 2013). Patients with these "high-risk" genetic patterns therefore need to be treated accordingly. Recent clinical trials have shown that "high-risk" patients should be treated with a bortezomib-based induction followed by ASCT (Stella, 2015). Furthermore, high risk patients harboring t(4;14) or del(17p) may benefit from ASCT followed by an allogeneic stem cell transplantation (Kroger, 2013).

In summary, multiple myeloma remains an incurable hematologic disease of the elderly, despite major therapeutic advances in the past decades. Therefore, the exact understanding of the underlying biology and pathogenesis is of great importance for the further development of more targeted and specific drugs.

1.2 Immunomodulatory Drugs (IMiDs)

1.2.1 Thalidomide and teratogenicity

The discovery of IMiDs dates back to the late 1950s, when "Chemie-Grünenthal", a German pharmaceutical company, developed thalidomide as a new non-barbiturate sedative. Due to its additional anti-emetic potential, one major application of the drug named "Contergan" in Germany was the treatment of morning sickness in pregnant women. It became very popular and was licensed and marketed as a completely safe and non-addictive drug worldwide, given that it had shown no adverse effects in mice (Vargesson, 2015). However, first occurrences of peripheral neuropathy in patients and severe birth defects in children of treated mothers were reported shortly thereafter. In 1961, two physicians independently published their concerns about the safety of thalidomide (Lenz, 1962; McBride, 1961). Thalidomide was soon withdrawn from the markets, having affected more than 10 000 children. Malformations included amelia, phocomelia, syndactyly and abnormal development of the heart, gallbladder, esophagus and duodenum. Interestingly, Frances Kelsey, a scientist at the US-American drug approval agency FDA managed to prevent thalidomide from ever being sold in the US. Her decision was based on lack of safety data (Rehman, 2011). The devastating teratogenic effects led to the implementation of new drug approval regulations, including the obligation to test drugs *in vitro* and *in vivo* in several species. Thalidomide has been shown to be teratogenic in several animal models, including rabbits and non-human primates, whereas mice do not seem to be affected. The reason for this still remains unclear (Vargesson, 2015). Retrospective analyses found the teratogen-sensitive period to be 34-50 days after the last menstrual cycle. A single exposure to thalidomide within this period is thought to be sufficient to cause severe disfigurement (Smithells, 1992). Thalidomide is a chiral molecule, of which only the R(+)-enantiomer is responsible for the formerly

appreciated sedative effect, while the S(-)-enantiomer causes birth defects. Both enantiomers are interconverted rapidly *in vivo*, thereby reducing specific effects of only one enantiomer (Franks, 2004). Many theories as to how thalidomide mediates teratogenicity exist, including anti-angiogenic effects (see below), however, the exact molecular mechanism of thalidomide-mediated teratogenicity remained elusive.

1.2.2 The revival of thalidomide

After being banned from most markets in 1962, thalidomide was rediscovered as a useful therapeutic drug as early as 1965, when a dermatologist by chance observed a beneficial effect of thalidomide in leprosy patients suffering from erythema nodosum leprosum and assumed anti-inflammatory effects (Sheskin, 1965). The drug was further evaluated in graft-versus-host disease as well as in various inflammatory diseases, such as rheumatoid arthritis, ankylosing spondylitis and inflammatory bowel diseases (Rehman, 2011). In 1991, scientists could show that thalidomide decreases the secretion of tumor-necrosis-factor alpha (TNFα) in stimulated human monocytes. TNFα is an important cytokine elevated in cancer, chronic inflammatory diseases and opportunistic infections related to the acquired-immunodeficiency syndrome (AIDS) (Sampaio, 1991). A milestone was set by D'Amato and colleagues, who identified thalidomide as a potent inhibitor of angiogenesis. They managed to show that thalidomide selectively inhibits the formation of new blood vessels in a rabbit cornea micropocket assay in a TNF-α-independent manner (D'Amato, 1994). Judah Folkman, D'Amato's supervisor, had suggested angiogenesis to be of vital importance for tumor development many years earlier and in fact, angiogenesis is nowadays considered to be one of the hallmarks of cancer (Folkman, 1971; Hanahan, 2000). In a follow-up study, thalidomide's vascular-endothelial growth factor (VEGF)-mediated antiangiogenic activity could be linked to its S(-)-enantiomer's teratogenicity (Kenyon, 1997). Another group has demonstrated that thalidomide exerts its anti-inflammatory and immunomodulatory activity partly by suppressing NF-κB activation induced by H_2O_2 and TNF-α (Majumdar, 2002). Furthermore, thalidomide's anti-inflammatory and immunomodulatory activity may partially be due to IL-10 elevation and subsequent inhibition of cyclooxygenase-2 (Payvandi, 2004). Of note, thalidomide also inhibits the production of matrix metalloproteinases (MMP) by B-cell lines and primary myeloma cells (Segarra, 2010).

1.2.3 Thalidomide and IMiDs in MM and other malignancies

It is thanks to Beth Wolmer that Dr. Bart Barlogie, an oncologist at the University of Arkansas, began to investigate thalidomide in the context of multiple myeloma. Wolmer's husband was suffering from multiple drug-refractory MM, and in her desperation, she sought out many scientists for help and new ideas. One was Judah Folkman, whose lab had been working with thalidomide (see above). Taking

on her cause, Folkman was able to convince Barlogie to try thalidomide on Ira Wolmer in 1997. Unfortunately, the treatment did not help to stop Wolmer's disease from progressing (Stolberg, 1999). Nevertheless, in a following clinical trial with 84 patients suffering from advanced MM, Barlogie and colleagues found thalidomide to have substantial anti-myeloma activity. Thalidomide was able to reduce serum or urine M-protein levels in 32 patients, some of them reaching complete remission (Singhal, 1999). A follow-up trial confirmed the initial results and showed improved overall survival for patients on thalidomide monotherapy (Barlogie, 2001). The combination of thalidomide with dexamethasone further increased response rates compared to thalidomide monotherapy, suggesting synergistic effects (von Lilienfeld-Toal, 2008). Next, thalidomide was evaluated as first line therapy of MM in combination with dexamethasone and bortezomib and showed improved complete response rates of 32% (Cavo, 2010). In the past decade, Celgene, the pharmaceutical company marketing thalidomide released two structural analogues, lenalidomide (CC-5013, Revlimid) and pomalidomide (CC-4047, Pomalyst or Imnovid) (Figure 1). While being potent anti-inflammatory and anti-tumor analogues of thalidomide, they show a more favorable side effect profile (Rehman, 2011). Two

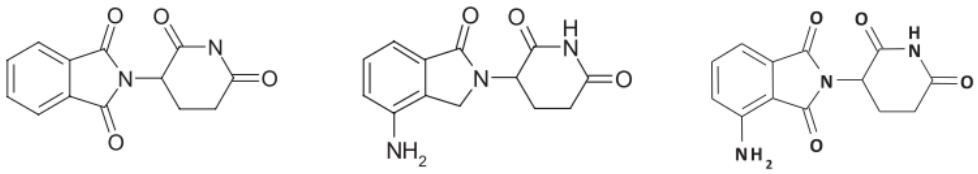

Thalidomide Lenalidomide Pomalidomide

Figure 1: Chemical structure of the three IMiDs thalidomide, lenalidomide and pomalidomide. Adapted from (Lacy, 2013).

initial trials with lenalidomide and dexamethasone treatment in relapsed MM resulted in high overall response rates and led to the approval of this combination (Dimopoulos, 2007; Weber, 2007). Similarly, the combination of pomalidomide with dexamethasone also achieved high response rates, leading to drug approval (San Miguel, 2013). A phase II clinical trial evaluating induction therapy with lenalidomide, bortezomib and dexamethasone followed by ASCT and lenalidomide maintenance as first-line treatment in MM showed impressive results, with 87% of patients achieving very good partial response rates or better after consolidation, suggesting synergy of the novel agents (Roussel, 2014). Apart from MM, lenalidomide has been approved in the treatment of myelodysplastic syndrome (MDS) with deletion of chromosome 5q [del(5q)] and is being investigated in various other hematologic as well as solid malignancies (Zeldis, 2011).

Common side effects of thalidomide include neuropathy, constipation, sedation and deep vein thrombosis. Patients taking lenalidomide may suffer from

myelosuppression, skin rashes and deep vein thrombosis, while myelosuppression and fatigue seem to be the predominant side effects of pomalidomide-therapy (Lacy, 2013). In Germany, the use of IMiDs is strictly regulated. Patients, both women and men, of childbearing age need to guarantee reliable contraception and IMiDs can only be prescribed by specially qualified doctors (BfArM, 2011).

Despite the clear clinical results, which continuously affirm the important role of IMiDs in various diseases, the exact molecular mechanisms by which these drugs exert their multitude of effects remained largely unknown.

1.3 Cereblon

Cereblon (CRBN) was originally assigned a role in memory and learning, because a nonsense mutation, leading to an abnormal C-terminal truncation of the protein, was discovered as the cause of an autosomal recessive nonsyndromic form of mental retardation (Higgins, 2004; Higgins, 2000). This role of CRBN was validated in a forebrain-specific conditional and full $CRBN^{-/-}$ knockout mouse model (Rajadhyaksha, 2012). CRBN was further characterized to have a ubiquitous subcellular localization pattern, with enrichment in the perinuclear region and to be expressed in various tissues (Jo, 2005; Xin, 2008). It contains a Lon domain, important for oligomerization of adenosine triphosphate (ATP)-dependent proteases and chaperones, a regulator of G-protein signaling (RGS) domain and a leucine zipper motif important for protein-protein interaction (Jo, 2005; C. K. Smith, 1999). Furthermore, CRBN associates with and regulates the function of voltage-gated ion-channels (Hohberger, 2009; Jo, 2005).

1.3.1 CRBN and IMiDs

In their landmark study, Ito and colleagues identified CRBN as the cellular target of thalidomide. Using thalidomide-conjugated beads, they searched for thalidomide-interacting proteins in whole cell extracts of HeLa cells and found CRBN and damaged DNA binding protein 1 (DDB1) in mass-spectrometric analyses (Ito, 2010). DDB1, cullin 4 (CUL4), the regulator of cullins 1 (ROC1) and a substrate receptor, usually form a cullin4-RING E3 ubiquitin ligase (CRL4), a multisubunit protein complex shown to polyubiquitinate proteins meant for proteasomal degradation (Angers, 2006). They proposed CRBN to function as the substrate receptor, or DDB1-CUL4-associated factor (DCAF), and indeed could show ubiquitin ligase activity of the complex and found it to be inhibited by thalidomide. Furthermore, they demonstrated that a knockdown of CRBN specifically phenocopies the teratogenic effects of thalidomide in zebrafish- and chicken-models by modulating fibroblast growth factor 8 (fgf8) levels. They therefore postulated that thalidomide exerts its teratogenic activity by binding to CRBN and inhibiting its

ubiquitin ligase activity (Ito, 2010). The next obvious question, whether CRBN is also responsible for thalidomide's actions in MM, was answered by Zhu and colleagues. Using flow cytometry and proliferation assays, they unveiled that knockdown of CRBN in MM cell lines is cytotoxic and leads to a decrease in proliferation. The loss of CRBN in myeloma cells also leads to lenalidomide- and pomalidomide-specific resistance and vice versa, acquired IMiD-resistance is associated with low CRBN levels. In addition, lenalidomide-mediated changes in gene expression are substantially reduced in CRBN-depleted cells. Their findings suggest that CRBN is necessary for lenalidomide's anti-myeloma actions and provide evidence for a common pathway of the teratogenic and anti-myeloma effects of IMiDs (Zhu, 2011). Another group further succeeded to clarify the interaction of IMiDs and CRBN (Lopez-Girona, 2011; Lopez-Girona, 2012): Namely, thalidomide's inhibitory effect on CRBN autoubiquitylation extends to both lenalidomide and pomalidomide. Moreover, depletion of CRBN abrogates lenalidomide's and pomalidomide's anti-proliferative potency in MM cell lines. Lenalidomide and pomalidomide also downregulate interferon-regulatory factor 4 (IRF4), an established MM cell survival factor and induce the cell cycle inhibitory protein $p21^{WAF-1}$ in a CRBN-dependent manner (Lopez-Girona, 2011). Furthermore, CRBN is necessary for IMiD-induced activation of the cytokines interleukin-2 (IL-2) and TNF-α in T cells (Lopez-Girona, 2012). These findings link CRBN both to the anti-proliferative and immunomodulatory activity of IMiDs.

1.3.2 IMiDs modulate CRBN ligase activity

The identification of CRBN as the key cellular IMiD-interacting protein clearly improved the understanding of IMiD biology. However, exactly how CRBN mediates the effect of IMiDs remained unclear. In an attempt to identify downstream interactors/substrates of CRBN, four groups simultaneously performed luciferase-assay and mass spectrometry-based analyses of cells with or without IMiD treatment. They identified two zinc finger transcription factors of the Ikaros family, Ikaros (IKZF1) and Aiolos (IKZF3), to be affected by IMiD treatment (A. K. Gandhi, 2014a; Kronke, 2014; Lu, 2014; Zhu, 2014). IKZF1 and IKZF3 are lymphoid transcription factors that have been implicated in various stages of B- and T-cell differentiation (Cortes, 1999). Particularly IKZF3 has been shown to be crucial in the development of long-lived high-affinity plasma cells in the bone marrow (Cortes, 2004). IKZF1 and IKZF3 protein levels are downregulated upon IMiD treatment of MM cell lines and patient-derived primary MM cells, while mRNA-levels remain stable. Depletion of IKZF1 and IKZF3 leads to a downregulation of IRF4 and decreases the proliferation of IMiD-sensitive MM cell lines. This links IKZF1 and IKZF3 downregulation to the anti-myeloma activity of IMiDs (Kronke, 2014; Lu, 2014). It has been previously demonstrated that IKZF1 and IKZF3 are negative regulators of IL-2 expression (R. Gandhi, 2010). Gandhi and colleagues observed

that IMiD-induced IL-2 secretion is mimicked by the depletion of IKZF1 or IKZF3 in T-cells. They therefore conclude that lenalidomide- and pomalidomide-induced IL-2

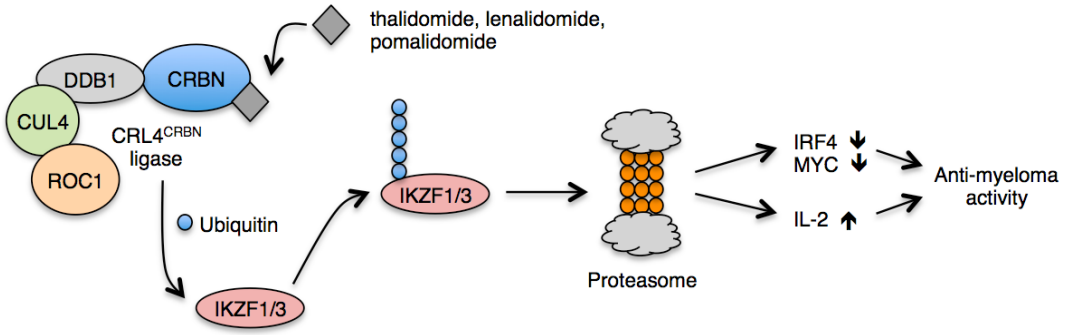

Figure 2: IMiDs modulate the CRL4^{CRBN} complex to ubiquitinate IKZF1/3. This leads to protein degradation in the proteasome and is responsible for some anti-myeloma effects of IMiDs. Adapted from (Stewart, 2014)

elevation in T-cells is mediated by CRBN-dependent degradation of the IKZF1 and IKZF3 transcription factors and the resulting de-repression of IL-2 transcription. The same group also assessed IKZF1 and IKZF3 expression levels in peripheral blood-derived T-cells of healthy volunteers before and after lenalidomide treatment and observed a decrease in IKZF3 levels upon treatment. They therefore propose IKZF3 as a new biomarker for lenalidomide activity in MM (A. K. Gandhi, 2014a).

On the mechanistic side, IKZF1 and IKZF3 were shown to interact with CRBN within the CRL4^{CRBN} ubiquitin ligase complex. This interaction, however, only occurs upon IMiD treatment. While previous studies suggested IMiDs to inhibit CRBN ubiquitin ligase activity, Ghandi, Lu, Krönke, Zhu and colleagues have shown that lenalidomide reprograms the CRBN ligase complex to bind to its substrates IKZF1 and IKZF3, leading to their polyubiquitynation and subsequent proteasomal degradation. These findings suggest an attractive model, in which a ubiquitin ligase complex such as CRL4^{CRBN} can be steered by small molecules to target specific proteins. Further, the authors assumed that teratogenicity and IMiD activity in the non-lymphoid context might be mediated by different CRBN substrates (Kronke, 2014; Lu, 2014). Indeed, in a follow-up study in del(5q) MDS, Krönke and colleagues have shown lenalidomide-induced degradation of casein kinase 1A1 (CK1α) to be responsible for IMiD activity in this hematologic entity (Kronke, 2015). Crystal structure analyses of CRBN with thalidomide, lenalidomide and pomalidomide have revealed that IMiDs bind to a hydrophobic pocket in the C-terminal region of CRBN with their common glutarimide ring. The phthalimide moiety, which varies among IMiDs (Figure 1), is exposed on the surface of the CRBN protein, creating an interface of unsatisfied bonding potential for new interactions. Of note, the hydrophobic IMiD-binding pocket is highly conserved and therefore physiologic IMiD-competing endogenous ligands are very likely (Chamberlain, 2014; Fischer, 2014). In

an elegant approach, a group at the Dana-Farber Cancer Institute combined a thalidomide analogue with a small molecule inhibitor of bromodomain-containing protein 4 (BRD4), which is involved in MYC signaling, and demonstrated that $CRL4^{CRBN}$ selectively degrades BRD4 upon exposure to this thalidomide-conjugated inhibitor. They infer that many previously intractable proteins might be selectively degradable by using phthalimide-conjugated ligands with or without intrinsic inhibitory activity (Winter, 2015).

The IMiD-induced selective degradation of IKZF1, IKZF3 or CK1α by an E3 ubiquitin ligase complex involving CRBN explains some of the anti-proliferative and immunomodulatory effects in MM and del(5q) MDS. Nevertheless, this theory lacks explanations for the anti-angiogenic and teratogenic potential of IMiDs. Furthermore, it creates a paradox, because in patients, proteasome inhibitors like bortezomib, carfilzomib and ixazomib show synergistic activity with IMiDs (S. K. Kumar, 2014a; Richardson, 2010; Roussel, 2014; Stewart, 2015). In theory, however, proteasome inhibition would antagonize the IMiD induced degradation of IKZF1, IKZF3 and CK1α. A ubiquitin-independent physiologic function of CRBN might be able to explain these unanswered questions.

1.3.3 CRBN exerts a chaperone-like function for the CD147/MCT1 complex

In their search for physiological CBRN interactors, my colleagues in the lab of Prof. Bassermann performed an affinity purification of CRBN, followed by mass spectrometry and identified cluster of differentiation 147 (CD147), which is also known as basigin or extracellular matrix metalloproteinase inducer (EMMPRIN), and monocarboxylate transporter 1 (MCT1) as specific interactors. Functions of these proteins are investigated in 1.4. They found that the interaction between CRBN and these two membrane proteins, in contrast to IKZF1 and IKZF3, is lost upon lenalidomide exposure (Eichner, 2016). Moreover, knockdown of CRBN leads to CD147 and MCT1 destabilization, while forced expression stabilizes both proteins (Eichner, 2016). This suggests that CRBN exerts a stabilizing, e.g. chaperone-like function on CD147 and MCT1, which compete with IMiDs for CRBN-binding. Indeed, CRBN interacts with freshly synthetized CD147 and MCT1, while lenalidomide treatment or CRBN depletion result in accumulation of the membrane proteins at the

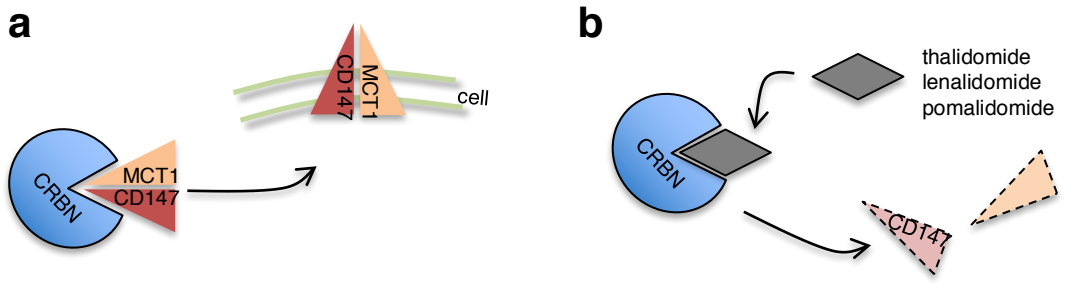

Figure 3: CRBN exerts a chaperone-like function for the CD147/MCT1 complex. a) CRBN promotes complex formation and proper localization to the cell membrane. b) IMiDs bind competitively to CRBN and abrogate complex assembly and correct localization.

endoplasmatic reticulum (Eichner, 2016). Their size exclusion chromatography experiments of CRBN immunoprecipitates showed that CRBN exists in two different complexes, one containing the usual components of the $CRL4^{CRBN}$ ligase and another with CD147 and MCT1. In addition, immunoprecipitation of CUL4A failed to retrieve both CD147 and MCT1. Taken together, these findings imply that CRBN exerts a ubiquitin-independent chaperone-like function on CD147 and MCT1 and plays an important role in the maturation of these two membrane proteins. The functional relevance of this mechanism in MM is presented in the results section of this thesis. Apart from the relevance in MM, further studies from our group have linked CD147 to IMiD-induced teratogenicity in a zebrafish model. The morpholino-induced specific knockdown of CD147 phenocopies the teratogenic effects of thalidomide, resulting in a dose-dependent reduction of fin-, head- and eye-size (Eichner, 2016). Likewise, CD147 depletion reduces the expression of fgf8 in pectoral fin buds, an effect also observed in thalidomide-treated zebrafish (Ito, 2010). This effect is thalidomide-specific and does not extend to lenalidomide or pomalidomide, which is in line with the fact that in zebrafish, CD147 is only destabilized by thalidomide (Eichner, 2016).

1.4 CD147 & MCT1

1.4.1 CD147 and its role in malignant diseases

CD147 is a transmembrane glycoprotein related to the immunoglobulin superfamily of receptors. It exists in various species and is also known as EMMPRIN or basigin. It is made up of 269 amino acids and can be divided into an extracellular domain, which contains two immunoglobulin-like structures with three glycosylation sites, a short highly-conserved hydrophobic transmembrane-region and a 39 amino acid C-terminal intracellular domain. The molecular weight of CD147 varies from 29-65kDa, depending on the glycosylation pattern. The low molecular weight core-glycosylated protein is the immature form, while the highly glycosylated form of CD147 is considered to be the active form. CD147 has been shown to interact with several proteins including integrins, cyclophilin-A, caveolin-1 and two members of the moncarboxylate transporter family MCT1 and MCT4 (Iacono, 2007). The name extracellular matrix metalloproteinase inducer (EMMPRIN) derives from the observations that CD147 mediates tumor invasion, growth, progression and metastasis by inducing MMP

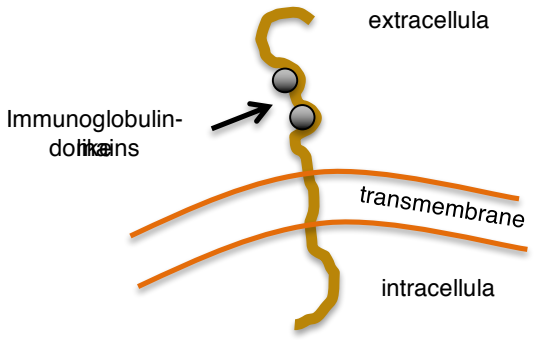

Figure 4: Schematic representation of the CD147 protein. Adapted from (Xiong, 2014)

production (Xiong, 2014). In addition, several studies could demonstrate that CD147 plays a crucial role in angiogenesis by promoting the secretion of VEGF both by tumor cells directly and by inducing VEGF secretion in the microenvironment (Bougatef, 2009; Y. Chen, 2012; Tang, 2005). CD147 is expressed in various tissues, including actively proliferating and differentiating epithelial, myocardial, vascular endothelial cells of the brain, most cells of the hematopoietic system and in almost all types of cancer tissue (Riethdorf, 2006). It is overexpressed and described as a marker of poor prognosis in some tumor entities, such as breast cancer, serous ovarian and bladder carcinoma (Weidle, 2010). CD147 has also been implicated in multidrug resistance in different types of cancer (Weidle, 2010). CD147-directed monoclonal antibodies are currently being evaluated pre-clinically in hepatocellular carcinoma and head and neck squamous cell carcinoma and show promising results regarding prevention of metastasis, invasion and angiogenesis (Xiong, 2014).

1.4.2 Cancer cell metabolism and the Warburg Effect

In regular cellular metabolism, under normoxic conditions, cells take up glucose and process it to pyruvate by glycolysis. Pyruvate is then passed on to the mitochondrial citric acid cycle and oxidative phosphorylation resulting in carbon dioxide, water and 36 molecules of ATP per processed molecule of glucose. Under anaerobic or hypoxic conditions, cells neglect oxidative phosphorylation and instead upregulate the less efficient anaerobic glycolytic pathway, which produces lactate and 2 molecules of ATP (Berg, 2002). In the 1920s, Otto Warburg, while comparing metabolic respiratory rates of tumor tissues with those of normal liver and kidney tissues, observed that cancer cells with functioning mitochondria retain a glycolytic metabolic pattern even under normoxic conditions. This phenomenon has been named “aerobic glycolysis” or the Warburg Effect (Liberti, 2016; Warburg, 1925). Aerobic glycolysis has been shown to be associated with hypoxia-independent activation of hypoxia-inducible factors (HIF) by well-known oncogenes like RAS, MYC and mutated tumor suppressors (Hanahan, 2011). The reasons for the glycolytic switch are still not fully understood, there are, however, several theories. One reason may be the rapid generation of ATP by glycolysis. The rate of lactate-producing glycolysis is 10-100 times faster compared to oxidative phosphorylation and therefore the net ATP obtained by both pathways is almost equal (Liberti, 2016). Another theory states that aerobic glycolysis might aid cancer cells by increasing glucose uptake and synthesis of amino acids, nucleotides and lipids, which are urgently needed in cells with uncontrolled proliferation. In addition to ATP, the biosynthesis of such macromolecules relies on the reducing equivalents NADH and NADPH, which are generated as a byproduct of glycolytic metabolism (Vander Heiden, 2009). Next, the tumor microenvironment is influenced by elevated lactate levels and decreased extracellular pH. Reports have shown that H^+ ions diffuse into neighboring healthy tissue causing tissue remodeling, which ultimately favors

invasion and metastasis (Estrella, 2013). Finally, the Warburg Effect has been proposed to directly affect signal transduction in tumor cells, by generating and modulating reactive oxygen species and altering chromatin structure and the epigenetic pattern of certain growth genes (Liberti, 2016). The complex deregulation of normal energy metabolism is considered to be one of the new emerging hallmarks of cancer (Hanahan, 2011). Indeed, a recent study has demonstrated that MM cells also depend on aerobic glycolysis and produce significantly higher amounts of lactate compared to normal blood mononuclear cells under normoxic conditions (Sanchez, 2013). The interruption of the glycolytic pathway by dichloroacetate induces apoptosis, superoxide production, decreases proliferation and increases sensitivity to proteasome inhibitors like bortezomib in MM cell lines (Sanchez, 2013). In addition, pyruvate dehydrogenase kinase 1 (PDK1), which inhibits pyruvate dehydrogenase (PDH), the gatekeeping enzyme limiting the conversion of pyruvate to acetyl-CoA used in the citric acid cycle, and other glycolytic enzymes such as glucose transporter 1 (GLUT1) and lactate dehydrogenase A (LDHA) are overexpressed in MM patient samples (Fujiwara, 2013).

1.4.3 Hypoxia, the bone marrow and MM

Hypoxia is a state of imbalance between oxygen consumption and availability. It is a common feature of the tumor microenvironment and has been implicated in disease progression and treatment resistance. Hypoxia in solid tumors can be explained by massive cell proliferation and concurrent shortage of perfusion by pre-existing blood vessels or frequently aberrant and insufficient neo-vascularization. Therefore, hypoxic tumor cells rely on oxygen diffusion and acquire more aggressive and drug resistant phenotypes by upregulating hypoxia inducible factor-1α (HIF-1α) (Martin, 2011). Notably, the bone marrow microenvironment is characterized by local hypoxia. This has been established by invasive studies in orthopedic and MM patients (Colla, 2010; Watanabe, 2007). Studies conducted on murine bone marrow using markers for hypoxia have shown that oxygen tension varies within the bone marrow. Lowest oxygen tensions were observed in compartments close to the edge of the bone marrow, which coincide with a high abundance of hematopoietic stem cells (Martin, 2011; Parmar, 2007). In MM cells, HIF-1α is upregulated both due to local hypoxia and oxygen-independent aberrant signaling. HIF-1α contributes to MM pathogenesis by deregulating energy metabolism and inducing anti-apoptotic proteins as well as the secretion of angiogenic factors like VEGF (Borsi, 2015). Specific inhibition of HIF-1α causes reduced viability in MM cell lines via cell cycle arrest and apoptosis (Borsi, 2014). TH-302, a prodrug of a cytotoxin, is only activated under hypoxic conditions and is currently being studied in phase I and II clinical trials in combination with dexamethasone alone or with bortezomib for patients with relapsed or refractory MM

(Borsi, 2015; Hu, 2010). To conclude, selective targeting of MM via the hypoxic bone marrow niche seems like a very promising therapeutical approach.

1.4.4 MCT1 and its role in malignant diseases

Until the 1970s, it was believed that lactate, pyruvate and acetate cross the plasma membrane by simple diffusion. However, Halestrap and colleagues found that this transport could be specifically inhibited by α-cyano-4-hydroxycinnamate (CHC) and therefore proposed the involvement of transporters (Halestrap, 1974). The solute carrier 16 (SLC16) or monocarboxylate transporter (MCT) family consists of 14 members and is characterized by 12 transmembrane domains, an N- and C-terminal intracellular tail and an intracellular loop between the transmembrane domains 6 and 7 (Halestrap, 2004). MCTs catalyze the symport of monocarboxylate anions together with a proton across membranes, following a concentration gradient in a process that does not require ATP. They also mediate the exchange of intra- and extracellular monocarboxylates (Halestrap, 2013). MCT1, encoded by the SLC16A1 gene, is ubiquitously expressed and is the most characterized member of the MCT family. MCT1 can transport monocarboxylates equally well across membranes in both directions. Due to its high abundance and its leading role in anaerobic and aerobic glycolysis, L-lactate is by far the most relevant substrate (Halestrap, 2013). MCT1-facilitated lactate and proton efflux across the plasma membrane contributes to the regulation of intracellular pH and therefore is of vital importance to cell survival during periods of hypoxia or ischemia. Some tissues such as white muscle and some invasive tumors preferentially use MCT4, while MCT1 serves as a lactate importer in red skeletal muscle cells, supplying these cells with lactate for oxidative metabolism (Halestrap, 2012). MCT1 is overexpressed in various solid tumors including lung cancer, colorectal carcinoma, pancreatic carcinoma, glioma, neuroblastoma and melanoma (Kennedy, 2010). Because lactate efflux is important in tumor cell metabolism, MCTs have recently been investigated as potential targets in anti-cancer therapy. Knockdown of MCT1 via siRNA or treatment with the MCT1/2-specific inhibitor AR-C155858 increases intracellular lactate levels, reduces rates of glycolysis and displays anti-proliferative and cytotoxic effects in fibroblasts and a xenograft mouse model (Le Floch, 2011). Similar results have been achieved in small cell lung cancer cell lines in normoxia and hypoxia with the MCT1-specific inhibitor AZD3965, which

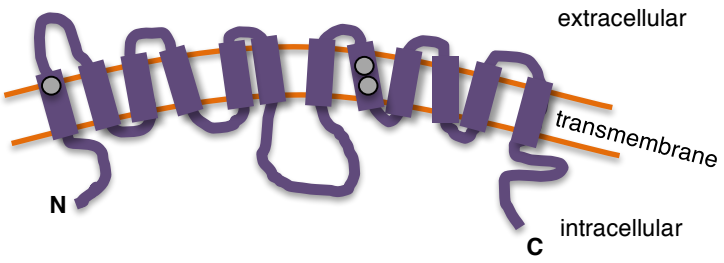

Figure 5: Schematic representation of the MCT1 protein. Grey circles indicate residues involved in proton and monocarboxylate binding. Adapted from (Halestrap, 2013)

is currently being evaluated in a phase I clinical trial for patients with advanced solid tumors in the United Kingdom (Polanski, 2014).

1.4.5 CD147, MCT1 and MM

CD147 and MCT1 have been shown to interact strongly and form a transmembrane complex, most likely through the transmembrane and intracellular domain of CD147 (Kirk, 2000). Co-transfection experiments have shown that correct co-localization at the cell membrane occurs only upon interaction of CD147 and MCT1, suggesting that CD147 acts as a chaperone for MCT1 and thereby facilitates lactate transport (Kirk, 2000; Le Floch, 2011). Likewise, proper maturation of CD147 partly depends on MCT1 expression, as a knockdown of MCT1 leads to an accumulation of the immature core-glycosylated form of CD147. This implies that CD147 and MCT1 regulate each other by acting as co-chaperones to form a transmembrane complex (Deora, 2005).

Both CD147 and MCT1 are implicated in MM pathogenesis. CD147 is elevated in MM cells compared to MGUS and normal B cells, on both mRNA and protein level. Progression of disease correlates with increased CD147 cell surface expression levels (Arendt, 2012). The natural CD147 ligand and activator cyclophillin B increases proliferation of MM cells in a CD147-dependent manner (Arendt, 2012). High CD147 cell surface levels are associated with rapid proliferation, whereas downregulation of CD147 decreases proliferation (Arendt, 2012). Microvesicles are thought to mediate intercellular communication and those released by MM cells show high CD147 levels. These microvesicles with high CD147 levels are able to stimulate MM cell proliferation, while microvesicles derived from CD147-silenced cells fail to do so (Arendt, 2014). Recently, CD147 has been shown to be involved in MM cell homing to the bone marrow (D. Zhu, 2015). Zhu and colleagues propose a model, in which a cyclophilin A gradient, created by bone marrow endothelial cells, promotes the migration and colonization of CD147-overexpressing MM cells to the bone marrow. Extravasation is induced by cyclophilin A-mediated CD147 activation and secretion of MMPs. Treatment of MM cell xenografted mice with a CD147 antibody significantly reduces tumor burden (D. Zhu, 2015). Another recent study has confirmed CD147 overexpression in MM patient-derived bone marrow aspirates, while secretion of MMP-2 and MMP-9 was found to be significantly elevated in comparison to control samples (Urbaniak-Kujda, 2016).

According to gene expression data, MCT1 is significantly overexpressed in MM patients compared to MGUS patients or healthy individuals (Walters, 2013). CD147 and MCT1 also co-localize at the plasma membrane of MM cells. RNAi-mediated knockdown of MCT1 leads to significantly decreased proliferation of MM cell lines, however this is not due to an increased apoptotic fraction (Walters, 2013). Finally, CD147 and MCT1-depletion in MM also results in higher extracellular pH-values and decreased concentrations of extracellular lactate (Walters, 2013).

Another study has shown that blocking lactate export with the MCT inhibitor CHC or the MCT1/2-specific inhibitor AR-C155858 is also cytotoxic in MM (Hanson, 2015). This cytotoxicity is enhanced by an acidic microenvironment, thus making MM cells in acidic bone lesions particularly targetable. MCT-inhibition also leads to reduced MM cell migration (Hanson, 2015).

In summary, CD147 and MCT1 promote progression of various malignancies by inducing angiogenesis, the secretion of matrix-degrading pro-invasive proteases and by facilitating the export of excess lactate. Both proteins are overexpressed in MM and thus represent promising druggable targets in the treatment of this currently incurable disease.

2 Aim of the study

Thalidomide became infamous in the 1960s for causing severe birth defects, after having been promoted as a safe anti-emetic and sedative drug for pregnant women (Vargesson, 2015). Together with its derivatives lenalidomide and pomalidomide, it has been rediscovered as an effective agent in the therapy of several malignancies, including MM and del(5q) MDS (Rehman, 2011). The introduction of these novel agents, which display immunomodulatory, anti-angiogenic, anti-proliferative and anti-invasive properties has, significantly improved the prognosis of MM patients in the past decades (S. K. Kumar, 2014b; S. K. Kumar, 2008). While the identification of CRBN as direct IMiD-binding protein and effector of anti-myeloma activity and teratogenicity (Ito, 2010; Lopez-Girona, 2012; Zhu, 2011) and the IMiD-induced degradation of the lymphoid transcription factors IKZF1/3 has shed some light on the molecular mechanism of IMiDs (A. K. Gandhi, 2014a; Kronke, 2014; Lu, 2014; Zhu, 2014), the exact mechanism by which IMiDs exert their various anti-tumor effects remained unclear. The aim of this present study was to functionally validate and characterize the two newly identified CRBN interactors CD147 and MCT1 in the context of MM. Deciphering IMiD biology and the role of CD147 and MCT1 in this context would contribute to the understanding of acquired IMiD resistance and could help to select patients, who could profit from an IMiD-based therapy regimen.

3 Materials and Methods

3.1 Materials

3.1.1 Devices, machines and instruments

Object	Manufacturer
Agarose electrophoresis chamber Mini-Sub Cell GT	Bio-Rad, Munich, Germany
Analytical balance ABJ	Kern&Sohn, Balingen, Germany
Bacterial shaker/incubator innova 40	Eppendorf, Hamburg, Germany
Cell Culture CO_2-Incubator Hera cell 150i	Thermo Scientific, Waltham, US
Centrifuge Heraeus Multifuge 3SR+	Thermo Scientific, Waltham, US
Chamber for ready gels	Invitrogen, Karlsruhe, Germany
Cobas 8000 modular analyzer series	Roche, Grenzach-Wyhlen, Germany
Cooling-Centrifuge 5417R	Eppendorf, Hamburg, Germany
Cooling-Centrifuge 5430R	Eppendorf, Hamburg, Germany
FACS Calibur	BD Biosciences, San Jose, US
Hypoxia Incubator, CB 160	Binder, Tuttlingen, Germany
Magnetic Thermo Stirrer RCT basic	IKA, Staufen, Germany
Microplate Reader Sunrise	Tecan Group, Männedorf, Switzerland
Microscope Axiovert 40 CFL	Carl Zeiss AG, Oberkochen, Germany
Microscope PrimoStar	Carl Zeiss AG, Oberkochen, Germany
Nano-Photometer	Implen, Munich, Germany
Neubauer hemocytometer	Marienfeld, Lauda-Königshofen, Germany
PCR peqSTAR 2x Gradient Thermocycler	Peqlab, Erlangen, Germany
pH-meter pH720 InoLab	WTW, Weilheim, Germany
Pipetboy acu 2	Integra Biosciences, Zizers, Switzerland
Pipettes PIPETMAN Neo P2, P10, P20, P100, P200, P1000	Gilson, Middleton, US
Power Supply PowerPac Basic	Bio-Rad, Munich, Germany
Power Supply PowerPac HC High Current	Bio-Rad, Munich, Germany
Precision Balance 572	Kern&Sohn, Balingen, Germany
Rotating wheel L29	Fröbel Labortechnik, Lindau, Germany
Rotating wheel, horizontal, RM10W	Fröbel Labortechnik, Lindau, Germany
RT-PCR System LightCycler 480	Roche, Grenzach-Wyhlen, Germany
Safety hood, Herasafe KS	Thermo Fisher Scientific, Waltham, US
Scanner V750 Pro	Epson, Meerbusch, Germany
SDS-gel electrophoresis chamber Mini-Protean	Bio-Rad, Munich, Germany
Sorvall Superspeed Centrifuge RC5B	Thermo Fisher Scientific, Waltham, US
Tabletop centrifuge 5424	Eppendorf, Hamburg, Germany
Thermomixer	Eppendorf, Hamburg, Germany
Vortexer MS3 basic	IKA, Staufen, Germany
Waterbath Aqualine AL 18	Lauda, Lauda-Königshofen, Germany
Waving platform shaker Polymax 2040	Heidolph Instruments, Kelheim, Germany
Western Blotting chamber Tetra Blotting Module	Bio-Rad, Munich, Germany

Western Blot Developer SRX-101A	Konica Minolta, Munich, Germany

3.1.2 Chemicals

Product	**Manufacturer**
Acetic acid	Roth, Karlsruhe, Germany
Acetone	Roth, Karlsruhe, Germany
Acrylamide/Bis Rotiphorese 40% (29:1)	Roth, Karlsruhe, Germany
Agarose powder	Roth, Karlsruhe, Germany
Ammonium persulfate (APS)	Roth, Karlsruhe, Germany
Ampicillin	Roth, Karlsruhe, Germany
Aqua ad injectabila, sterile	Braun, Melsungen, Germany
ATX Ponceau S red staining solution	Sigma-Aldrich, Taufkirchen, Germany
β-Mercaptoethanol	Sigma-Aldrich, Taufkirchen, Germany
Bacto agar	BD Bioscience, San Jose, US
Bacto typton	BD Bioscience, San Jose, US
Bacto yeast extract	BD Bioscience, San Jose, US
Bovine serum albumin	Roth, Karlsruhe, Germany
Bromophenol blue	Sigma-Aldrich, Taufkirchen, Germany
Calcium Chloride ($CaCl_2$)	Sigma-Aldrich, Taufkirchen, Germany
Coomassie Brilliant Blue	Roth, Karlsruhe, Germany
Deoxynucleotide triphosphate (dNTP) mix	Thermo Fisher Scientific, Waltham, US
Dimethyl sulfoxide (DMSO)	Roth, Karlsruhe, Germany
Ethanol 70%	Merck Millipore, Darmstadt, Germany
Ethanol 96%	Merck Millipore, Darmstadt, Germany
Ethidium bromide	Roth, Karlsruhe, Germany
Hydrochloric acid (HCl)	Roth, Karlsruhe, Germany
Glycerol	Sigma-Aldrich, Taufkirchen, Germany
Glycine	Roth, Karlsruhe, Germany
Isopropanol 70%	Roth, Karlsruhe, Germany
Kanamycin	Sigma-Aldrich, Taufkirchen, Germany
Lenalidomide	Selleckchem, Houston, US
Methanol	Merck Millipore, Darmstadt, Germany
Nonidet-P40 Subsitute (NP40)	Roche, Grenzach-Wyhlen, Germany
N,N-Bis(2-hydroxyethyl)taurine (BES)	Sigma-Aldrich, Taufkirchen, Germany
Polybrene (Hexdimethrine bromide)	Sigma-Aldrich, Taufkirchen, Germany
Pomalidomide	Selleckchem, Houston, US
Potassium chloride	Sigma-Aldrich, Taufkirchen, Germany
Puromycin	Sigma-Aldrich, Taufkirchen, Germany
Skim milk powder	Sigma-Aldrich, Taufkirchen, Germany
SOC medium	NEB, Ipswich, US
Sodium acetate	Merck Millipore, Darmstadt, Germany
Sodium azide	Merck Millipore, Darmstadt, Germany
Sodium chloride (NaCl)	Roth, Karlsruhe, Germany
Sodium dihydrogenphosphat	Merck Millipore, Darmstadt, Germany
Sodium dodecylsulfate (SDS)	Roth, Karlsruhe, Germany
Sodium fluoride (NaF)	Sigma-Aldrich, Taufkirchen, Germany
Sodium hydroxide	Roth, Karlsruhe, Germany
SuperSignal West Pico Chemiluminescent Substrate	Thermo Fisher Scientific, Waltham, US

SuperSignal West Femto Maximum Sensitivity Substrate	Thermo Fisher Scientific, Waltham, US
Tris/Borate/EDTA (TBE) Buffer, UltraPure 10X	Thermo Fisher Scientific, Waltham, US
Tetramethylethylenediamine (TEMED)	Sigma-Adrich, Taufkirchen, Germany
(±)-Thalidomide	Tocris Bioscience, Bristol, UK
Tris(hydroxymethyl)aminomethane (Tris)	Roth, Karlsruhe, Germany
Triton X-100	Sigma-Aldrich, Taufkirchen, Germany
Trypan blue	Life Technologies, Carlsbad, US
Tween 20	Sigma-Aldrich, Taufkirchen, Germany

3.1.3 Cell culture materials

Product	**Manufacturer**
Dulbecco's Modified Eagle's Medium (DMEM)	Life Technologies, Carlsbad, US
DMEM, no phenol red medium	Life Technologies, Carlsbad, US
RPMI 1640 GlutaMAX medium	Life Technologies, Carlsbad, US
RPMI 1640, no phenol red medium	Life Technologies, Carlsbad, US
Fetal Bovine Serum (FBS) Superior	Biochrom, Berlin, Germany
Newborn Calf Serum	Biochrom, Berlin, Germany
Human IL-6	R&D Systems, Wiesbaden, Germany
Opti-MEM, reduced serum media	Life Technologies, Carlsbad, US
Phosphate buffered saline (PBS)	Life Technologies, Carlsbad, US
Penicillin/Streptomycin (100X)	Life Technologies, Carlsbad, US
Trypsin-EDTA (10X) solution	Biochrom, Berlin, Germany
Trypsin-EDTA (10X) solution	Life Technologies, Carlsbad, US
Glutamine (100X)	Life Technologies, Carlsbad, US

3.1.4 Cell lines

Cell line	**Medium**	**Type**	**Obtained from**
AMO-1	RPMI	Human MM cells (ACC-538)	DSMZ, Braunschweig, Germany
HEK293T	DMEM	Human embryonic kidney cell-line (CRL-3216)	ATCC, Virginia, US
HeLa	DMEM	Human cervix carcinoma cell-line (CCL-2)	ATCC, Virginia, US
INA6	RPMI+IL6	Human MM cells	Kind gift of U. Keller
JJN3	RPMI	Human MM cells (ACC-541)	DSMZ, Braunschweig, Germany
KMS 12BM	RPMI	Human MM cells (ACC-551)	DSMZ, Braunschweig, Germany
L363	RPMI	Human MM cells (ACC-49)	DSMZ, Braunschweig, Germany
MM1S	RPMI	Human MM cells (CRL-2974)	ATCC, Virginia, US
OPM2	RPMI	Human MM cells (ACC-50)	DSMZ, Braunschweig, Germany

RPMI 8226	RPMI	Human MM cells (ACC-402)	DSMZ, Braunschweig, Germany
U266	RPMI	Human MM cells (ACC-9)	DSMZ, Braunschweig, Germany

Table 3: List of cell lines

3.1.5 Cell culture, Bench and other materials

Product	Manufacturer
0.2ml, 1.5ml, 2ml Eppendorf tubes	Sarstedt, Nümbrecht, Germany
15ml, 50ml Falcon tubes	Greiner Bio-One, Krems, Austria
1ml, 250µl, 20µl tips	Sarstedt, Nümbrecht, Germany
Gel-loading tips	Roth, Karlsruhe, Germany
T25, T75, T175 cell culture flasks	Sarstedt, Nümbrecht, Germany
6cm, 10cm, 15cm cell culture plates	TPP, Trasadingen, Switzerland
6-well, 12-well, 96-well plates	TPP, Trasadingen, Switzerland
Syringe-Filters 0.45µm, 0.2µm	TPP, Trasadingen, Switzerland
Immobilon-P Membrane, PVDF, 0.45 μm	Merck Millipore, Darmstadt, Germany
Microcon 30kDa Centrifugal Filter Units	Merck Millipore, Darmstadt, Germany
X-Ray Films for Western Blot, CL-XPosure	Thermo Fisher Scientific, Waltham, US

3.1.6 Transfection reagents & Enzymes

Product	Manufacturer
HiPerFect Transfection Reagent	Qiagen, Hilden, Germany
Pfu II Ultra DNA Polymerase	Agilent Technologies, Santa Clara, US
Restriction Enzymes: AgeI, BamHI, DpnI, EcoRI, HindIII, KpnI, XbaI, XhoI	Thermo Fisher Scientific, Waltham, US
SuperScript III Reverse Transcriptase	Life Technologies, Carlsbad, US

All enzymes were used with appropriate reaction buffers.

3.1.7 Inhibitors

Inhibitor	Manufacturer
cOmplete Protease Inhibitor Cocktail	Roche, Grenzach-Wyhlen, Germany
DL-Dithiotheritol (DTT)	Sigma-Aldrich, Taufkirchen, Germany
Glycerol 2-phosphate disodium salt pentahydrate (G2P)	Sigma-Aldrich, Taufkirchen, Germany
Ocadaic acid	Sigma-Aldrich, Taufkirchen, Germany
Phenylmethylsulfonylfluoride (PMSF)	Sigma-Aldrich, Taufkirchen, Germany
Peptidylprolyl isomerase inhibitor (PIN)	Sigma-Aldrich, Taufkirchen, Germany
Sodium orthovanadate (NaVa)	Sigma-Aldrich, Taufkirchen, Germany
Tosyl-L-lysyl-chloromethyl-ketone (TLCK)	Sigma-Aldrich, Taufkirchen, Germany
Tosyl-phenylalanyl-chloromethyl-ketone (TPCK)	Sigma-Aldrich, Taufkirchen, Germany

3.1.8 Buffers

250mM lysis buffer (for lactate measurements)	250mM NaCl 50mM Tris/HCl (pH 7.5) 0.1% Triton X-100 1mM EDTA 50mM NaF
1% Triton lysis buffer	250mM NaCl 50mM Tris/HCl (pH 7.5) 1% Triton X-100 1mM EDTA 50mM NaF
150mM lysis buffer	150mM NaCl 50mM Tris/HCl (pH 7.5) 0.1% NP40 1mM EDTA 5mM $MgCl_2$ 5% Glycerol
Inhibitors	1mM DTT 10mM G2P 0.1mM PMSF 0.1mM NaVa 5.0µg/ml TLCK 10.0µg/ml TPCK 1µg/ml aprotinin 1µg/ml leupeptin 10µg/ml soybean trypsin inhibitor
10X Running Buffer	250mM Tris/HCl (pH 7.5) 1.92 M Glycine 1% SDS
10X Blotting Buffer	250mM Tris/HCl (pH 7.5) 1.5M Glycine 1% SDS to prepare 1X: 1vol Buffer + 2vol Methanol + 7vol H_2O
Stripping Buffer	62.5mM Tris/HCl (pH 6.8) 0.867% β-Mercaptoethanol 2% SDS
Washing Buffer	PBS (1X) 0.1% Tween 20
Western Blot Blocking Buffer	PBS (1X) 0.1% Tween 20 5% Skim milk powder
Luria-Bertani (LB)	1% Bacto trypton

medium	0.5% Bacto yeast extract 1% NaCl Ampicillin or Kanamycin
LB-agar plates	1% Bacto trypton 0.5% Bacto yeast extract 1% NaCl 1.5% Bacto agar Ampicillin or Kanamycin
FACS Sample Buffer	PBS (1X) 1% FBS
Freezing medium	90% FBS 10% DMSO
5X Laemmli Buffer	300mM Tris/HCl (pH 6.8) 50% Glycerol 10% SDS 5% β-Mercaptoethanol 0.05% Bromophenol blue
Separating Gel Buffer	1.5M Tris/HCl (pH 6.8)
Stacking Gel Buffer	0.5M Tris/HCl (pH 6.8)
Coomassie Staining Buffer	0.25% Coomassie brilliant blue 45% Methanol 10% Acetic acid
Coomassie Destaining Buffer	45% Methanol 10% Acetic acid
10X Oligo annealing buffer	500mM NaCl 100mM Tris-HCl 100mM $MgCl_2$

All Buffers were prepared with dH_2O, if not mentioned otherwise.

3.1.9 Molecular Biology Kits

Product	**Manufacturer**
Bio-Rad DC Protein Assay	Bio-Rad, Munich, Germany
GeneJET Gel Extraction Kit	Thermo Fisher Scientific, Waltham, US
LightCycler 480 SYBR Green I Master	Roche, Grenzach-Wyhlen, Germany
L-Lactate Assay Kit II	Eton Bioscience, San Diego, US
MMP7 Human ELISA Kit, RAB0369	Sigma-Aldrich, Taufkirchen, Germany
peqGOLD Plasmid Mini Kit I	PEQLAB Biotechnologie, Erlangen, Germany
QIAGEN Plasmid Maxi Kit	Qiagen, Hilden, Germany
QIAshredder Kit	Qiagen, Hilden, Germany

QIAGEN RNeasy extraction Kit	Qiagen, Hilden, Germany
Rapid DNA Dephos and Ligation Kit	Roche, Grenzach-Wyhlen, Germany
VEGF Human ELISA Kit, RAB0507	Sigma-Aldrich, Taufkirchen, Germany

3.1.10 Protein/DNA molecular weight standards

Product	**Manufacturer**
GeneRuler 1kb DNA Ladder	Thermo Fisher Scientific, Waltham, US
6X DNA Loading Dye	Thermo Fisher Scientific, Waltham, US
PageRuler Prestained Protein Ladder	Thermo Fisher Scientific, Waltham, US

3.1.11 Antibodies

Primary antibodies:

Antibody	**Rabbit/ mouse**	**Dilution**	**Manufacturer**
β-Actin	Mouse	1:10000 milk	Sigma-Aldrich, Taufkirchen, Germany
CD147 (8D6)	Mouse	1:200 milk	Santa-Cruz Biotechnology, Dallas, US
CD147 (MEM)	Mouse	1:1000 milk	Sigma-Aldrich, Taufkirchen, Germany
CD147	Rabbit	1:1000 milk	LifeSpan BioSciences Inc., Seattle, US
CRBN	Rabbit	1:5000 BSA	Produced for this study (immunizing peptides MAGEDQQDAAHNMGNHLPC and CPTIDPTEDEISPDK) by Innovagen, Lund, Sweden
CUL1	Mouse	1:500 milk	Life Technologies, Carlsbad, US
IKZF1	Rabbit	1:1000 BSA	Cell Signaling, Cambridge, UK
IKZF3	Rabbit	1:1000 BSA	Cell Signaling, Cambridge, UK
IRF4	Rabbit	1:1000 BSA	Cell Signaling, Cambridge, UK
MCT1	Rabbit	1:1000 BSA	Merck Millipore, Darmstadt, Germany
MCT4	Rabbit	1:5000 BSA	Santa-Cruz Biotechnology, Dallas, US
MMP7	Mouse	1:1000 BSA	R&D Systems, Minneapolis, US
VEGF	Rabbit	1:200 BSA	Santa-Cruz Biotechnology, Dallas, US

Table 4: List of primary antibodies

Secondary antibodies:

Antibody	**Manufacturer**
Anti-mouse IgG, horseradish peroxidase	GE Healthcare, Chalfont St. Giles, UK
Anti-rabbit IgG, horseradish peroxidase	GE Healthcare, Chalfont St. Giles, UK

Table 5: List of secondary antibodies

3.1.12 Plasmids

Plasmid	origin	Antibiotic resistance
peGFP_C3	Clontech, France	Kanamycin
pMI-dsRed	Kind gift of T. Brummer	Ampicillin
pMD2G	Kind gift of U. Keller	Ampicillin
psPAX	Kind gift of U. Keller	Ampicillin
pLKO.1 puro TRC cloning vector	AddGene, Cambridge, US	Ampicillin
pLKO.1 TRC cloning vector dsred	Cloned for this study	Ampicillin
sh-scramble pLKO.1 puro	AddGene, Cambridge, US	Ampicillin
sh-scramble pLKO.1 dsred	Cloned for this study	Ampicillin
shMCT1 pLKO.1 puro	Kind gift of D. Sabbatini	Ampicillin
shMCT1 pLKO.1 dsred	Cloned for this study	Ampicillin
shCRBN #1 pLKO.1 puro	Cloned for this study	Ampicillin
shCRBN #1 pLKO.1 dsred	Cloned for this study	Ampicillin
shCRBN #2 pLKO.1 dsred	Cloned for this study	Ampicillin
shCRBN #3 pLKO.1 dsred	Cloned for this study	Ampicillin
shCRBN #4 pLKO.1 dsred	Cloned for this study	Ampicillin
shCD147 pLKO.1 dsred	Cloned for this study	Ampicillin
shIKZF1 pLKO.1 dsred	Cloned for this study	Ampicillin
shIKZF3 pLKO.1 dsred	Cloned for this study	Ampicillin

Table 6: List of plasmids

3.1.13 Oligonucleotides (cloning, sequencing, qPCR, shRNA)

Oligonucleotides were synthesized by Eurofins MWG GmbH, Ebersberg Germany. “salt free” purity was used for oligonucleotides shorter than 30 base pairs (bp). Longer shRNA oligonucleotides were additionally purified by high performance liquid chromatography (HPLC).

Oligo	Sequence	Use
shCD147_fw (Arendt, 2012)	CCGGGTACAAGATCACTGACTCTGACTCG AGTCAGAGTCAGTGATCTTGTACTTTTTG	shRNA
shCD147_rv	AATTCAAAAAGTACAAGATCACTGACTCTG ACTCGAGTCAGAGTCAGTGATCTTGTAC	shRNA
shCRBN1_fw	CCGGGCTTGCAACTTGAATCTGATACTCGA GTATCAGATTCAAGTTGCAAGCTTTTTG	shRNA
shCRBN1_rv	AATTCAAAAAGCTTGCAACTTGAATCTGATA CTCGAGTATCAGATTCAAGTTGCAAGC	shRNA
shCRBN2_fw	CCGGGCCCACGAATAGTTGTCATTTCTCGA GAAATGACAACTATTCGTGGGCTTTTTG	shRNA
shCRBN2_rv	AATTCAAAAAGCCCACGAATAGTTGTCATT TCTCGAGAAATGACAACTATTCGTGGGC	shRNA
shCRBN3_fw	CCGGCGCTGGCTGTATTCCTTATATCTCGA GATATAAGGAATACAGCCAGCGTTTTTG	shRNA
shCRBN3_rv	AATTCAAAAACGCTGGCTGTATTCCTTATAT CTCGAGATATAAGGAATACAGCCAGCG	shRNA

shCRBN4_fw	CCGGCCAGAAACATCTACTTGGGTACTCG AGTACCCAAGTAGATGTTTCTGGTTTTTG	shRNA
shCRBN4_rv	AATTCAAAAACCAGAAACATCTACTTGGGT ACTCGAGTACCCAAGTAGATGTTTCTGG	shRNA
shIKZF1_fw	CCGGCTACGAGAAGGAGAACGAAATCTCG AGATTTCGTTCTCCTTCTCGTAGTTTTTG	shRNA
shIKZF1_rv	AATTCAAAAACTACGAGAAGGAGAACGAAA TCTCGAGATTTCGTTCTCCTTCTCGTAG	shRNA
shIKZF3_fw	CCGGGCCTGAAATCCCTTACAGCTACTCG AGTAGCTGTAAGGGATTTCAGGCTTTTTG	shRNA
shIKZF3_rv	AATTCAAAAAGCCTGAAATCCCTTACAGCT ACTCGAGTAGCTGTAAGGGATTTCAGGC	shRNA
sh-scramble_fw	CCGGCCTAAGGTTAAGTCGCCCTCGCTCG AGCGAGGGCGACTTAACCTTAGGTTTTTG	shRNA
sh-scramble_rv	AATTCAAAAACCTAAGGTTAAGTCGCCCTC GCTCGAGCGAGGGCGACTTAACCTTAGG	shRNA
DsRed_BamHI_fw	CCCGGATCCGCCACCATGGATAGCACTGA GAAC	Cloning
DsRed_KpnI_rv	CCCGGTACCCTACTGGAACAGGTGGTGG	Cloning
pLKO.1 dsred sequencing	CGCACGTCGGCAGTCGGCTCC	Seq.
pLKO.1 sh-insert sequencing	GATACAAGGCTGTTAGAGAGATAATT	Seq.
ARPPA_fw	GCACTGGAAGTCCAACTACTTC	qPCR
ARPPA_rv	TGAGGTCCTCCTTGGTGAACAC	qPCR
CD147_fw	GATCACTGACTCTGAGGACAAGGC	qPCR
CD147_rv	TGCGAGGAACTCACGAAGAACC	qPCR
CRBN_fw	ACAGCTGGTTTCCTGGGTATGC	qPCR
CRBN_rv	ACAGAGCAGATCGCGTTAAGCC	qPCR
MCT1_fw	TGGCTGTCATGTATGGTGGAGGTC	qPCR
MCT1_rv	GAAGCTGCAATCAAGCCACAGC	qPCR

Table 7: List of oligonucleotides

3.1.14 Bacteria

Bacteria	**Supplier**
NEB 5-alpha Competent *E. coli* (High Efficiency)	New England BioLabs, Ipswich, US

3.1.15 Software

Software	**Use**
FlowJo Version 10 OSX	FACS data analysis
GraphPad Prism 6	Statistical analysis
Image J	Quantification of Western Blots
MacVector 14	Sequencing data analysis
QuantPrime	qPCR primer design

3.2 Methods

3.2.1 Eucaryotic Cell culture

3.2.1.1 Culturing of cell lines

All cell lines were cultured at 37°C, 95% humidity and 5% CO_2. The adherent human embryonic kidney cell line HEK293T and human cervix carcinoma cell line HeLa were cultured on 6-15 cm plates with Dulbecco's modified Eagle's medium (DMEM). The multiple myeloma cell lines MM1S, U266, KMS12BM, RPMI8226, OPM2, AMO1, L363, INA6 and JJN3 were cultured as suspension cells in RPMI 1640 medium, in cell culture flasks or 6-well plates, depending on the experimental setting. DMEM and RPMI 1640 media were supplemented with 10% fetal bovine serum (FBS) and the antibiotics penicillin/streptomycin. Newborn calf serum was used instead of FBS to culture HEK293T cells. For MM cell culture, FBS was heated to 60°C for 60 minutes to reduce complement activity. Medium for the IL-6 dependent MM cell line INA6 was additionally supplemented with 2ng/ml human IL-6. Cell culture media were exchanged at least every 2-3 days, or when the pH indicator phenol red shifted to orange/yellow, indicating more acidic conditions. In addition, cells were split according to density, to achieve cell densities of 1.5-5 x 10^5 cells/ml for suspension cells and 40-80% confluency for adherent cells. To split suspension cells, cells were transferred to falcons and centrifuged for 4 minutes at 1200 rpm, followed by removal of the supernatant. Cells were resuspended in fresh medium and returned to original flask. Fresh flasks were used at least 1-2 times per week. To split adherent cells (HEK293T, HeLa), the medium was removed. After a brief wash with PBS, 1-2 ml of 1X trypsin-EDTA solution was dropped onto the plate, followed by an incubation at 37°C for 3-5 minutes to loosen cells from the plate. The cells were then collected with fresh medium to inactivate trypsin and transferred to falcons for centrifugation (4 min, 1200 rpm). After removal of the supernatant, cells were resuspended in fresh medium (6 ml for 6 cm-, 10 ml for 10 cm- and 20 ml for 15 cm-plates) and transferred to fresh plates. Cells that had been lentivirally infected (see below) were treated with special precaution. All media and cell culture plastic in contact with those cells were disposed in containers containing bleach for a minimum of 48 hours to inactivate viral residues. 14 days post infection cells were considered virus-free and therefore treated as usual.

3.2.1.2 IMiD-treatment of cells

For certain experiments the MM cell lines mentioned above were treated with the IMiDs lenalidomide, pomalidomide and thalidomide. Lenalidomide and thalidomide powder was dissolved in DMSO according to the manufacturers instructions to yield a stock of 500 mM. For some experiments, a stock of 1000 mM was mixed for thalidomide to allow for higher concentrations in cell culture. A 50 mM

stock solution was pepared for pomalidomide. The stocks were aliquotted to batches of 10-20 µl to reduce freeze/thawing effects. On the first day of MM cell time courses, cells were plated at a concentration of 150 000 cells/ml in 10 ml of medium containing different IMiD concentrations. For longer time courses, MM cells were centrifuged at least every 48 hours and expanded by resuspending the pellets in 15-20 ml (depending on growth rate) of medium containing fresh IMiDs to ensure full drug efficiency. Control samples were supplemented with corresponding amounts of DMSO in order to rule out any unspecific solvent-mediated effects.

3.2.1.3 Long-term storage of cells

To allow for long-term storage, cells were frozen in liquid nitrogen at -196°C. To prevent cell bursting or lysis, FBS was supplemented with 10% dimethyl sulfoxide (DMSO). Approximately $1x10^6$ cells were collected from a growing culture, centrifuged (4 min, 1200 rpm), resuspended in 1 ml of freezing medium and transferred to cryotubes. These were slowly cooled down by 1°C per minute to -80°C using freezing containers containing isopropanol. In a following step, cryotubes were transferred to a liquid nitrogen tank. To take cells back into culture, they were unthawed by resuspension in fresh medium. After centrifugation (4 min, 1200 rpm), the supernatant was quickly removed in order to prevent DMSO-mediated cytotoxicity and cells were transferred to plates/flasks in fresh medium.

3.2.1.4 Harvesting cells

To harvest cells for further experiments, cells were transferred to falcons with or without prior trypsinization depending on the cell type. After centrifugation (4 min, 1200 rpm) and removal of the supernatant, the pellet was washed in PBS and transferred to 1.5 ml tubes. After a quick-spin (10 sec, 14 000 rpm), PBS was removed and the pellet temporarily frozen at -80°C.

3.2.2 Hypoxia

Some experiments were carried out under hypoxic conditions to simulate the low oxygen levels of the bone marrow. To this end, we used a hypoxia-incubator that was kindly provided by Prof. Schilling's Lab for Plastic and Hand-surgery. The incubator was set to 1% O_2, 5% CO_2 and 37°C. MM cells were treated with lenalidomide or DMSO for a total of 96 hours and incubated at normoxic (21% O_2) conditions for the first 48 hours. After this, media were exchanged as described above and one set of cells was transferred to hypoxic conditions. Another batch of cells was placed in the hypoxia-incubator 24 hours prior to harvesting. A set of cells was kept at normoxic conditions for the entire 96 hours. Flasks with sealable lids were used to prevent reoxygenation during transport. To further minimize the exposure to oxygen, cells were harvested quickly in small batches and snap-frozen in liquid nitrogen, before being stored at -80°C.

3.2.3 Transfection

3.2.3.1 Calcium phosphate method

To transiently express genes for various purposes in HEK293T cells, these cells were transfected using the calcium phosphate ($CaPO_4$) method. (C. Chen, 1987; Kingston, 2003) Depending on the setting, up to 40 µg of plasmid DNA was diluted with 450 µl of dH_2O. 50 µl of 2.5 M calcium chloride ($CaCl_2$) was added to obtain a final concentration of 0.25 M $CaCl_2$. After a 5 minute incubation at room temperature (RT), 500 µl of 2X N,N-Bis(2-hydroxyethyl)taurine (BES) was added to the solution, while gently shaking the tube. After a 20 minute incubation at RT, allowing DNA-complex formation, the solution was added dropwise onto a 10 cm dish of HEK293T cells at 60-70% confluency. Cells were incubated with this mixture for 4 hours, allowing the DNA-complexes to enter the cells. Following this incubation, culture medium was exchanged and incubation continued for another 24-48 hours. Transfection efficiency could be assessed under the fluorescent microscope when using dsredExpress2 containing pLKO.1 vectors. In some experiments the peGFP vector was transfected into control cells to monitor transfection rates.

3.2.3.2 HiPerFect method

The HiPerFect method was used to silence protein expression via siRNA interference in HeLa cells. In brief, 2.4 µl of a 20 µM siRNA stock (corresponding to 600 ng siRNA) was diluted in 1 ml Opti-MEM serum-free medium. 40 µl of HiPerFect transfection reagent was added and the solution mixed by gentle vortexing. After a 15-minute incubation at RT, the solution was dropped onto HeLa cells followed by an overnight incubation. Media was exchanged the next day and Western Blot and Lactate analysis conducted 48 hours after transfection.

3.2.4 Lentiviral transduction

Since the transfection methods listed above can only be used for transient expression of DNA plasmids, we went on to produce lentiviral particles to infect and stably integrate sequences coding for shRNAs into the infected cell's genome.

3.2.4.1 Lentivirus production

HEK293T cells were used to produce lentiviral particles. They were seeded as usual to 60-70% confluency and transfected using the $CaPO_4$-method (see 3.2.3.1). The transfection solution contained the following plasmids:

Construct	Purpose	Amount
pLKO.1-construct	shRNA-coding	20 µg
psPAX	packaging vector	15 µg
psMD2.G	envelope vector	5 µg

Table 8: Plasmid-mix for lentiviral transduction

24 hours following the transfection, the medium was discarded and replaced by fresh medium matching the cell line to be infected. For instance, when planning to infect MM cells, RPMI 1640 medium was added to HEK293T cells for the final incubation. 48 hours post transfection, the medium was collected and filtered through a 0.45 µm syringe-filter to remove cellular debris. The lentivirus containing medium was used for immediate infection, or stored at 4°C for later usage.

3.2.4.2 Lentiviral infection

For lentiviral infection, $2x10^6$ cells were seeded onto 6-well plates in 1 ml of fresh medium. 2 ml of corresponding lentivirus containing medium was added. It has previously been described that Polybrene, a cationic polymer, increases infection rates significantly, when added to viral media (Davis, 2002). Therefore, polybrene was diluted with 1X PBS to 4 µg/µl from a 250 µg/µl stock solution and added to the cells to yield a final concentration of 8 µg/ml. To assess infection rates by flow cytometry or fluorescent microscopy, control cells were seeded in 3 ml of virus-free medium and supplemented with polybrene. The 6-well plates were then subjected to a 30-minute spin at 1000 rpm to further facilitate infection. Following this spin-infection, 1 ml of fresh medium was added to each well and cells were left to incubate with the lentiviral particles for another 24 hours. Cells were then centrifuged, virus-containing media was removed and cells resuspended in 10 ml fresh medium in T25 cell culture flasks. Western blot and lactate analyses were usually performed at 96 hours post spin-infection.

3.2.5 Proliferation analysis

To compare proliferation rates and detect changes in proliferation upon IMiD

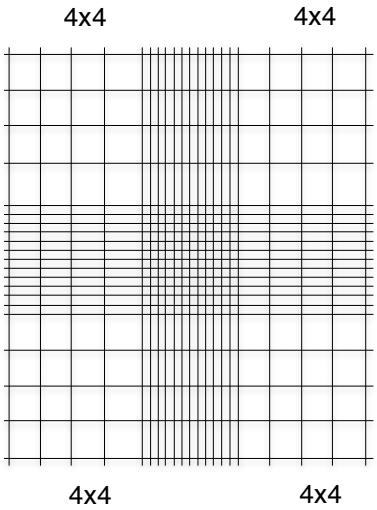

Figure 6: Schematic representation of a Neubauer hemocytometer under the microscope. To determine the number of cells in a given volume, Trypan Blue negative cells were counted in all four 4x4 squares (kept in white here). To finally calculate the number of cells, the following equation was used: $\boldsymbol{number\ of\ cells\ per\ ml} = \frac{\boldsymbol{cell\ count}}{\mathbf{2}} \times \mathbf{10^4}$

or shRNA treatment, viable cells were counted using the Trypan Blue exclusion method. Control cells, as well as cells treated with either IMiDs or shRNA were expanded at same ratios and were subjected to proliferation analysis at the times indicated in respective figures. At these time-points, cells were thoroughly mixed and a 50 µl sample was taken from each cell suspension for counting. 50 µl of Trypan Blue were added and thoroughly mixed. Viable (=brightly shimmering, Trypan Blue negative) cells were then counted under a microscope using a Neubauer hemocytometer (Fig. 6). Counting was always performed at least in duplicates. Relative ratios were then calculated by dividing cell counts of treated cells by cell counts of untreated control cells (DMSO or sh-scramble).

3.2.6 Flow cytometry

Flow cytometry is a method allowing analysis of specific cell surface markers or intracellular proteins on a single cell level. Lasers with specific wavelengths excite fluorochromes inside cells and can quantitatively detect their emission. At the same time, flow cytometers can determine cell size and granularity by measuring forward scatter (FSC) and sideward scatter (SSC), respectively. For the purpose of this project, flow cytometry was used to determine the infection rates of MM cells, after lentiviral infection with pLKO.1 shRNA constructs containing a DsRedExpress2 sequence, coding for a red fluorochrome with excitation and emission maxima of 554 and 591 nm, respectively. 4 days after spin-infection, 1 ml of MM cells were taken from the growing culture and centrifuged for 4 minutes at 1200 rpm. The supernatant was removed and the pellet washed with 1X PBS followed by another spin (4 min, 1200 rpm). The pellet was resuspended in 250 µl FACS-Buffer and analyzed with the FACSCalibur. Flow cytometry data were analyzed using the Flow-Jo software. After pre-gating in a FSC against SSC plot to exclude debris, the fraction of infected, fluorescent MM cells was measured using the FL3-H channel.

3.2.7 Cell lysis

To prepare whole cell extracts for protein or lactate analysis, cells were lysed with different buffers. A 250 mM NaCl buffer was used for lactate analysis. For protein analytics and Western Blotting, cells were lysed on ice in a 150 mM NaCl lysis buffer, supplemented with inhibitors to reduce the activity of proteases, kinases and other enzymes. Cell lysates were thoroughly mixed and incubated on ice for 20 minutes, followed by centrifugation for 20 minutes at 14 000 rpm and 4°C. The supernatant was transferred to fresh tubes on ice and protein concentration was measured using the Bio-Rad DC protein assay following the manufacturers instructions. After addition of 5X Lämmli buffer, the uncooked lysates were directly used for gel separation or stored at -20°C.

3.2.8 Protein analysis

3.2.8.1 SDS-Polyacrylamide Gel-Electrophoresis

Protein analytics were conducted as previously described (Bassermann, 2005; Baumann, 2014; Fernandez-Saiz, 2013). Proteins can be separated according to their molecular weight using SDS-Polyacrylamide Gel-Electrophoresis (SDS-PAGE). Coating of proteins with negatively charged SDS-containing Lämmli buffe results in denaturation. Therefore, if a charge is applied across the gel, proteins move towards the positively charged anode. Polyacrylamide gels were cast by radical polymerization of acrylamide with bisacrylamide. Addition of ammonium persulfate (APS) and tetramethylethylenediamine (TEMED) started the reaction. Polyacrylamide gels consist of two separate regions. Protein samples were loaded into pockets in the stacking gel, a gel with a greater pore size and a pH of 6.8. A protein ladder with colored bands at specific molecular weights was used as a marker. After passing through the stacking gel, proteins accumulate at the border to the following separating gel, which is characterized by smaller pores and a higher pH of 8.8, which leads to an overall negative charge of SDS molecules. While migrating through the separating gel, proteins are separated according to their size. Changing the concentration of acrylamide alters the resolution of the separating gel. A charge of 80V was applied for 15 minutes to allow migration through the stacking gel. After this, the voltage was raised to 150V for another 60 minutes until the samples completely passed through the gel.

3.2.8.2 Western Blotting

To immobilize proteins, they were transferred from polyacrylamide gels onto polyvinylidene fluoride (PVDF) membranes by wet Western Blotting. PVDF membranes were briefly activated in methanol. The set up of a wet blotting chamber can be seen in Figure 7. Up to two blotting cassettes were placed into a blotting chamber filled with blotting buffer. A charge of 100 V was applied for 1 hour. Alternatively, proteins were transferred at 30 V overnight. After blotting, membranes were stained with Ponceau S solution, a red dye solution that stains all proteins, to

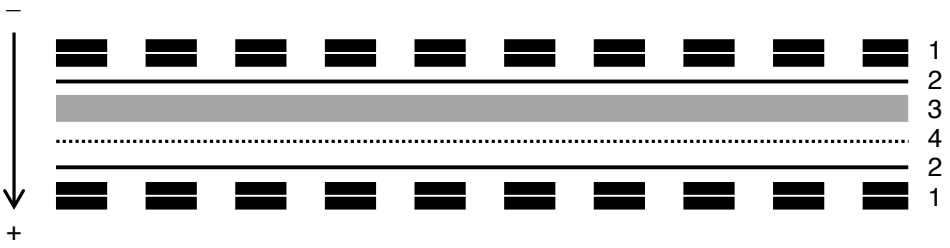

Figure 7: Western Blot cassette set-up. (1) Sponge, (2) Whatman paper, (3) Polyacrylamide gel, (4) PVDF membrane. After applying a charge, the proteins move towards the anode (+) and thus are transferred from the gel (3) to the membrane (4).

ensure equal loading. A representative Ponceau-stained membrane can be seen in Figure 8. Membranes were then cut into smaller stripes according to different molecular weights, to allow analysis of different proteins, and blocked in milk for 30 minutes to prevent unspecific antibody binding in the following steps. After blocking, membranes were incubated with protein specific primary antibodies overnight at 4°C. The next day, membranes were washed 3x10 minutes with washing buffer (WB) and incubated with matching secondary antibodies coupled to horseradish peroxidase in

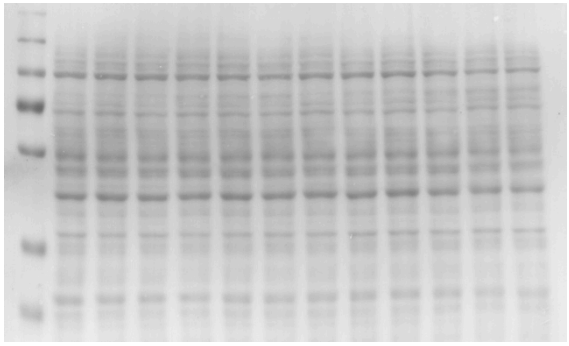

Figure 8: Representative Ponceau-stained PVDF membrane. Equal brightness of lanes signifies equal loading. A molecular weight marker was loaded in the first lane.

5% milk (1:5000) for 60 minutes at RT. Following 3x10 minutes washing with WB and short rinsing in 1X PBS, membranes were developed using enhanced chemiluminescent substrates pico and femto at ratios depending on the primary antibodies, and light-sensitive X-ray films. Enhanced chemilumicescence occurs when substrates emit a luminescent signal after reacting with horseradish peroxidase bound to the secondary antibody. Light-sensitive X-ray films then capture this signal. Quantification of developed Western Blots films was performed using ImageJ software.

3.2.9 Quantitative PCR

Quantitative PCR (qPCR) was used to determine changes in mRNA levels upon IMiD-treatment in MM cells. qPCR primers were designed using the internet-based public software QuantPrime. Cells were harvested as usual (see 3.2.1.4) and thawed from -80°C for RNA extraction. Cells were lysed and total RNA was extracted using QIAshredder columns and the Qiagen RNeasy extraction kit according to the manufacturers instructions. In the final step, RNA was eluted with 30 µl RNAse free dH_2O and total RNA concentration measured on a nano-spectrophotometer. RNA was either temporarily stored at -80°C or used directly for reverse transcription, a reaction where complimentary DNA (cDNA) is synthesized by an enzyme called reverse transcriptase using RNA as a template. In the first step of this reaction, 1 µg of RNA was diluted with dH_2O to a total of 17.5 µl and incubated with 1 µl of random hexamers for 5 minutes at 70°C to allow annealing. Random hexamers serve as primers for the reverse transcriptase in the following step. After cooling down to RT,

the reverse transcription was initiated following the manufacturers instructions. In brief, 6 µl of 5X reaction buffer, 3 µl 0.1M DTT, 1 µl 0.1M dNTPs, 0.5 µl RNAse Out and 1 µl SuperScript III reverse transcriptase were added and incubated with gentle agitation for 1 hour. The obtained total cDNA was diluted 1:10 with dH_2O and quantitative PCR performed using the SYBR Green kit according to the instructions. SYBR green intercalates into DNA molecules, therefore the intensity of green signal measured by the LightCycler is proportional to the amplified DNA. Before starting the reaction, 1 µl of forward and reverse sequence specific primers (10 pmol/µl), 3 µl dH_2O, 5 µl of diluted cDNA and 10 µl SYBR Green master mix were pipetted into each well on a 96-well plate. After sealing and briefly centrifuging the plate, the reaction was performed by running 30 PCR cycles on a LC480 LightCycler. Each sample was pipetted and measured in triplicates and results were normalized to the results of the stably expressed housekeeping gene ARPPA (acidic ribosomal phosphoprotein P0), using advanced relative quantification.

3.2.10 Lactate measurements

3.2.10.1 Extracellular lactate using L-lactate kit

In initial experiments, lactate was measured in cell culture supernatants of HeLa and MM cells, either treated with IMiDs or CRBN/CD147/MCT1 knockdown via siRNA/shRNA. $5x10^5$ cells were collected and washed 2x in PBS. In a first approach, the pellet was resuspended in 300 µl Opti-MEM medium and plated onto 96-well plates as previously described (Walters, 2013), while in various other approaches, $5x10^5$ cells were resuspended in 1 ml DMEM or RPMI medium lacking the pH-indicator phenol red and plated onto 12-well plates. Following a 3-hour incubation at 37°C, supernatants were collected and snap frozen in liquid nitrogen or immediately put on ice for subsequent lactate measurements. 500 µl supernatant were pipetted onto 30 kDa exclusion columns and centrifuged for 15 min at 14 000 rpm at 4°C to remove lactate dehydrogenase (LDH) from the samples. LDH has a molecular weight of 36 kDa and needs to be removed due to possible interference with the L-lactate assay kit. Samples were diluted 2-20 fold with medium and lactate concentration measured in duplicates following the manufacturers instructions. In short, 25 µl sample or lactate standard were incubated with 25 µl reagent for 30 minutes at 37°C. The colorimetric reaction was terminated by addition of 25 µl of 0.5 M acetic acid and absorbances were measured at 492 nm wavelength on a microplate reader. Absorbance values of lactate standards were used to plot a linear standard curve, from which individual values were calculated by interpolation.

3.2.10.2 Optimizing extracellular lactate measurements

In subsequent approaches, lactate concentrations were measured in collaboration with the Department of Clinical Chemistry on campus, with the kind

help of Prof. Luppa. Initial experiments showed that normal cell culture medium supplemented with FBS contained significant amounts of lactate. In addition to this, repeated measurements showed that the values obtained with the L-lactate kit were not accurate. Further experiments were, therefore, conducted mainly on the cobas8000 machine in the Department of Clinical Chemistry, which can measure lactate concentrations in the range of 0.2 to 40 mmol/l. Samples were thawed from -80°C and transported on ice to be measured immediately.

3.2.10.3 Intracellular lactate

To determine intracellular lactate concentration, MM cells were treated with lenalidomide or lentiviral shRNA-constructs as indicated in the respective figures. Cells were harvested and pellets lysed using the 250 mM NaCl lysis buffer (see 3.2.1.4 & 3.2.7). Whole cell extracts were kept on ice and measured on the cobas8000 in the Department of Clinical Chemistry. Intracellular lactate concentrations were normalized to protein concentration measured in the whole cell extracts of corresponding samples. Relative ratios were calculated by dividing normalized intracellular lactate concentrations of treated by untreated control cells.

3.2.11 VEGF/MMP7 ELISA

In order to assess changes in VEGF and MMP7 secretion by MM cells upon lenalidomide or lentiviral sh-treatment, we performed Enzyme-Linked Immunosorbent Assays (ELISA) specific to VEGF or MMP7 using commercially available ELISA kits according to the manufacturers instructions. In brief, supernatants of treated MM cells were collected at the times indicated in the figures and snap frozen in liquid nitrogen. For analysis, samples were unfrozen and diluted 1-4 fold, while protein standards were prepared by a series of dilutions with dH_2O. 100 µl of each sample and protein standard were pipetted in duplicates onto an antibody-coated ELISA plate and sealed for incubation overnight at 4°C, allowing complete binding of any VEGF/MMP7 in samples to the plate. The next day, samples and standards were removed and the plate washed 4x by rinsing wells with 300 µl wash buffer each, using a multi channel pipette. Next, 100 µl of a biotinylated VEGF or MMP7 detection antibody was added to each well, followed by a 60-minute incubation at RT. After a thorough wash as described above, 100 µl of Streptavidin coupled to horseradish peroxidase was added to each well, followed by a 45 minute incubation at RT. Streptavidin binds to the biotin molecule attached to the primary antibody, therefore horseradish peroxidase activity directly correlates with VEGF/MMP7 concentration of the sample. After another wash, 100 µl of horseradish peroxidase substrate solution was pipetted in each well. The plate was incubated at RT for 30 minutes and the reaction terminated by adding 50 µl of the Stop solution. Absorbances were immediately measured at 450 nm wavelength on a microplate reader. A standard curve was plotted using the absorbances of protein standards. VEGF/MMP7

concentrations of individual samples were calculated using the interpolation of non-linear standard curves function in GraphPad Prism. VEGF/MMP7 secretion was normalized to total protein concentration of corresponding samples and relative ratios calculated by dividing treated by untreated samples.

3.2.12 Design and Cloning of shRNA constructs

shRNA-mediated knockdown of specific proteins was done mainly following the instructions of The RNAi Consortium (TRC), based at the Broad Institute, Cambridge, Massachusetts, USA (Moffat, 2006).

3.2.12.1 Modifying pLKO.1 TRC cloning vector

The pLKO.1 TRC cloning vector is an 8901bp long lentiviral vector used to express shRNAs in human cells. It contains a spacer (1.9kb), located between the AgeI and EcoRI cutting sites, which needs to be removed prior to insertion of the shRNA oligo. Furthermore, it contains a puromycin resistance gene, which is located between the BamHI and KpnI cutting sites (Fig. 9). In order to reliably monitor infection rates, we replaced the puromycin resistance gene with the sequence of DsRedExpress2, which codes for a red fluorochrome.

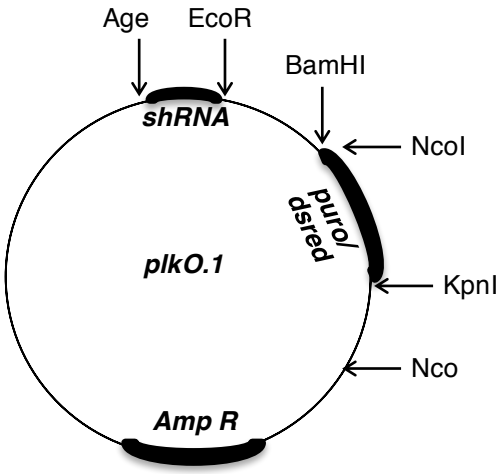

Figure 9: Simplified vector map of pLKO.1 construct. Restriction enzyme cutting sights are indicated with arrows.

3.2.12.2 Polymerase chain reaction

The 678bp DsRedExpress2 sequence was amplified using polymerase chain reaction (PCR), in which the vector pMI-dsRed served as template. 2 µl of template (100 ng/µl), 2 µl of each forward and reverse primers (10 pmol/µl), 2 µl dNTPs, 10 µl 10X Pfu buffer were mixed with 80 µl dH_2O and the reaction was started by adding 2 µl of the Pfu II ultra DNA polymerase.

PCR conditions were as follows: initial denaturation of 30s at 95°C, followed by 30 cycles of 30s denaturation at 95°C, 30s annealing at 55°C and 60s elongation at 68°C, followed by a final elongation step of 120s at 68°C and storage at 8°C. The amplified PCR products were then incubated with 11 µl 10X reaction buffer and 1 µl of DpnI-enzyme for 60 minutes at 37°C. DpnI degrades methylated template DNA. Samples were then purified using the gel extraction kit following the manufacturers instructions.

3.2.12.3 DNA restriction

Bacterial restriction enzymes can specifically recognize palindromic DNA sequences and cut DNA at these positions, creating overhanging ends. To replace the puromycin resistance sequence by the DsRedExpress2 sequence, both vector and amplified PCR product were cut by double digest with the enzymes BamHI and KpnI. Ideal reaction conditions for double digests can be derived from the Thermo Fisher Scientific homepage for all combinations of common restriction enzymes. Vector and insert were cut by incubation with 1 µl BamHI, 2 µl KpnI, 10X BamHI buffer for 90 minutes at 37°C.

3.2.12.4 Agarose gel electrophoresis

Agarose gels were cast by briefly cooking 1 g agarose in 100 ml Tris/Borate/EDTA (TBE) buffer. After addition of 6 µl ethidium bromide (EtBr), a fluorochrome, gels were left to cool down in desired forms. Digested DNA samples were supplemented with 6X DNA loading dye and loaded into sample pockets. By applying a 100 V charge for 60 minutes, DNA was separated according to size due to the negative charge of the DNA molecule. Because EtBr intercalates into the DNA, DNA was visualized under UV light and desired fragments were excised according to size (Fig. 10). DNA was extracted from the gel and purified using the gel extraction kit according to the manufacturers instructions. DNA concentrations were measured on a nano spectrophotometer.

3.2.12.5 Ligation

Purified vector and insert were ligated using the rapid ligation kit according to the manufacturers instructions. In brief, 50 ng vector, 150 ng insert and 2 µl DNA dilution buffer were diluted in dH_2O to a final volume of 10 µl, before mixing thoroughly with 10 µl T4 DNA ligation buffer. The reaction was started by adding 1 µl of T4 DNA ligase and incubating for 5 minutes at RT. Ligated DNA was either stored at -20°C or used for transformation immediately.

3.2.12.6 Bacterial transformation and culture

NEB5α competent high efficiency E.coli bacteria were used to amplify plasmid DNA. For transformation, 20 µl bacteria were unfrozen from -80°C, supplemented with 2 µl plasmid DNA and incubated for 30 minutes on ice. A heat

shock was performed by a 45 s incubation at 42°C, followed by another 2 minutes on ice. 500 µl of SOC recovery medium was added to the bacterial suspension, which was then incubated for 60 minutes at 37°C under gentle shaking. Samples were then centrifuged 3 minutes at 4000 rpm and 450 µl supernatant removed. The remaining medium was used to resuspend the pellet, which was subsequently plated onto LB agar plates, supplemented with the corresponding antibiotics (100 µg/ml ampicillin or 50 µg/ml kanamycin) and incubated at 37°C overnight. The next day, single colonies were picked and cultured overnight in 5 ml LB medium at 37°C under vigorous shaking. Plasmid DNA was extracted from 2 ml bacterial suspension using the peqGOLD plasmid mini extraction kit following the manufacturers instructions. DNA was subjected to test-restriction and agarose gel electrophoresis (see 3.2.12.3 and 3.2.12.4) to verify the integrity of the vector. DNA of positive clones was sent for sequencing (Eurofins MWG GmbH, Ebersberg) with corresponding primers to ensure appropriate integration of the insert. Sequences were verified using the alignment function of MacVector. Plasmid DNA was produced on a larger scale by incubating bacteria in 300 ml LB medium at 37°C overnight, and extracting DNA using the QIAGEN Maxi prep kit according to the manufacturers instructions.

3.2.12.7 Design and annealing of shRNA oligonucleotides

Specific shRNA sequences were derived from previous publications (see 3.1.13). Oligonucleotides (oligo) to be inserted into the lentiviral pLKO.1 TRC cloning vector were designed using the following templates:

fw oligo: 5' – CCGG – *21bp sense sh* – CTCGAG – *21bp antisense sh* – TTTTTG 3'
rv oligo: 5' – AATTCAAAAA – *21bp sense sh* – CTCGAG – *21bp antisense sh* – 3'

Oligonucleotides were dissolved in dH_2O to a final concentration of 100 pmol/µl by gentle shaking for 60 minutes at RT. To anneal oligonucleotides before cloning them into a vector, 1 µl of corresponding forward and reverse oligonucleotides, 5 µl of 10X annealing buffer and 43 µl of dH_2O were mixed and incubated at 95°C for 5 minutes. Next, the tubes were transferred to a flask containing 1l boiling water and let to cool down to RT for at least 4 hours.

3.2.12.8 Cloning sh-constructs

The DsRedExpress2-containing pLKO.1 vector was cut to remove the 1.9 kb spacer by double digestion with the enzymes AgeI and EcoRI with 10X Buffer O. Agarose gel electrophoresis, purification, ligation and transformation were carried out as described in sections 3.2.12.3 to 3.2.12.6. Test restrictions were performed by double digest with EcoRI and NcoI. The exchange of the puromycin resistance sequence with DsRedExpress2 resulted in the creation of a new NcoI cutting site.

Therefore positive clones showed three fragments of 5000 bp, 1250 bp and 750 bp length after test restriction (Fig. 10).

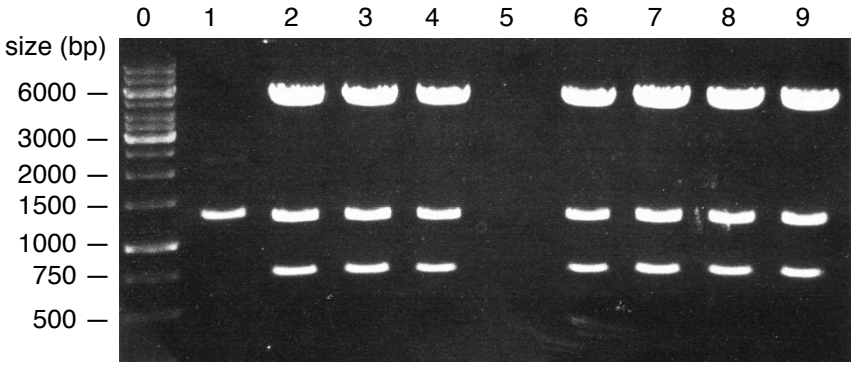

Figure 10: Representative image of sh-construct test restriction agarose gel electrophoresis. 2 x 4 samples were loaded onto a 1% agarose-gel and run at 100 V for 30 minutes. A marker is loaded in the far left lane. Numbers represent size of each marker lane in bp. Positive clones show 3 fragments of 750 bp, 1250 bp and 5000 bp. Therefore clones 2,3,4,6,7,8,9 were positive and sent for sequencing.

3.2.13 Statistical analysis

Statistical analysis was performed according to the experimental setting using GraphPad Prism software. One-sample t-tests were used to assess statistical significance of relative ratios. Regular Student's t-tests were used in case of absolute values. Most graphs show means ± SD. Significant results are shown by using the following representation: *: $P < 0.05$; **: $P < 0.01$; ***: $P < 0.001$; **** < 0.0001.

4 Results

This study is part of a larger collaborative project and mainly covers the biological and functional aspects of IMiD treatment in myeloma cells. Other aspects of the collaborative project are presented in the introduction and discussion sections. However, data in Figure 12b, obtained by Dr. med. Ruth Eichner, the supervisor of the submitting author, is integrated into the results section in order to improve comprehension and clarity of the study. This is indicated in the text and figure legend.

4.1 CRBN antibody testing

Because commercially available CRBN antibodies did not show satisfying sensitivity in Western Blot and low performance in the immunoprecipitation of CRBN, a polyclonal antibody against CRBN was generated by immunizing rabbits with a mixture of two peptides containing amino acids 1-19 and 424-437 of human CRBN (MAGEDQQDAAHNMGNHLPC and CPTIDPTEDEISPDK). In order to optimize the specificity of the newly generated, affinity-purified antibody for Western Blot application, whole cell extracts from untreated wt 293T cells were analyzed by SDS-PAGE and subsequent immunoblotting with the newly generated CRBN antibody at different dilutions in 5% milk or 5% BSA. Undiluted antibody stocks were stored at either 4°C, -20°C or -80°C. Figure 11a shows that best antibody performance was

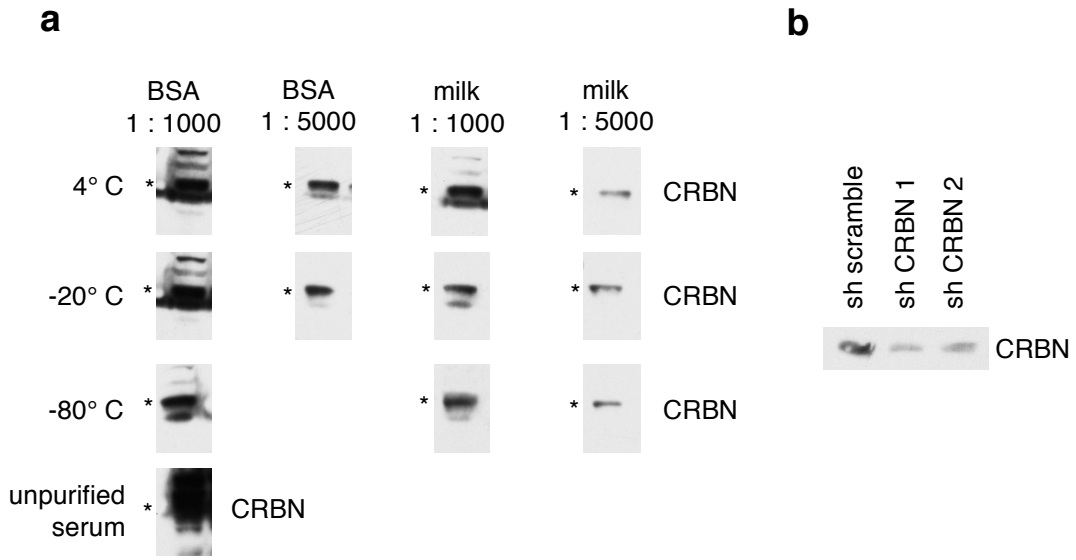

Figure 11: CRBN antibody testing. (a) Immunoblot analysis of whole cell extracts from untreated 293T wt cells with the generated polyclonal CRBN antibody. Identical samples were either loaded once or twice. Rows represent different storage conditions of the undiluted antibody. Columns represent different dilutions in 5% milk or 5% BSA. A control sample was probed with the unpurified rabbit serum diluted 1:2000 in BSA. An asterisk (*) marks the actual CRBN band. (b) Immunoblot analysis of whole cell extracts from MM1S , which were lentivirally infected with either scramble or CRBN-targeting shRNA constructs.

achieved at lower concentrations like 1: 5000. Even when using only the weaker SuperSignal West Pico Chemiluminescent Substrate developing solution and short exposure times, the use of 1:1000 dilutions resulted in unspecific signals right below the actual CRBN band. In addition, clearer blots were obtained by diluting the antibody in 5% milk as opposed to 5% BSA. All three storage temperatures (4°C, -20°C, -80°C) of the undiluted CRBN antibody showed similar results. Specificity of the antibody was ascertained by lentivirally knocking down CRBN with two independent shRNA constructs (Fig. 11b).

4.2 IMiDs destabilize CD147/MCT1 in MM cells

4.2.1 IMiDs destabilize CD147/MCT1 dose and time dependently

In order to assess the effect of IMiDs on CD147 and MCT1 in multiple myeloma cells, the IMiD-sensitive cell line MM1S was treated with increasing concentrations (1,25 µM to 100 µM) of lenalidomide for 72 hours (Fig. 12a). In a parallel approach, Ruth Eichner treated MM1S cells with a standard lenalidomide concentration of 10 µM for different periods of time, ranging from 6 hours to 96 hours (Fig. 12b). Control cells were treated with DMSO. Cells were harvested, lysed, and subjected to SDS-PAGE separation and immunoblot analysis. Western Blots showed a striking dose- and time-dependent decrease of CD147 and MCT1 protein levels in

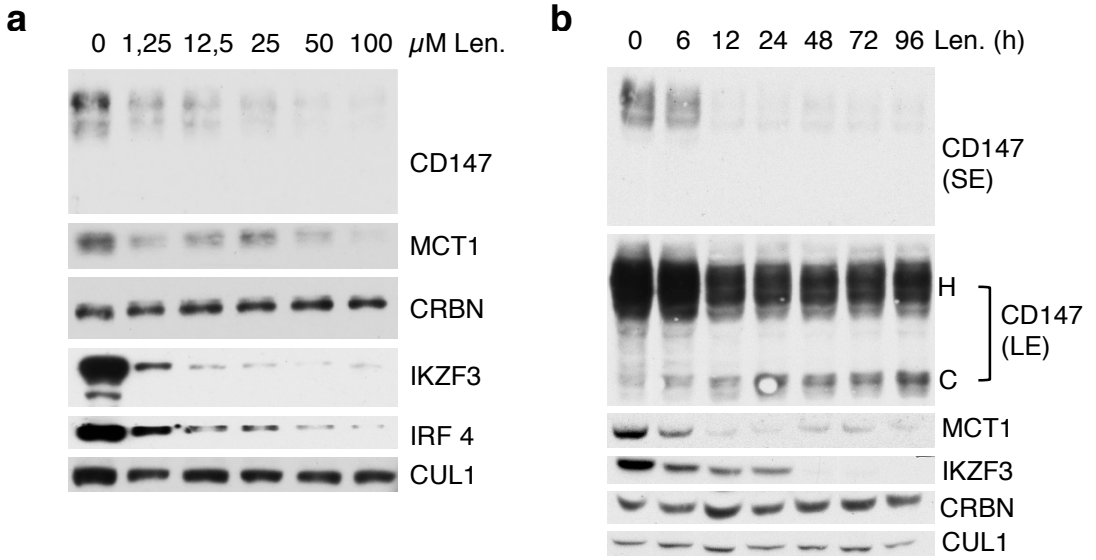

Figure 22: Lenalidomide treatment of MM cells decreases CD147 and MCT1 protein levels in a dose and time dependent manner. (a) Immunoblot analysis of MM1S cells, treated with the indicated concentrations of lenalidomide for 72 hrs. Whole cell extracts were probed with the indicated antibodies. (b) Immunoblot analysis of MM1S cells, treated with 10µM lenalidomide for the indicated length of time. Control cells were treated with DMSO. SE: short exposure, LE: long exposure, CG: core glycosylation, HG: high glycosylation. (Data in (b) provided by Ruth Eichner)

whole cell extracts upon lenalidomide treatment. These decreased protein levels could be observed after only 6 hours of lenalidomide treatment and with concentrations as low as 1,25 µM. IKZF3 levels served as controls, as IKZF3 has been reported to be degraded upon IMiD-treatment (A. K. Gandhi, 2014a; Kronke, 2014; Lu, 2014; Zhu, 2014). IRF4, which is upregulated in MM and decreases upon IMiD treatment, is shown as an additional positive control for IMiD efficacy (Lopez-Girona, 2011). In addition to the overall decrease of CD147 and MCT1 protein levels, in a longer exposure, an increase of the immature core-glycosylated form of CD147 could be observed upon lenalidomide treatment (Fig 12b).

4.2.2 IMiDs destabilize CD147/MCT1 on a post-transcriptional level

Next, we wanted to determine, whether the lenalidomide-induced decrease of CD147 and MCT1 protein levels occurs on a transcriptional or post-transcriptional level. Transcriptional modulation could, in theory, result from IMiD-induced inhibition of transcription factors, or activation of transcriptional repressors of CD147 and MCT1 genes. In order to investigate this, we measured CRBN, CD147 and MCT1-mRNA levels upon IMiD treatment. IMiD-sensitive MM1S and U266 cells were treated with 10 µM lenalidomide for 96 hours. DMSO treated MM1S and U266 cells served as control. After harvesting the cells, total RNA was extracted and subjected to RT-PCR using random hexamers. Quantitative PCR using CRBN, CD147 and MCT1 specific qPCR primers was performed and the detected mRNA abundance was normalized to ARPPA, a housekeeping gene. Compared to DMSO-treated control cells, lenalidomide-treated MM1S and U266 cells showed similar mRNA levels of MCT1, while CRBN and CD147 mRNA levels even proved to be elevated (Fig. 13). This suggests a post-transcriptional effect of IMiDs on CD147 and MCT1 protein stability, supporting the mechanism proposed by Eichner et al.

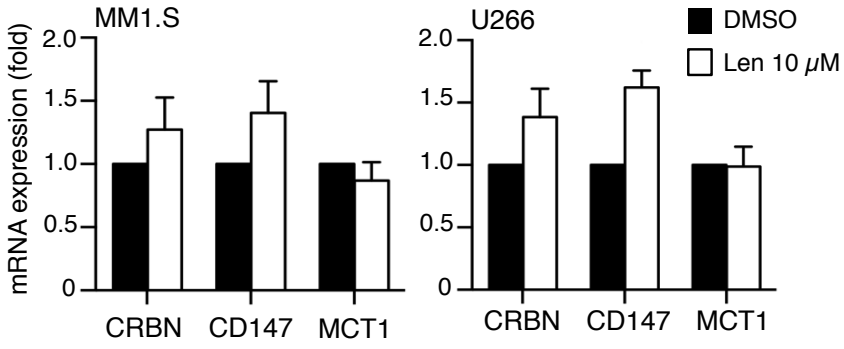

Figure 13: Lenalidomide-treated MM cells show similar or elevated CRBN, CD147 and MCT1 mRNA levels. MM1S (a) and U266 (b) cells were treated with 10 µM lenalidomide or DMSO for 96 hours. Indicated mRNA levels were measured by qPCR and normalized to ARRPA. The mRNA levels of DMSO-treated control cells were set to 1. Graphs show means ± SD of 3 independent experiments.

4.2.3 Lenalidomide reduces proliferation in IMiD-sensitive MM cells

Lenalidomide, as well as the other clinically available IMiDs thalidomide and pomalidomide have previously been shown to reduce proliferation in certain MM cell lines. Other cell lines have been shown to be resistant to the anti-proliferative effects of IMiDs (A. K. Gandhi, 2014b; Kronke, 2014; Lu, 2014). In order to reproduce these findings and establish both IMiD-sensitive and -resistant cell lines for further experiments in our lab, we chose the eight MM cell lines MM1S, U266, AMO1, L363, KMS12BM, RPMI8226, JJN3 and INA6. Each cell line was treated with 10 µM lenalidomide or DMSO as control for a total of 6 days (144 hrs). On days 4 and 6 (96 hrs. and 144 hrs.), proliferation was assessed by counting using the Trypan Blue exclusion method. We could confirm that MM1S, U266, AMO1 and L363 were

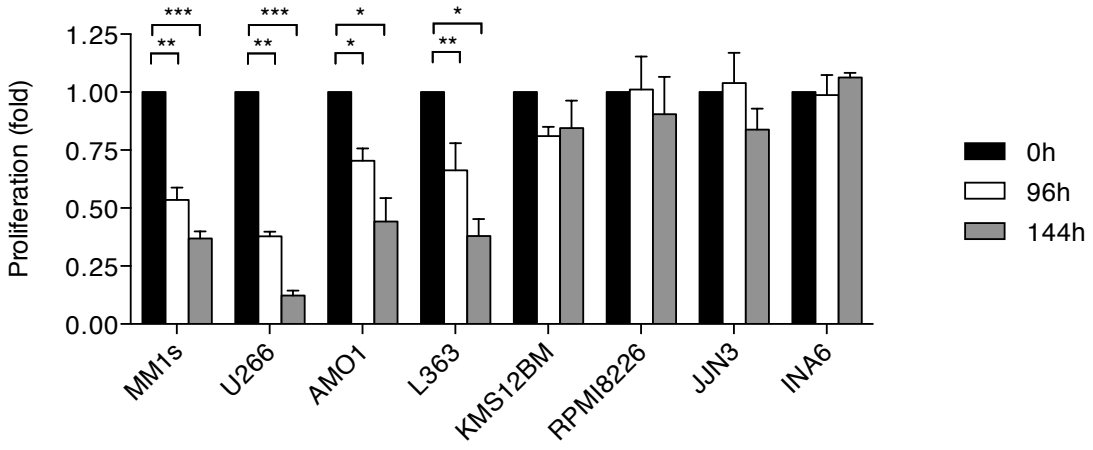

Figure 14: Lenalidomide reduces proliferation in certain MM cell lines. Indicated cell lines were treated with 10 µM lenalidomide or DMSO for 144 hrs. Cell proliferation was measured using Trypan Blue-exclusion cell counting at times indicated. Proliferation is shown as fold change relative to control cells. Graphs show mean ± SD of 3 independent experiments. Statistical analysis using a one sample t-test. *: $P < 0.05$; **: $P < 0.01$; ***: $P < 0.001$

lenalidomide-sensitive, as proliferation decreased significantly by 46.4% (MM1S), 62.1% (U266), 29.5% (AMO1) and 33.7% (L363) on day 4, and 63.1%, 87.7%, 55.8% and 62.1% on day 6, respectively. In contrast, KMS12BM, RPMI8226, JJN3 and INA6 cells showed no significant difference in proliferation under IMiD treatment compared to control cells. (Fig. 14)

4.2.4 CD147/MCT1 destabilization is limited to IMiD-sensitive cell-lines

Next, we wanted to check if the lenalidomide-induced CD147/MCT1 destabilization differs between the sensitive and resistant cell lines analyzed in chapter 4.2.3. In order to do so, lenalidomide-sensitive cell lines MM1S, U266, AMO1, L363 and -resistant cell lines KMS12BM, RPMI8226, JJN3 and INA6 were as described above and harvested, lysed and subjected to SDS-PAGE, followed by

Western Blot analysis. CD147 and MCT1 protein levels decreased in the four lenalidomide-sensitive cell lines MM1S, U266, AMO1 and L363, whereas no change could be observed in the resistant cell lines KMS12BM, RPMI8226, JJN3 and INA6. Interestingly, IKZF3 levels were decreased in both lenalidomide-sensitive and -resistant cell lines upon lenalidomide treatment. (Fig. 15) Taken together, these results show that destabilization of CD147 and MCT1 correlates with IMiD-sensitivity, suggesting that CD147 and MCT1 are critically involved in lenalidomide-mediated toxicity in MM cell lines.

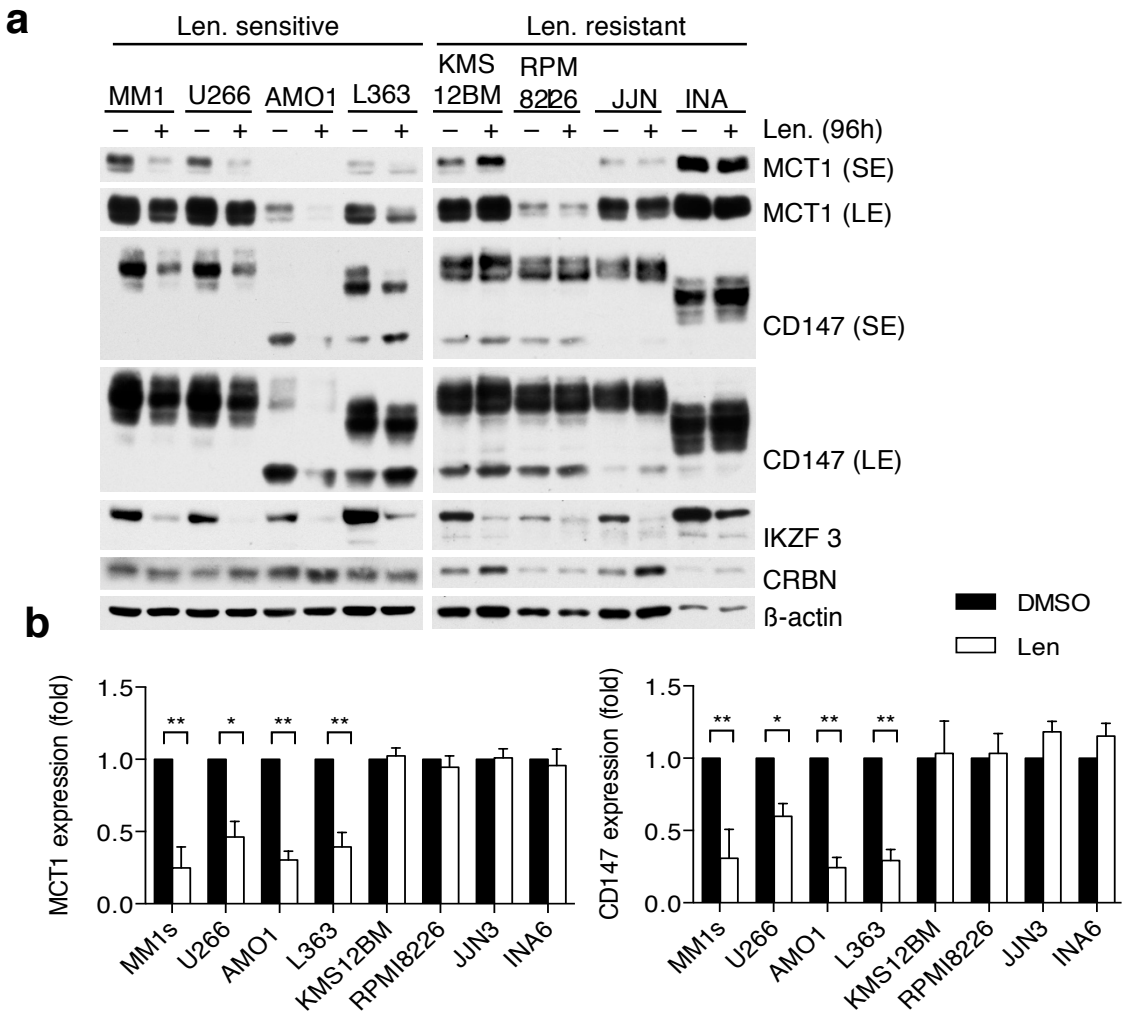

Figure 15: CD147/MCT1 destabilization is limited to lenalidomide-sensitive cell lines. (a) Immunoblot analysis of IMiD-sensitive (MM1S, U266, AMO1, L363) and -resistant (KMS12BM, RPMI 8226, JJN3, INA6) cell lines treated with 10 µM lenalidomide for 96 hours. Whole cell extracts were probed with the indicated antibodies. Representative blot of three independent experiments. (b) Quantification of Immunoblots presented in (a) averaged with two independent experiments. Graphs show mean ± SD; n=3. Statistical analysis using a one sample t-test. *: $P < 0.05$; **: $P < 0.01$.

4.2.5 CD147/MCT1 levels do not correlate with IMiD response

The identification of the CRBN/CD147/MCT1 axis could serve as a marker to predict response to IMiD treatment in a clinical setting. Low CRBN levels have previously been shown to correspond to poor IMiD sensitivity (A. K. Gandhi, 2014b; Zhu, 2011). We therefore wanted to check, whether on top of the predictive value of CD147/MCT1 destabilization (see 4.2.4), baseline protein levels of CD147 and/or MCT1 correlated to IMiD-sensitivity in several MM cell lines. We took samples from several growing cultures of MM cell lines, which have been described to be either IMiD-sensitive (U266, OPM2, MM1S) or -resistant (JJN3, KMS12BM, RPMI8226) (A. K. Gandhi, 2014b; Kronke, 2014; Lu, 2014). The expression levels of CD147 and MCT1 were diverging and we were unable to conclude any correlation between IMiD-response and baseline CD147 or MCT1 levels (Fig. 16). Of note, we could also not confirm any correlation of CRBN or IRF4 expression levels with IMiD sensitivity in the analyzed cell lines (Fig. 16).

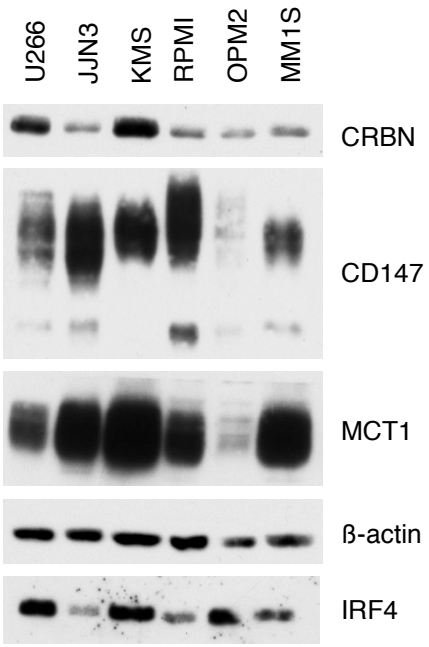

Figure 16: Baseline CD147/MCT1 levels do not correspond to IMiD-sensitivity. Immunoblot analysis of whole cell extracts from IMiD-sensitive (U266, OPM2, MM1S) and -resistant (JJN3, KMS12BM, RPMI8226) cell lines using the indicated antibodies.

4.2.6 CD147/MCT1 destabilization also occurs under hypoxic conditions

Multiple myeloma primarily is a disease of the bone marrow, which is characterized by local hypoxia (Colla, 2010; Parmar, 2007; Watanabe, 2007). Moreover, MCT1 is particularly important for the export of excess lactate generated during aerobic and anaerobic glycolysis (Halestrap, 2013). We asked, whether the lenalidomide-induced destabilization of CD147 and MCT1 also occurred under hypoxic conditions. This could be of relevance in assessing drug efficacy at its actual site of action. The IMiD-sensitive cell line MM1S was therefore treated with 10 µM lenalidomide or DMSO for 48 hours and incubated in 1% oxygen for 0, 24 and 48 hours to simulate hypoxic conditions. Cells were harvested and pellets snap frozen immediately after leaving the hypoxic incubator. They were lysed and subjected to SDS-PAGE and immunoblotting. A set of cells that had been incubated at hypoxic conditions for 96 hours showed severe signs of cell death under the microscope and therefore was excluded from further analysis. While overall CD147 and MCT1 levels

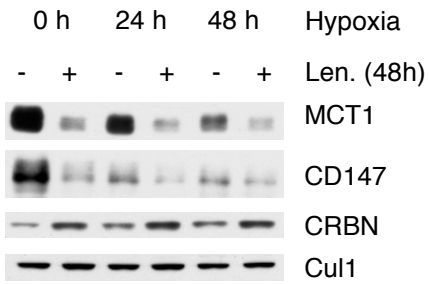

Figure 17: The lenalidomide-induced destabilization of CD147 and MCT1 is conserved under hypoxic conditions. Immunoblot analysis of MM1S whole cell extracts using the indicated antibodies. Cells were treated with 10 µM lenalidomide or DMSO for 48 hours and incubated at normoxic or hypoxic (1% O_2) conditions for different periods of time. The "24 h" cells were treated for 24 h in normoxia, followed by 24 h of hypoxia.

seemed to be reduced under hypoxic conditions, the destabilizing effect of lenalidomide on CD147 and MCT1 remained conserved (Fig. 17). This further underlines the importance of the CRBN/CD147/MCT1-axis in the treatment of multiple myeloma.

4.2.7 Thalidomide and pomalidomide also destabilize CD147/MCT1

Next, we sought to determine, whether the other two clinically established IMiDs thalidomide and pomalidomide show similar effects as lenalidomide. In analogy to previous experiments performed with lenalidomide, the sensitive MM cell line MM1S was treated with varying doses of thalidomide, lenalidomide or pomalidomide. All three established IMiDs destabilized CD147 and MCT1 levels in a dose dependant manner (Fig. 18). Thalidomide induced only a slight destabilization of CD147 at low doses, while higher concentrations could achieve similar effects to those observed with lenalidomide. Pomalidomide showed an even stronger destabilizing effect than lenalidomide (Fig. 18). The other known CRBN substrates IKZF1 and IKZF3 seemed to be only marginally affected by thalidomide. The fact that all three clinically established IMiDs have a common effect on CD147 and MCT1 suggests a common mechanism and general drug-class specific effect, while IKZF1 and IKZF3 are predominantly targeted by lenalidomide and pomalidomide.

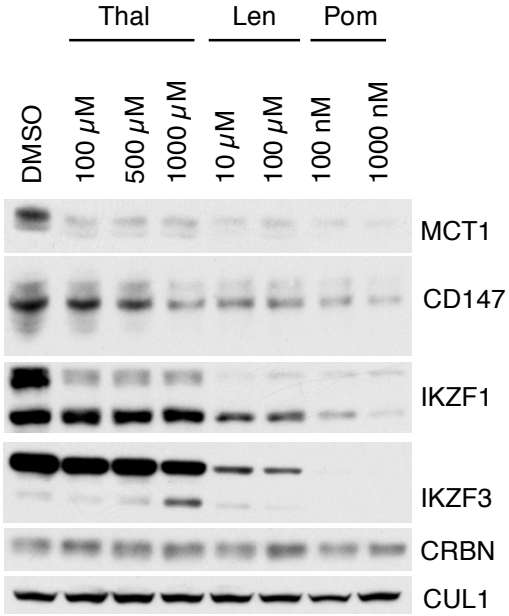

Figure 18: Thalidomide and pomalidomide also destabilize CD147/MCT1. Immunoblot analysis of MM1S whole cell extracts using the indicated antibodies. MM1S cells were treated with increasing concentrations of thalidomide, lenalidomide and pomalidomide (as indicated) for 96 hours.

This suits the current mechanistic model, in which only certain IMiDs modify CRBN to create an interface, which enables the degradation of IKZF1/3, while all IMiDs can outcompete CD147/MCT1 from binding to CRBN.

4.3 Knockdown of CRBN, CD147 and MCT1 leads to decreased proliferation of MM-cells

CRBN, CD147 and MCT1 have been previously identified to play an important role in MM cell proliferation. Low levels or knockdown of any of these proteins have been shown to reduce proliferation significantly (Arendt, 2012; Walters, 2013). However, this has only been shown in IMiD-sensitive cell lines.

4.3.1 Infection of myeloma cells with lentiviral shRNA constructs can be confirmed by flow cytometry

In order to validate existing data on the role of CD147 and MCT1 in MM cell proliferation, these proteins were knocked down using shRNA constructs, which were cloned into the lentiviral pLKO.1 TRC vector. In order to reliably assess infection rates, the originally included puromycin-resistance gene was replaced by cDNA encoding for DsRedExpress2, a red fluorescent protein. The infection rates could therefore easily be monitored using fluorescence microscopy or flow cytometry with

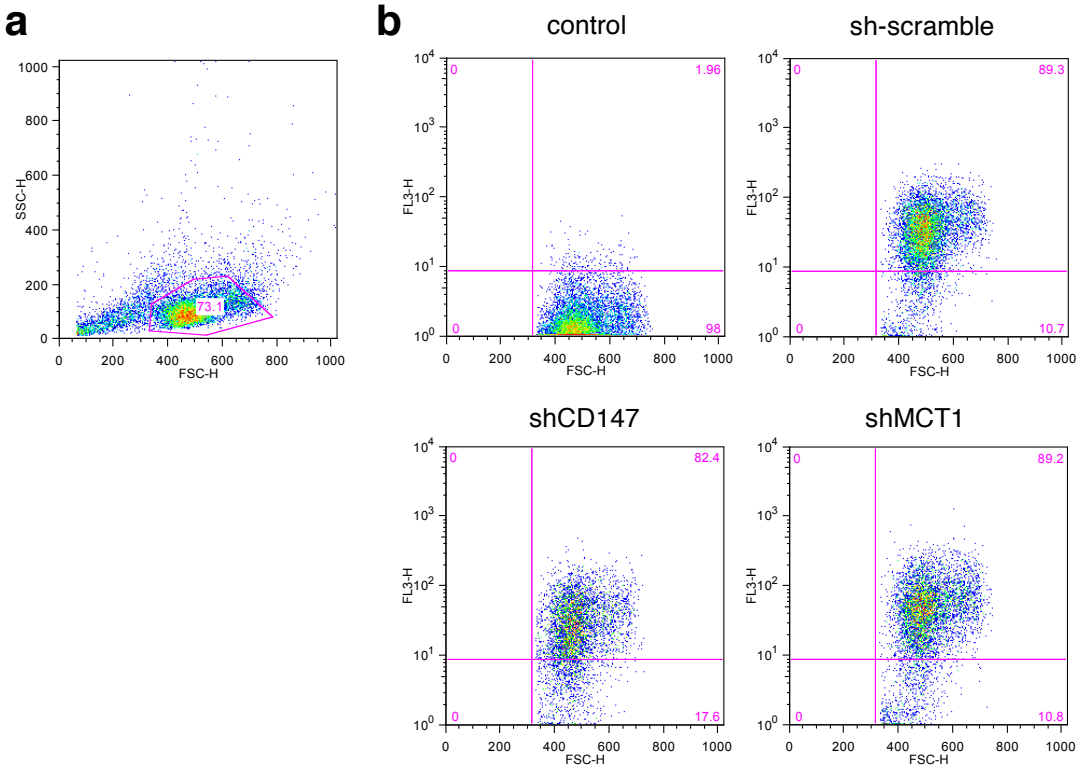

Figure 19: Lentiviral infection rates analyzed by flow cytometry. MM1S cells were infected with lentiviral sh-constructs containing a DsRedExpress2 sequence. Control cells were treated identically, only lacking the virus. (a) Representative flow cytometry plot, in which single cells were pre-gated in a sideward vs. forward scatter plot. (b) Representative plots of MM1S cells, infected with the indicated sh-constructs. The channel FL3-H, plotted on the y-axis, indicates the intensity of red fluorescence. Uninfected non-fluorescing control cells were used to set appropriate gates. Numbers in the top right corner of each plot show the percentage of fluorescent (= infected) cells.

uninfected cells serving as control. Optimization of infection protocols gave rise to a protocol including spin infection at 1000 rpm for 30 minutes and subsequent further incubation with virus for 24 hours, yielding infection rates above 80%. A set of representative flow cytometry data is shown in Figure 19. Cells were pre-gated in a forward vs. sideward-scatter plot to exclude debris (Fig. 19a). Within this gate, red fluorescence was measured in the FL3H channel, which measures red fluorescence. When setting an appropriate border range, infection rates of 89,3% (sh-scramble), 82,4% (shCD147) and 89,2% (shMCT1) were calculated in the experiment depicted (Fig. 19b).

4.3.2 Knockdown of CD147 and MCT1 decreases MM cell proliferation

Having achieved high infection rates in two IMiD-sensitive (MM1S, U266) and two -resistant (KMS12BM, RPMI8226) MM cell lines, we went on to verify the knockdown on protein level. For this purpose, MM cells were harvested four days

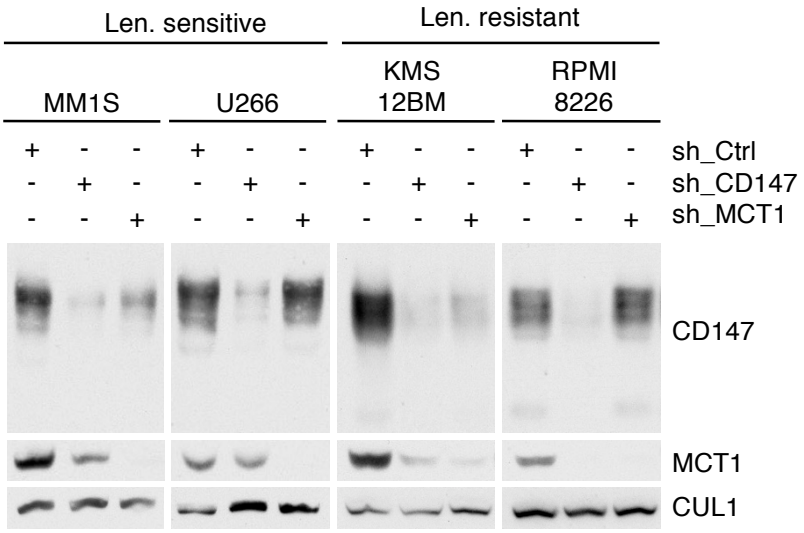

Figure 20: Knockdown of CD147 and MCT1 in MM cell lines. Immunoblot analysis of the lenalidomide-sensitive (MM1S, U266) and -resistant (KMS12BM, RPMI8226) MM cell lines on day 4 after lentiviral infection with the indicated specific shRNA-constructs. Control samples were infected with an sh-scramble sequence. Whole cell extracts were probed with the indicated antibodies.

after spin infection, lysed and subjected to Western Blot analysis. A convincing knockdown of CD147 and MCT1 protein levels could be observed in all four examined cell lines (Fig. 20).

In parallel, we continued to expand the infected MM cells in order to assess proliferation at a later time point. On day 8 after spin infection, cell samples were taken from the growing culture, counted using the Trypan Blue-exclusion method and related to cell counts of the control cells. Indeed, both the knockdown of CD147 and

MCT1 led to a significant decrease in proliferation relative to control cells, with an average decrease of 81,8% (MM1S), 77,2% (U266), 66,7% (KMS12BM) and 63,7% (RPMI8226) for CD147-knockdown and 62,8% (MM1S), 88,1% (U266), 59,7% (KMS12BM) and 49,2% (RPMI8226) for MCT1 (Fig. 21). Importantly, the knockdown affected the lenalidomide-resistant cell lines KMS12BM and RPMI8226 to a similar

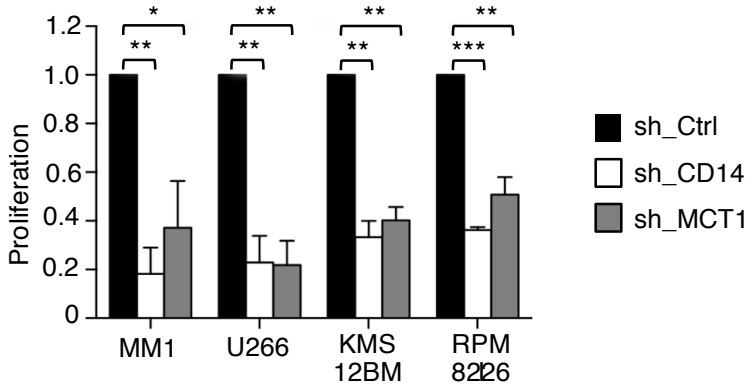

Figure 21: Knockdown of CD147 and MCT1 reduces proliferation in lenalidomide-sensitive and -resistant cell lines. Proliferation was assessed on day 8 after lentiviral infection with indicated shRNA constructs by Trypan Blue-exclusion counting in lenalidomide-sensitive (MM1S, U266) and -resistant (KMS12BM, RPMI8226) MM cell lines. Proliferation of control cells was set to 1. Graph shows means ± SD; n=3. Statistical analysis using a one sample t-test. *: $P < 0.05$; **: $P < 0.01$; ***: $P < 0.001$.

extent as the lenalidomide-sensitive lines MM1S and U266. This suggests that myeloma cells, even after having acquired resistance to IMiDs like lenalidomide, are still sensitive to depletion of CD147 and MCT1.

4.4 IMiDs influence MCT1-mediated lactate export

MCT1, a member of the family of monocarboxylate transporters, is responsible for the transport of lactate across the cell membrane. Many tumor cells rely on this mechanism to export excess lactate produced by anaerobic glycolysis (Halestrap, 2013; Le Floch, 2011). We thus hypothesized that IMiDs alter this transport system via destabilization of the CD147/MCT1 complex. So far, the only attempt to measure lactate in multiple myeloma cells revealed decreased extracellular lactate levels upon CD147 or MCT1 silencing, the difference was, however, not statistically significant (Walters, 2013). Thus, an important part of this project was to establish a reliable method to assess the impact of IMiDs and the role of CD147 and MCT1 for lactate transport in MM cell lines. Initial lactate measurements were performed using a lactate measuring kit. To improve the

accuracy of lactate analysis, later measurements were carried out using a cobas8000 (see also chapter 3.2.10).

4.4.1 Knockdown of CRBN and CD147 decreases lactate export in HeLa cells

To analyze lactate export, HeLa cells were transfected with siRNA specifically targeting CRBN, CD147 or Lacz as a control, in a first step. 48 hours after siRNA transfection, cells were counted and equal amounts of cells were incubated with fresh medium for another 3 hours. The extracellular lactate concentration in the medium was then measured using the lactate measurement kit. As expected,

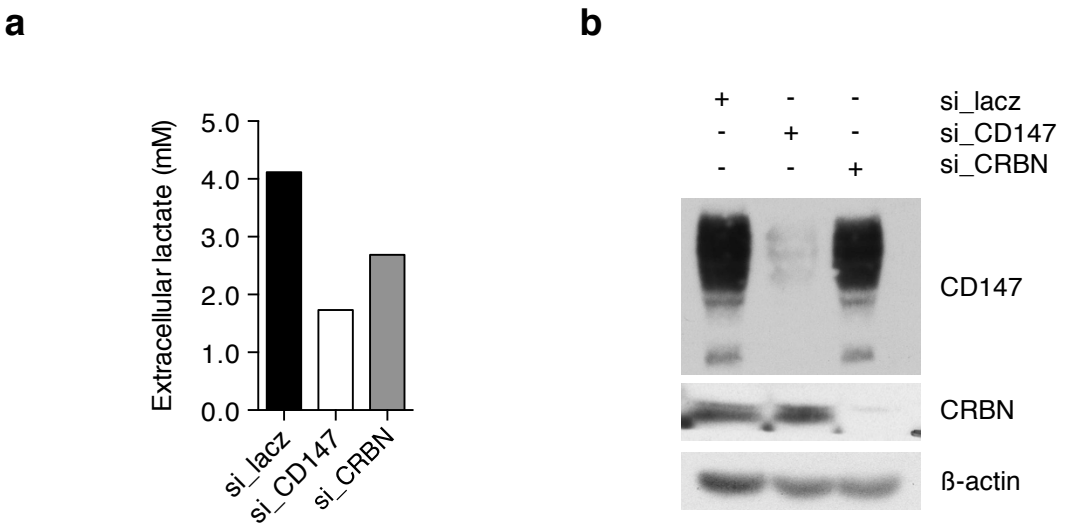

Figure 22: Knockdown of CD147 or CRBN decreases lactate export in HeLa cells. (a) Extracellular lactate measured in cell culture media supernatant of HeLa cells, 48 hours after having been transfected with the indicated siRNA constructs. The concentration of the control sample was set to 1. (b) Immunoblot analysis with the indicated antibodies of corresponding whole cell extracts.

extracellular lactate levels were found to be decreased in the supernatant of HeLa cells which had been transfected with siRNA targeting CD147 or CRBN, compared to those transfected with control siRNA (Fig. 22a). The decrease was 57,8% for siCD147 and 34,7% for siCRBN. In parallel, HeLa cells were harvested, lysed and subjected to SDS-PAGE and Western Blot analysis (Fig. 22b). A good knockdown of CRBN and CD147 could be observed, whilst the expected subsequent destabilization of MCT1 could not be shown, most probably due to preliminary difficulties in finding an ideal buffer to extract MCT1, a highly hydrophobic protein.

4.4.2 Lenalidomide treatment decreases lactate export

If downregulation of MCT1 via knockdown of CD147 or CRBN leads to impeded lactate transport across the cell membrane, this should likewise apply to IMiD-mediated destabilization of the CD147/MCT1 membrane complex. Since our model was established in multiple myeloma, we decided to conduct further lactate experiments in the MM cell lines mentioned above. The IMiD-sensitive cell line MM1S was treated with 10 µM, 100 µM lenalidomide or DMSO for 96 hours. Cells

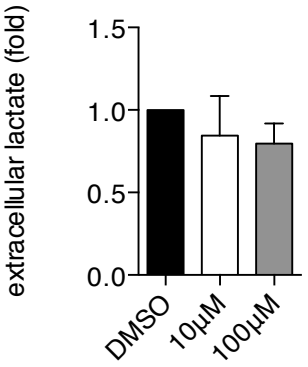

Figure 23: Lenalidomide treatment decreases lactate transport. Extracellular lactate levels of MM1S cells, treated with the indicated concentrations of lenalidomide for 96 hours. Lactate concentration of control sample, treated with DMSO, was set to 1. Graph shows means ± SD; n=3.

were then resuspended in fresh medium with lenalidomide or DMSO for another 3 hours, followed by harvesting of cells and supernatants and measurement of extracellular lactate. Extracellular lactate concentrations were decreased upon lenalidomide treatment by 15,5% for 10 µM and 21,4% for 100 µM lenalidomide compared to DMSO treated controls (Fig. 23). This proposes decreased lactate export as an additional effect of IMiDs on MM cells. The difference in extracellular lactate concentration was however not significant, because only a small proportion of the lactate in the medium originated from the cells.

4.4.3 Lenalidomide treatment of IMiD-sensitive cells increases intracellular lactate levels

To optimize the analysis of lactate export in MM cells, we next sought to measure intracellular lactate levels. In theory, by impeding MCT1-mediated lactate export across the cell membrane, lactate should accumulate inside the cells. In order to see whether lenalidomide treatment affects intracellular lactate concentrations, the lenalidomide-sensitive (MM1S, U266, AMO1) and -resistant (KMS12BM, RPMI8226, JJN3) MM cell lines were treated with 10 µM, 100 µM lenalidomide or DMSO for 96 hours. After harvesting, cells were lysed and lactate concentrations were measured in whole cell extracts using the cobas8000 instrument in the Department of Clinical

Chemistry. Indeed, intracellular lactate levels were significantly increased by on average 34.4% (MM1S), 25.1% (U266), 97.8% (AMO1) at 10 µM and 48.8%

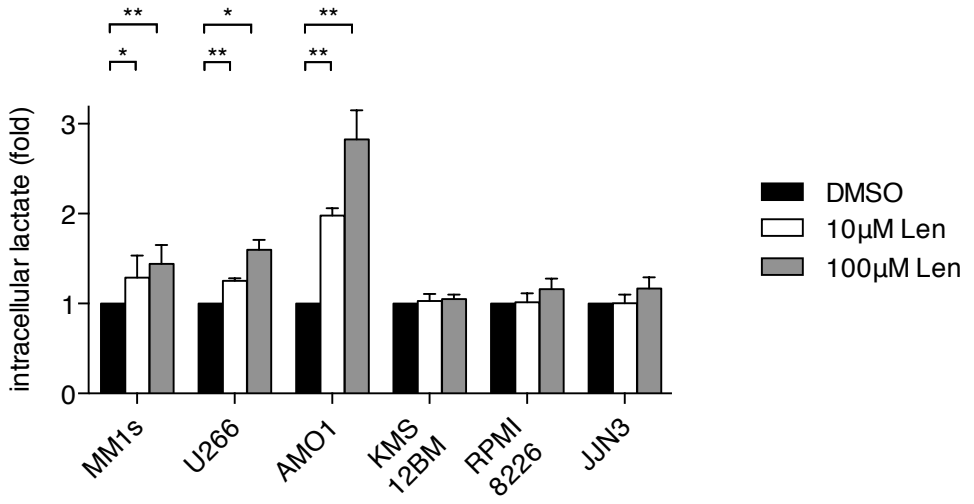

Figure 24: Lenalidomide increases intracellular lactate levels in IMiD-sensitive cell lines. Intracellular lactate concentrations in whole cell extracts of the lenalidomide-sensitive (MM1S, U266, AMO1) and -resistant (KMS12BM, RPMI8226, JJN3) MM cell lines. Concentrations of DMSO-treated control samples were set to 1. Graph shows means ± SD; n=5 (MM1S, RPMI8226); n=3 (U266, AMO1, KMS12BM, JJN3). Statistical analysis using one sample t-tests. *: $P < 0.05$; **: $P < 0,01$.

(MM1S), 59.7% (U266) and 282.3% (AMO1) at 100 µM lenalidomide in the sensitive cell lines, while no significant difference could be observed in the three resistant cell lines tested (Fig. 24). These results suggest that IMiD-induced destabilization of MCT1 indeed inhibits lactate export, thus adding a novel metabolic mechanism, by which IMiDs exert their anti-myeloma effects.

4.4.4 Knockdown of CRBN or MCT1 increases intracellular lactate levels

In order to prove the functional link between IMiDs, the CRBN/CD147/MCT1 axis and inhibition of lactate export in MM cells, we went on to measure intracellular lactate levels upon shRNA-mediated knockdown of CRBN or MCT1. A knockdown of these proteins should, in analogy to the IMiD effects and the effects in HeLa cells, lead to increased intracellular lactate levels. To verify this hypothesis, MM1S cells were infected with lentiviral shRNA constructs specifically targeting CRBN or MCT1 mRNA respectively or a scrambled control shRNA. Five days after lentiviral spin infection, cells were collected, lysed and subjected to intracellular lactate measurement and Western Blot analysis (Fig. 25). As expected, intracellular lactate levels were significantly increased in whole cell extracts from MM1S cells, which had been infected with shCRBN (19,8%) or shMCT1 (37,8%) constructs compared to

control cells. This finding provides a functional link between IMiD-induced destabilization of the CD147/MCT1 complex and MCT1-dependent lactate transport.

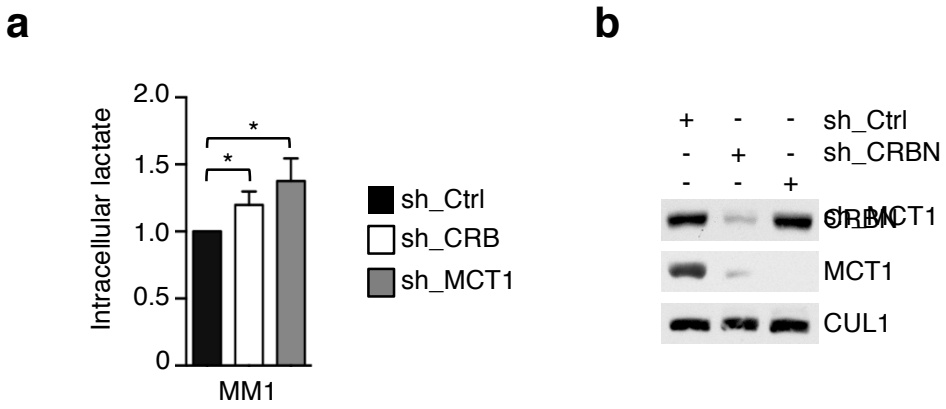

Figure 25: Knockdown of CRBN or MCT1 increases intracellular lactate levels. (a) Intracellular lactate levels in whole cell extracts of MM1S cells on day 5 following lentiviral infection with the indicated shRNA constructs. A scrambled shRNA sequence was used as control and lactate levels in control cells were set to 1. Graph shows means ± SD; n=4. Statistical analysis using one sample t-tests. *: $P < 0.05$. (b) Immunoblot analysis of samples presented in (a) to verify knockdown of CRBN and MCT1. Whole cell extracts were probed with the indicated antibodies.

4.5 IMiDs attenuate CD147-mediated secretion of pro-invasion and angiogenic factors

CD147 has previously been reported to play an important role in regulating the secretion of several pro-invasive and pro-angiogenic factors (Bougatef, 2009; Y. Chen, 2012; Tang, 2005; Xiong, 2014). On the other hand, IMiDs have been shown to be anti-angiogenic (D'Amato, 1994). We therefore hypothesized that IMiDs mediate their anti-invasive and anti-angiogenic effects by altering the secretion of pro-invasive factors like MMPs and angiogenic factors like VEGF, which have both been described to be secreted by MM cells (Borsi, 2015; Urbaniak-Kujda, 2016).

4.5.1 Lenalidomide treatment of IMiD-sensitive cells leads to decreased secretion of VEGF and MMP7

To substantiate this hypothesis, the multiple myeloma cell lines MM1S and AMO-1 (IMiD-sensitive) as well as RPMI8226 and KMS12BM (IMiD-resistant) were treated with 10 µM lenalidomide or DMSO for 96 hours. After a brief (3 hour) incubation in fresh medium, cell culture medium supernatants were collected in order to assess changes in MMP7 and VEGF secretion. MMP7 and VEGF concentrations in supernatants were measured using specific Enzyme-Linked Immunosorbent Assays (ELISA). Additionally, cells were harvested and lysed, and total protein

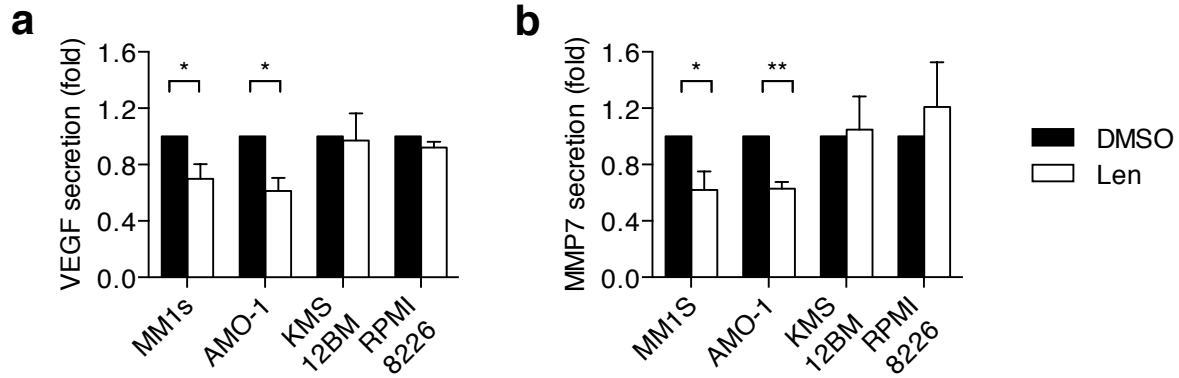

Figure 26: Lenalidomide reduces VEGF/MMP7 secretion in IMiD-sensitive MM cells. IMiD-sensitive (MM1S, AMO-1) and -resistant (RPMI8226, KMS12BM) MM cell lines were exposed to 10 µM lenalidomide for 96 hours as indicated. Control cells were treated with DMSO for the equal amount of time. (a) Concentration of VEGF in cell culture supernatants measured by ELISA. (b) Concentration of MMP7 in cell culture supernatants measured by ELISA. Concentrations of VEGF/MMP7 in control cells were set to 1. Graphs show means ± SD; n=3. Statistical analysis using one sample t-tests. *: $P < 0.05$; *: $P < 0.01$.

concentration was measured for normalization. In IMiD-sensitive MM cell lines, decreased concentrations of both MMP7 (38.2% in MM1S and 37.4% decrease in AMO1 cells) and VEGF (30.2% in MM1s and 38.8% decrease in AMO1 cells) could be observed in the supernatants upon lenalidomide treatment. As expected, this effect did not extend to the IMiD-resistant cell lines KMS12BM and RPMI8226, where concentrations of MMP7 and VEGF remained unchanged or even were elevated in the case of MMP7 (Fig. 26). This suggests that lenalidomide significantly alters the secretion of MMP7 and VEGF via destabilization of CD147 in IMiD-sensitive MM cell lines.

4.5.2 Knockdown of CRBN, CD147 and MCT1 leads to decreased secretion of VEGF

Next, we wanted to provide further evidence that the lenalidomide-induced decrease of VEGF secretion in MM cells is mediated via the CRBN-dependent destabilization of CD147 and MCT1. Therefore, CRBN, CD147 and MCT1 were individually knocked down via shRNA constructs. A scrambled shRNA construct was used as control. MM1S cells were lentivirally infected with the named constructs and cultured for 96 hours. Following a three-hour incubation in fresh medium, supernatants were collected and VEGF concentrations were measured using a specific VEGF-ELISA as in 4.5.1 In parallel, cells were harvested, lysed and protein concentrations were measured to normalize results. As anticipated, knockdown of

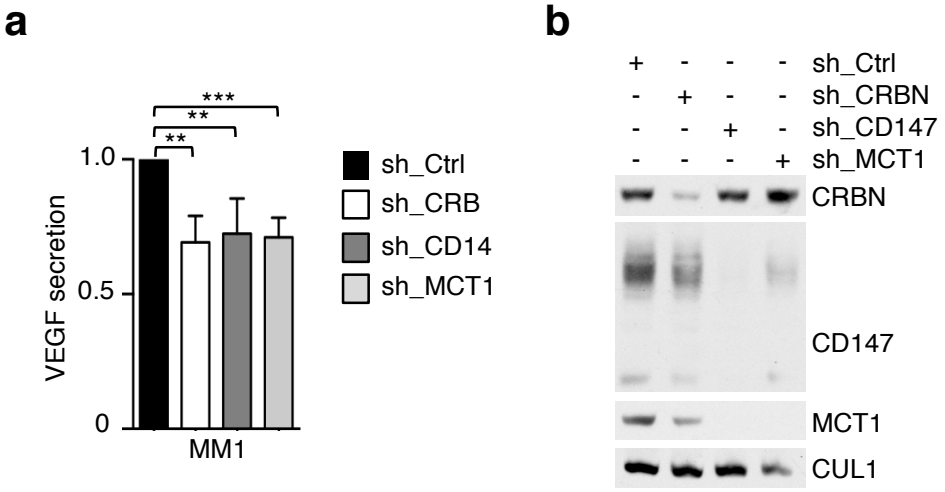

Figure 27: Knockdown of CRBN, CD147 or MCT1 decreases VEGF secretion. (a) VEGF concentration determined by ELISA in supernatants of MM1S cells 96 hours after lentiviral spin-infection with the indicated shRNA constructs. VEGF concentration in the control sample was set to 1. Graph shows means ± SD; n=5. Statistical analysis using one sample t-tests. **: $P < 0.01$; ***: $P < 0.001$. (b) Immunoblot analysis of samples presented in (a) to verify knockdown of CRBN, CD147 and MCT1. Whole cell extracts were probed with the indicated antibodies.

CRBN, CD147 and MCT1 individually lead to significantly decreased concentrations of VEGF in respective supernatants compared to control. The decrease amounted on average to 30.8% for shCRBN, 27.5% for shCD147 and 28.8% for shMCT1 (Fig. 27). These data further support the hypothesis that IMiDs reduce VEGF secretion in MM1S cells via destabilization of the CD147/MCT1 complex.

5 Discussion

5.1 Lenalidomide, thalidomide and pomalidomide destabilize CD147 and MCT1 post-transcriptionally

This study identifies CD147 and MCT1 as physiologically relevant CRBN-interacting proteins and characterizes their functional role in IMiD-sensitive and resistant MM cell lines. Lenalidomide reduced protein expression levels of CD147 and MCT1 in a dose- and time-dependent manner in IMiD-sensitive MM cell lines, while giving rise to unchanged or slightly elevated mRNA levels of CD147 and MCT1. These findings indicate a specific effect, which occurs independent of transcriptional regulation by the previously described IMiD-induced degradation of the lymphoid transcription factors IKZF1/3 (A. K. Gandhi, 2014a; Kronke, 2014; Lu, 2014; Zhu, 2014). The independence from IKZF1/3 degradation is further underscored by data showing unchanged CD147 and MCT1 levels upon RNAi mediated IKZF1/3 depletion in MM cells (Eichner, 2016). Furthermore, the present study reveals that thalidomide and pomalidomide, the other two established IMiDs, induce CD147 and MCT1 destabilization comparable to lenalidomide, which suggests a drug-class specific effect. By contrast, IKZF1 and especially IKZF3 levels were only mildly affected by thalidomide treatment in MM cells. Indeed, so far, thalidomide-induced degradation of IKZF1 only has been shown in the del(5q) MDS cell line MDS-L, while no effect could be observed in another del(5q) MDS cell line KG-1 (Kronke, 2015).

5.2 Destabilization of CD147/MCT1 mediates anti-myeloma activity of IMiDs

The present study shows that the IMiD-induced destabilization and inactivation of the CD147/MCT1 transmembrane complex mediates the various anti-myeloma effects of IMiDs, by directly reducing cell proliferation, as well as by inhibiting angiogenesis and invasion via decreased secretion of VEGF and MMP7. In line with our data, both CD147 and MCT1 have been previously implicated in MM biology and RNAi-mediated depletion of CD147 or MCT1 individually results in reduced proliferation of MM cells (Arendt, 2012; Walters, 2013). In addition, both CD147 and MCT1 are overexpressed in MM patients, compared to MGUS or healthy patients (Arendt, 2012; Walters, 2013).

CD147 is also known as an extracellular matrix metalloproteinase inducer and has been shown to mediate tumor invasion, growth, progression and metastasis by inducing MMP secretion (Biswas, 1995; Xiong, 2014). Indeed, MMPs likely play an important role in MM pathogenesis and disease progression, by mediating the infiltration of MM cells into bone and other tissues. Moreover, they induce the

remodeling of the extracellular matrix by activating bone marrow stromal cells (BMSC), as well as by activating osteoclasts to promote osteolytic bone destruction (Kelly, 2000). Several studies using patient-derived cells and co-culture models have shown that both BMSCs and MM cells themselves produce MMPs. Furthermore, the balance between MMPs and the specific tissue inhibitors of metalloproteinases (TIMP) seems to be shifted towards high levels of MMPs and lower levels of TIMPs in MM cells (Barille, 1997; Kaushal, 1999; Urbaniak-Kujda, 2016; Vacca, 1999; Zdzisinska, 2008). Our data is in line with the finding that thalidomide inhibits the production and activity of MMP2 and MMP9 in primary myeloma cells and other B-cell lines (Segarra, 2010). A recent study however, performed in human glioma, colon and lung adenocarcinoma lines and mouse embryonic fibroblasts, claims that the knock-out of CD147 does not influence the secretion and activity of MMPs, thus revoking the dogma and name-giving feature of CD147-induced MMP secretion (Marchiq, 2015). However, the investigators did not include MM cells, and even though many MMP subtypes, such as MMP2, MMP3, MMP9, MMP9, MMP11 and MMP13 were measured, MMP7, the read-out used in the present study, was not analyzed (Marchiq, 2015). The finding that both IMiD-treatment and CD147-knockdown lead to decreased MMP7 levels is further substantiated by a murine xenograft experiment with MM1S cells, which shows reduced MMP7 staining in immunohistochemical analysis of tumors from lenalidomide treated mice, or CD147/MCT1 depleted tumors (Eichner, 2016).

Apart from MMPs, this study shows that lenalidomide as well as knockdown of CD147 or MCT1 reduces the secretion of VEGF, thus suggesting that lenalidomide-induced inhibition of angiogenesis is mediated by destabilization of the CD147/MCT1 complex. This is relevant for the following reasons: First, active MM and MGUS are characterized by a high degree of angiogenesis and high microvessel density is associated with disease progression (Vacca, 1994). Indeed, tumor induced angiogenesis is associated with reduced event-free survival, overall survival and median duration of reponse (Munshi, 2001). VEGF, a key regulator of angiogenesis and endothelial cell migration, is highly expressed and actively secreted both in MM cell lines and MM patient samples (S. Kumar, 2003). The corresponding receptors vascular endothelial growth factor receptor 1 (VEGFR) and VEGFR2 are additionally expressed in MM cells, suggesting autocrine stimulation (S. Kumar, 2003). Moreover, Dankbar and colleagues propose a paracrine stimulatory loop between MM cells and BMSCs. This group has shown that MM cells secrete active VEGF, which stimulates BMSCs to release interleukin-6, which in turn stimulates MM cells to proliferate and produce more VEGF (Dankbar, 2000). Apart from its stimulatory effects on bone marrow angiogenesis and endothelial cell migration, VEGF also directly promotes MM cell migration via protein kinase C and MM cell proliferation via Raf-1, MEK-1 and ERK signaling (Podar, 2001). Blocking VEGF is an attractive therapeutic

strategy that is successful in various types of cancer. Accordingly, pre-clinical studies have documented the effectiveness of a VEGF-directed pan-receptor inhibitor in MM cells (Podar, 2004). However, while demonstrating good tolerability and achievement of adequate plasma drug levels, several phase II clinical trials with different small molecule VEGF-inhibitors or the clinically established VEGF-antibody bevacizumab have failed to show relevant clinical efficacy in relapsed or refractory MM (Kovacs, 2006; Prince, 2009; Somlo, 2011; White, 2013; Zangari, 2004). Second, in line with our data, a number of studies have linked CD147 to VEGF expression and secretion. CD147 interacts and co-localizes with VEGFR2 in human endothelial cell lines, melanoma cell lines and in different cancer tissues *in vivo* and is required for VEGF-induced VEGFR2 activation and signaling (Khayati, 2015). Furthermore, CD147 positively regulates VEGF production, both on mRNA and protein level, and stimulates tumor angiogenesis *in vivo* (Tang, 2005). The CD147-promoted secretion of soluble VEGF occurs independently of MMPs and is in part mediated by an upregulation of HIF2α (Bougatef, 2009). In a co-culture model of hepatocellular carcinoma cells with human umbilical vein endothelial cells (HUVEC), CD147 induces the secretion of VEGF and insulin-like growth factor 1, as well as the formation of neo-vasculature, proliferation, migration and tube formation of HUVECs (Y. Chen, 2012). Third, IMiDs have been described to exert anti-angiogenic activity. Orally administered thalidomide inhibits basic fibroblast growth factor triggered angiogenesis in a rabbit cornea micropocket assay and this anti-angiogenic potential has been linked to its teratogenic effects (D'Amato, 1994). In a murine cornea model, specifically the S(-)-enantiomer of thalidomide also reduces VEGF-induced neovascularization independent of thalidomide-induced reduction of TNFα (Kenyon, 1997). The anti-angiogenic activity also extends to lenalidomide, which inhibits microvessel formation in a rat aorta assay and a HUVEC angiogenesis assay (Dredge, 2002). Furthermore, lenalidomide inhibits vascularization *in vivo* in a dose-dependent manner and attenuates growth factor-induced endothelial cell migration (Dredge, 2005). In the context of MM, thalidomide and pomalidomide reduce the secretion of VEGF in MM cell lines, BMSCs and in co-culture of MM cells with BMSCs (Gupta, 2001). In line with our results, Gupta and colleagues have demonstrated that pomalidomide significantly reduces VEGF secretion in IMiD-sensitive U266 cells, while only a minor difference was seen in the IMiD-resistant cell line RPMI8226. In contrast to our data, they did not observe any change in VEGF levels in another IMiD-sensitive cell line MM1S (Gupta, 2001). This could be explained by the different techniques used, the use of pomalidomide instead of lenalidomide, the use of other ELISA kits or different subclones of MM1S cells. Indeed, they measured VEGF concentrations in supernatants after 48 hours of incubation, while in this study MM cells were incubated in fresh medium for 3 hours after 96 hours of initial incubation.

Taken together, this study demonstrates that IMiDs exert their anti-myeloma activity partly by inhibiting angiogenesis and invasion through decreased levels of MMP7 and VEGF, two well-described oncogenic effectors downstream of CD147 via destabilization of the CD147/MCT1 complex.

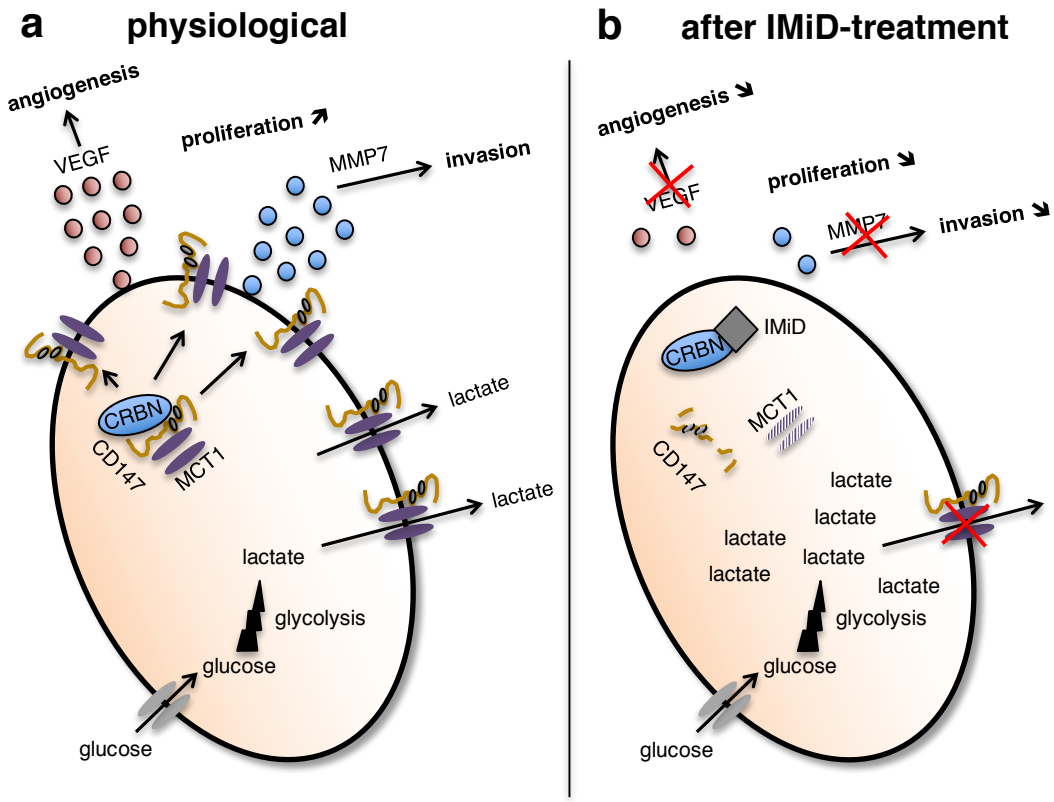

Figure 28: IMiDs mediate their anti-myeloma activity through destabilization of the CD147/MCT1 complex. Schematic representation of the proposed mechanism. a) Under physiologic conditions, CRBN promotes proper formation of the CD147/MCT1 membrane complex, which regulates lactate export, MMP7 and VEGF secretion, leading to proliferation, invasion and angiogenesis. b) Binding of IMiDs to CRBN abrogates the interaction with CD147/MCT1 and proper complex formation. Lactate accumulates in the intracellular compartment and secretion of MMP7 and VEGF is reduced, leading to a reduction of proliferation, invasion and angiogenesis. red spheres = VEGF, blue spheres = MMP7, grey square = IMiD

5.3 Metabolic alteration as new IMiD function

Importantly, this study establishes metabolic alteration via disruption of MCT1-mediated lactate transport as a previously unknown function of IMiDs. As many other tumors, MM has been described to employ aerobic glycolysis as a source of energy (Fujiwara, 2013). MM cells overexpress glycolytic enzymes and produce significantly higher amounts of lactate compared to normal peripheral-blood

mononuclear cells (Sanchez, 2013). Inhibition of glycolysis by dichloroacetate suppresses MM cell proliferation and induces superoxide production as well as apoptosis (Sanchez, 2013). In agreement with our results, MCT1 has previously been shown to be involved in lactate transport in MM cells and specific inhibition of MCT1 has been shown to be cytotoxic (Fujiwara, 2015; Walters, 2013). Walters and colleagues have shown that RNAi-induced silencing of MCT1 or CD147 leads to a decrease of extracellular lactate levels and increased extracellular pH. Their findings were not statistically significant, however, they are in line with data of this study, which shows that depletion of CD147 or MCT1 in MM cells significantly increases intracellular lactate levels (Walters, 2013). To our best knowledge, this is the first report that IMiDs alter lactate transport, via the disruption and inactivation of the CD147/MCT1 membrane complex, thus leading to increased intracellular lactate levels. This adds metabolic alteration as a previously unknown function of IMiDs in MM. Of note, MM cells treated with glycolysis inhibitors show increased sensitivity to proteasome inhibitors, such as bortezomib (Sanchez, 2013). This is in agreement with the clinical observation that IMiDs show strong synergistic effects with the proteasome inhibitors bortezomib, carfilzomib, ixazomib and marizomib (Das, 2015; S. K. Kumar, 2014a; Richardson, 2010; Roussel, 2014; Stewart, 2015).

The identification of lenalidomide-mediated inhibition of MCT1-associated lactate export nevertheless raises several questions regarding lactate metabolism in the context of MM. First, most studies suggest that cancer cells employ aerobic glycolysis (the so called Warburg Effect) to obtain energy and accumulate intracellular lactate, which needs to be removed from the cytoplasm via MCTs (Liberti, 2016). However, there is evidence that cancer cells can also import lactate via MCTs and utilize it for oxidative metabolism (Bouzier, 1998b). Nuclear magnetic resonance spectroscopy studies in glioma cells have demonstrated that even though these cells exhibit a net lactate production via glycolysis and lactate export, they also import exogenous lactate as a major source for oxidative metabolism, which implies the existence of two functionally different pools of lactate (Bouzier, 1998a). Indeed, a recent study in MM cells using radioactively labeled ^{14}C-lactate suggests that MM cells not only produce lactate, but also incorporate exogenous lactate from the microenvironment via MCT1. In line with our results, the inhibition of MCT1 by RNAi was cytotoxic in this study (Fujiwara, 2015). Based on their studies in human cervix squamous carcinoma cell lines, Sonveaux and colleagues propose a model in which tumors with a heterogeneous O_2-distribution consist of lactate exporting hypoxic cells, performing mainly glycolysis, and well oxygenated cells that take up excess lactate to facilitate oxidative metabolism (Sonveaux, 2008). This process of lactate exchange has been termed metabolic symbiosis or reverse Warburg Effect (Doherty, 2013). A similar mechanism could be envisioned for MM, as oxygen tension has been described to vary within the bone marrow (Parmar, 2007). However, several

reports confirming low oxygen tension in the bone marrow microenvironment *in vivo* support the theory that MM cells mainly perform glycolysis and rely on MCTs for lactate export, as demonstrated in our experiments (Colla, 2010; Watanabe, 2007).

Second, due to its high abundance in the mass spectrometric analysis of the CRBN interactome, the present study focused on MCT1 as representative of the MCT family. Preliminary data, which has not been included in this study, however, suggests that IMiDs also destabilize MCT4 to a similar extent. MCT4, another isoform from the monocarboxylate transporter family, is also described to function as a lactate transporter and is up-regulated via HIF-1α under hypoxic conditions (Ullah, 2006). IMiD-induced destabilization of MCT4 is conceivable, since maturation of MCT4 is also described to be CD147-dependent (Kirk, 2000). Based on enzyme kinetics data showing significantly higher lactate affinity of MCT1, MCT1 has traditionally been attributed the function of lactate importer and MCT4 of lactate exporter (Kennedy, 2010). However, inhibition of lactate export can be achieved by blocking either MCT1 or MCT4 or both, resulting in reduced growth of fibroblasts. In addition, the inhibition of one specific transporter can be compensated by upregulation of the other (Le Floch, 2011). This could also explain why intracellular lactate levels were higher upon IMiD treatment, which possibly restrains the activity of both MCT1 and MCT4, than upon RNAi-mediated knockdown of only MCT1 (Fig. 24). The finding, that blocking of multiple MCTs potentiates the cytotoxic and metabolic effects of blocking a single MCT in MM cell lines further underscores the relevance of blocking multiple MCTs (Hanson, 2015) and the importance to further elucidate the role of MCT4 in MM lactate metabolism in future investigations.

5.4 CD147/MCT1 destabilization is predictive of IMiD-response

The numerous CD147/MCT1-mediated anti-myeloma effects of lenalidomide uncovered in this study were limited to lenalidomide-sensitive MM cell lines, while naturally lenalidomide-resistant MM cell lines remained unaffected (Fig. 14-15). Taken together with fully matching data from MM cell lines, *in vivo* xenograft experiments and IMiD-naïve and IMiD-refractory MM patient sample analyses (Eichner, 2016), the above finding suggests that the destabilization of CD147/MCT1 proteins predicts IMiD sensitivity and therefore response to IMiD treatment. This could serve as a new early biomarker to determine which MM patients might benefit from an IMiD-based therapy regimen. By contrast, lenalidomide-induced reduction of IKZF3 levels occurred to a similar extent both in lenalidomide-sensitive and lenalidomide-resistant MM cell lines in this study (Fig. 15), which is consistent with previously published data (Lu, 2014). So far, only one study performing murine xenograft experiments with human MM1S cells succeeded to show that IKZF1/3 levels decrease upon lenalidomide or pomalidomide treatment, whereas this decrease was no longer observed once tumors became resistant to either treatment

(Ocio, 2015). However, IKZF1 has been found to be lower in 3 of 5 IMiD-resistant MM cell lines and low IKZF1 gene expression levels in MM patients predict poor IMiD response rates and reduced overall survival rates (Zhu, 2014). Next to IKZF1/3, a few other potential predictive indicators of IMiD response have been evaluated, but they remain controversial and broadly available clinical biomarkers are far from being established.

Two studies with newly diagnosed MM patients receiving thalidomide-based treatment have identified low levels of CRBN in gene expression profiles to correlate with drug resistance, while high CRBN expression was associated with longer progression free survival (Bedewy, 2014; Broyl, 2013). Similar relationships between treatment response and CRBN gene expression data were also observed in patients treated with lenalidomide or pomalidomide with or without dexamethasone (Heintel, 2013; Schuster, 2014; Zhu, 2011). MM patients with low CRBN expression have significantly reduced progression free and overall survival (Schuster, 2014). In line with these findings, immunohistochemical analyses of MM patient samples have shown superior response to thalidomide or lenalidomide in patients with high CRBN signal (Huang, 2014). These clinical observations were confirmed in cell culture experiments, where a naturally IMiD-resistant MM cell line expressed no detectable CRBN protein and acquired resistance in another MM cell line was accompanied by a reduction in CRBN protein levels (Lopez-Girona, 2012). By contrast, a study by Greenberg and colleagues, comparing CRBN protein abundance on Western Blot level in lenalidomide-sensitive and lenalidomide-resistant MM cell lines, showed no differences in upfront CRBN levels. Furthermore, this group could not identify a correlation between cytogenetic subtypes and IMiD response (Greenberg, 2013). However, due to the low number of cell lines analyzed, the conclusions that can be drawn from this study are very limited.

Complementary to MM, a first study in lower risk del(5q) MDS patients has demonstrated that high CRBN mRNA levels correlate with good response to lenalidomide treatment, while loss of CRBN expression during the course of therapy was associated with drug resistance and progression of MDS (Jonasova, 2015). Similarly, the activity of lenalidomide in an aggressive subtype of diffuse large cell B lymphoma (DLBCL) was shown to depend on CRBN (Zhang, 2013). As further complication, several isoforms of CRBN exist and a study using a highly sensitive and specific CRBN antibody has shown discrepancies between CRBN mRNA and protein levels. Together, these findings call for the standardization of study conditions and infer the superiority of protein level assessment, when trying to establish CRBN as a biomarker (A. K. Gandhi, 2014b; Ren, 2015). Apart from CRBN, IRF4 has been investigated as a marker for IMiD-response. IRF4 is a haematopoetic transcription factor, which is important for differentiation and immune response regulation (Acquaviva, 2008; Lopez-Girona, 2011). It was originally identified as a product of a

proto-oncogene in MM but is supposed to function as a tumor-suppressor in early B-cell development (Acquaviva, 2008). High levels of IRF4 have been shown to correlate with poor survival rates in patients with MM (Heintel, 2008). However, in MM cell lines high IRF4 levels correlate with lenalidomide sensitivity and MM patients with high IRF4 expression have longer overall survival under lenalidomide treatment compared to other treatments (Lopez-Girona, 2011).

CD147 has already been reported to function as a prognostic marker in several solid tumors (Bovenzi, 2015). For example, high expression of CD147 correlates with advanced stages and poor prognosis in hepatocellular carcinoma, glioblastoma, pediatric glioma and gastric cancer (Gu, 2009; Shou, 2012; Yang, 2013; S. Zhu, 2015). The present study could not identify a relationship between baseline CD147 levels and lenalidomide sensitivity in MM cell lines. However, the full correlation of CD147/MCT1 destabilization and IMiD response both in our MM cell line data and MM patient sample analyses (Fig. 15) (Eichner, 2016), together with the fact that CD147 expression can be easily assessed by flow cytometry, highlights these two proteins as attractive potential biomarkers for IMiD response. However, the analysis of larger patient cohorts and standardized protocols will be necessary to further evaluate their role in the clinical setting.

The identification and characterization of CD147 and MCT1 as myeloma-relevant IMiD-effectors might not only serve to select IMiD-sensitive patients, but might also help to reveal the mechanism by which myeloma cells and ultimately MM patients become resistant to IMiD treatment. This phenomenon still remains a major challenge in the treatment of MM (Ocio, 2015). The investigation of CD147/MCT1-related resistance mechanisms therefore will be the goal of subsequent investigations.

5.5 IMiD-resistant cells remain sensitive to anti-CD147/MCT1 targeted therapies

Strikingly, in the present study, IMiD-resistant MM cell lines continued to be affected by RNAi-induced CD147/MCT1-silencing (Fig. 21), thus distinguishing CD147 and MCT1 as attractive targets in IMiD-refractory or relapsed MM patients. Both CD147-targeting monoclonal antibodies and MCT1-specific inhibitors, such as AZD3965, are currently undergoing clinical investigation for the treatment of different advanced-stage solid tumors and, based on our findings, should be explored in the context of MM (Polanski, 2014; Xiong, 2014). The finding that inhibition of lactate export with the pan-MCT inhibitor CHC or the MCT1/2-specific inhibitor AR-C155858 is cytotoxic in MM cells furthermore supports the hypothesis that MCT inhibitors could be clinically effective in MM and should be investigated in clinical trials (Hanson, 2015). Another strategy, which is in part already being assessed in phase I/II clinical trials, is the specific targeting of MM cells in their hypoxic bone marrow

niche by the prodrug TH-302. TH-302 is the prodrug of cytotoxic bromo-isophosphoramide mustard, which becomes activated under hypoxic conditions and leads to a cell cycle arrest and induces apoptosis (Borsi, 2015; Hu, 2010). It would be especially interesting to analyze the response of IMiD-refractory patients within this study. Considering that PDK1, which promotes glycolysis by inhibiting PDH, is overexpressed in MM cells relative to normal tissues, this enzyme may provide a further therapeutic opportunity to target MM cell metabolism both in the IMiD-sensitive and -resistant setting (Fujiwara, 2013). HIF-1α is a further experimental target in the therapy of MM. Indeed, RNAi-induced knock-down of HIF-1α in the lenalidomide-resistant MM cell line JJN3 led to a dramatic loss of tumor burden and decreased VEGF-mediated angiogenesis in a subcutaneous xenograft injection model and additionally reduced bone destruction in an intratibial xenograft model (Storti, 2013). It would be interesting to see the effect of HIF-1α inhibitors in the treatment of IMiD sensitive or resistant MM patients and analyze potential synergies.

5.6 Validation and further inquiry of the CD147/MCT1-axis in primary MM-cells, *in vivo* and del(5q)-MDS

To further validate the functional results observed in this study and to apply the findings in primary MM cells, as well as in the other clinically IMiD-relevant entity del(5q)-MDS (Zeldis, 2011), my colleagues in the Bassermann lab performed several experiments. Most importantly, they were able to demonstrate that forced overexpression of exogenous CD147 and MCT1 in the IMiD-sensitive MM cell line MM1S attenuates the cytotoxic and anti-proliferative effect of lenalidomide (Eichner, 2016). This rescue experiment specifically proves the importance of CD147 and MCT1 for mediation of IMiD effects in MM. Moreover, primary CD138+ MM cells were purified from patient-derived bone marrow aspirates, taken into culture and treated with lenalidomide. In line with the results in the established MM cell lines, samples derived from newly diagnosed or IMiD-naïve MM patients showed a destabilization of CD147 and MCT1, while CD147/MCT1-levels remained stable in cells obtained from lenalidomide-refractory MM patients (Eichner, 2016). To further investigate the proposed mechanism *in vivo*, murine xenograft experiments with subcutaneous injection of human MM1S cells were performed. One approach showed that RNAi-mediated silencing of both CD147 and MCT1 in injected MM1S cells leads to an impressive reduction in tumor growth compared to control tumors (Eichner, 2016). In another approach, CD147 and MCT1 were overexpressed in MM1S cells prior to injection. After the appearance of tumors, mice were treated orally with lenalidomide. While control tumors ceased to grow under lenalidomide treatment, tumors with forced CD147/MCT1 expression continued to grow to a similar extent as tumors in untreated control mice during initial treatment (Eichner,

2016). All these findings further underscore the clinical relevance of the model in the treatment of MM.

To translate the findings in MM to the other main IMiD-seinsitive entity del(5q) MDS, several experiments were performed using del(5q)- and non-del(5q)-MDS cell lines. Baseline CD147 and MCT1 levels were found to be elevated in del(5q) compared to non-del(5q) MDS cell lines. This finding is in line with data from primary MDS patient-derived erythroid cells, where levels of CD147 were considerably higher in del(5q) patients as compared to del(5q) patients after lenalidomide treatment or non-del(5q) patients (Eichner, 2016). Analogous to the observations in MM, lenalidomide and pomalidomide destabilized CD147 and MCT1 in del(5q) MDS cell lines and the anti-proliferative effects of lenalidomide were abated by CD147/MCT1 overexpression (Eichner, 2016). Furthermore, RNAi-mediated silencing of CD147 or MCT1 significantly reduced proliferation in a del(5q) MDS cell line, underlining the relevance of CD147 and MCT1 in this entity (Eichner, 2016). Flow cytometric analyses of *in vivo* differentiated and lenalidomide-treated primary del(5q) cells further delineated that erythroid cells specifically losing CD147 expression upon lenalidomide treatment undergo apoptosis, while cells with unchanged CD147 levels did not undergo apoptosis (Eichner, 2016). Taken together, these observations advocate the hypothesis that, as in MM, IMiDs mediate their anti-tumor activity via CD147 and MCT1 destabilization in del(5q) MDS. Other than IKZF1 and IKZF3, which are lymphoid transcription factors (Cortes, 1999), CD147 and MCT1 are broadly expressed and may explain IMiD activity in various other malignancies (Kennedy, 2010; Riethdorf, 2006). The involvement of CD147 and MCT1 in the treatment of other IMiD-sensitive and resistant tumors must therefore be the goal of follow-up investigations.

6 Summary

The introduction of new therapeutic agents in the treatment of MM, the second most common hematologic malignancy, has greatly improved the overall survival, progression-free survival and post-relapse survival in recent years. Apart from proteasome inhibitors, IMiDs like thalidomide and its derivatives lenalidomide and pomalidomide have significantly contributed to the improved treatment options of this still incurable disease (Costa, 2013; S. K. Kumar, 2014b; S. K. Kumar, 2008; D. Smith, 2013). In the early 1960s, thalidomide was marketed as a safe anti-emetic drug in the treatment of morning sickness in pregnant women, but was soon uncovered to be highly teratogenic (Vargesson, 2015). Thalidomide was later found to be effective in the treatment of various inflammatory diseases and its derivatives lenalidomide and pomalidomide have emerged as key players in the treatment of MM and del(5q) MDS (Rehman, 2011; Shortt, 2013). IMiDs exert their anti-tumor and teratogenic activity by directly interacting with CRBN, the substrate recognition factor of a CRL4 ubiquitin ligase (Chamberlain, 2014; Fischer, 2014; Ito, 2010; Lopez-Girona, 2012; Zhu, 2011). While the recently reported lenalidomide-induced degradation of IKZF1 and IKZF3, two lymphoid transcription factors, may explain some IMiD effects, it remained unclear, how IMiDs exert their anti-angiogenic, anti-proliferative and anti-invasive activity in various tumor entities and mediate teratogenicity (A. K. Gandhi, 2014a; Kronke, 2014; Lu, 2014; Zhu, 2014). Against this background, this study now identifies CD147 and MCT1 as physiologically relevant CRBN-interactors and characterizes their functional role in MM cell lines. The three clinically available IMiDs lenalidomide, thalidomide and pomalidomide all destabilized CD147 and MCT1 post-transcriptionally in a dose- and time-dependent manner. Furthermore, this effect was conserved under hypoxic conditions. The destabilization and inactivation of the CD147/MCT1 transmembrane complex was shown to mediate various anti-myeloma effects of IMiDs, by directly reducing cell proliferation, as well as by inhibiting angiogenesis and invasion via decreased secretion of VEGF and MMP7. Importantly, this study establishes metabolic alteration via disruption of MCT1-mediated lactate transport as a previously unknown function of IMiDs. The numerous CD147/MCT1-mediated anti-myeloma effects of lenalidomide uncovered in this study were limited to lenalidomide-sensitive MM cell lines, while naturally lenalidomide-resistant cell lines remained unaffected. This implies that CD147/MCT1-destabilization could serve as a new biomarker for IMiD response. Finally, IMiD-resistant MM cell lines remained sensitive to CD147/MCT1-silencing. This finding distinguishes CD147 and MCT1 as attractive targets particularly in IMiD-refractory or relapsed patients with MM.

7 Literature

Acquaviva, J., Chen, X., & Ren, R. (2008). IRF-4 functions as a tumor suppressor in early B-cell development. *Blood, 112*(9), 3798-3806. doi: 10.1182/blood-2007-10-117838

Angers, S., Li, T., Yi, X., MacCoss, M. J., Moon, R. T., & Zheng, N. (2006). Molecular architecture and assembly of the DDB1-CUL4A ubiquitin ligase machinery. *Nature, 443*(7111), 590-593. doi: 10.1038/nature05175

Arendt, B. K., Walters, D. K., Wu, X., Tschumper, R. C., Huddleston, P. M., Henderson, K. J., Dispenzieri, A., & Jelinek, D. F. (2012). Increased expression of extracellular matrix metalloproteinase inducer (CD147) in multiple myeloma: role in regulation of myeloma cell proliferation. *Leukemia, 26*(10), 2286-2296. doi: 10.1038/leu.2012.91

Arendt, B. K., Walters, D. K., Wu, X., Tschumper, R. C., & Jelinek, D. F. (2014). Multiple myeloma dell-derived microvesicles are enriched in CD147 expression and enhance tumor cell proliferation. *Oncotarget, 5*(14), 5686-5699. doi: 10.18632/oncotarget.2159

Attal, M., Lauwers-Cances, V., Marit, G., Caillot, D., Moreau, P., Facon, T., Stoppa, A. M., Hulin, C., Benboubker, L., Garderet, L., Decaux, O., Leyvraz, S., Vekemans, M.-C., Voillat, L., Michallet, M., Pegourie, B., Dumontet, C., Roussel, M., Leleu, X., Mathiot, C., Payen, C., Avet-Loiseau, H., & Harousseau, J.-L. (2012). Lenalidomide Maintenance after Stem-Cell Transplantation for Multiple Myeloma. *New England Journal of Medicine, 366*(19), 1782-1791. doi: doi:10.1056/NEJMoa1114138

Barille, S., Akhoundi, C., Collette, M., Mellerin, M. P., Rapp, M. J., Harousseau, J. L., Bataille, R., & Amiot, M. (1997). Metalloproteinases in multiple myeloma: production of matrix metalloproteinase-9 (MMP-9), activation of proMMP-2, and induction of MMP-1 by myeloma cells. *Blood, 90*(4), 1649-1655.

Barlogie, B., Desikan, R., Eddlemon, P., Spencer, T., Zeldis, J., Munshi, N., Badros, A., Zangari, M., Anaissie, E., Epstein, J., Shaughnessy, J., Ayers, D., Spoon, D., & Tricot, G. (2001). Extended survival in advanced and refractory multiple myeloma after single-agent thalidomide: identification of prognostic factors in a phase 2 study of 169 patients. *Blood, 98*(2), 492-494.

Bassermann, F., von Klitzing, C., Munch, S., Bai, R. Y., Kawaguchi, H., Morris, S. W., Peschel, C., & Duyster, J. (2005). NIPA defines an SCF-type mammalian E3 ligase that regulates mitotic entry. *Cell, 122*(1), 45-57.

Baumann, U., Fernandez-Saiz, V., Rudelius, M., Lemeer, S., Rad, R., Knorn, A. M., Slawska, J., Engel, K., Jeremias, I., Li, Z., Tomiatti, V., Illert, A. L., Targosz, B. S., Braun, M., Perner, S., Leitges, M., Klapper, W., Dreyling, M., Miething, C., Lenz, G., Rosenwald, A., Peschel, C., Keller, U., Kuster, B., & Bassermann, F. (2014).

Disruption of the PRKCD-FBXO25-HAX-1 axis attenuates the apoptotic response and drives lymphomagenesis. *Nat Med, 20*(12), 1401-1409. doi: 10.1038/nm.3740

Becker, N. (2011). Epidemiology of multiple myeloma. *Recent Results Cancer Res, 183*, 25-35. doi: 10.1007/978-3-540-85772-3_2

Bedewy, A. M. L., & El-Maghraby, S. M. (2014). Do baseline Cereblon gene expression and IL-6 receptor expression determine the response to thalidomide–dexamethasone treatment in Multiple myeloma patients? *Eur J Haematol, 92*(1), 13-18. doi: 10.1111/ejh.12207

Berg, J. M. T., J. L.; Stryer, L. (2002). *Biochemistry. 5th edition.* New York: W H Freeman.

Bergsagel, P. L., Mateos, M. V., Gutierrez, N. C., Rajkumar, S. V., & San Miguel, J. F. (2013). Improving overall survival and overcoming adverse prognosis in the treatment of cytogenetically high-risk multiple myeloma. *Blood, 121*(6), 884-892. doi: 10.1182/blood-2012-05-432203

BfArM. (2011). Verordnung über die Verschreibungspflicht von Arzneimitteln, §3a. *Bundesministerium für Arzneimittel und Medizinprodukte*.

Bird, J. M., Behrens, J., Westin, J., Turesson, I., Drayson, M., Beetham, R., D'Sa, S., Soutar, R., Waage, A., Gulbrandsen, N., Gregersen, H., & Low, E. (2009). UK Myeloma Forum (UKMF) and Nordic Myeloma Study Group (NMSG): guidelines for the investigation of newly detected M-proteins and the management of monoclonal gammopathy of undetermined significance (MGUS). *Br J Haematol, 147*(1), 22-42. doi: 10.1111/j.1365-2141.2009.07807.x

Bird, J. M., Owen, R. G., D'Sa, S., Snowden, J. A., Pratt, G., Ashcroft, J., Yong, K., Cook, G., Feyler, S., Davies, F., Morgan, G., Cavenagh, J., Low, E., & Behrens, J. (2011). Guidelines for the diagnosis and management of multiple myeloma 2011. *Br J Haematol, 154*(1), 32-75. doi: 10.1111/j.1365-2141.2011.08573.x

Birgegard, G., Gascon, P., & Ludwig, H. (2006). Evaluation of anaemia in patients with multiple myeloma and lymphoma: findings of the European CANCER ANAEMIA SURVEY. *Eur J Haematol, 77*(5), 378-386. doi: 10.1111/j.1600-0609.2006.00739.x

Biswas, C., Zhang, Y., DeCastro, R., Guo, H., Nakamura, T., Kataoka, H., & Nabeshima, K. (1995). The human tumor cell-derived collagenase stimulatory factor (renamed EMMPRIN) is a member of the immunoglobulin superfamily. *Cancer Res, 55*(2), 434-439.

Borsi, E., Perrone, G., Terragna, C., Martello, M., Dico, A. F., Solaini, G., Baracca, A., Sgarbi, G., Pasquinelli, G., Valente, S., Zamagni, E., Tacchetti, P., Martinelli, G., & Cavo, M. (2014). Hypoxia inducible factor-1 alpha as a therapeutic target in multiple myeloma. *Oncotarget, 5*(7), 1779-1792. doi: 10.18632/oncotarget.1736

Borsi, E., Terragna, C., Brioli, A., Tacchetti, P., Martello, M., & Cavo, M. (2015). Therapeutic targeting of hypoxia and hypoxia-inducible factor 1 alpha in multiple myeloma. *Transl Res, 165*(6), 641-650. doi: 10.1016/j.trsl.2014.12.001

Bougatef, F., Quemener, C., Kellouche, S., Naimi, B., Podgorniak, M. P., Millot, G., Gabison, E. E., Calvo, F., Dosquet, C., Lebbe, C., Menashi, S., & Mourah, S. (2009). EMMPRIN promotes angiogenesis through hypoxia-inducible factor-2alpha-mediated regulation of soluble VEGF isoforms and their receptor VEGFR-2. *Blood, 114*(27), 5547-5556. doi: 10.1182/blood-2009-04-217380

Bouzier, A. K., Goodwin, R., de Gannes, F. M., Valeins, H., Voisin, P., Canioni, P., & Merle, M. (1998a). Compartmentation of lactate and glucose metabolism in C6 glioma cells. A 13c and 1H NMR study. *J Biol Chem, 273*(42), 27162-27169.

Bouzier, A. K., Voisin, P., Goodwin, R., Canioni, P., & Merle, M. (1998b). Glucose and lactate metabolism in C6 glioma cells: evidence for the preferential utilization of lactate for cell oxidative metabolism. *Dev Neurosci, 20*(4-5), 331-338.

Bovenzi, C. D., Hamilton, J., Tassone, P., Johnson, J., Cognetti, D. M., Luginbuhl, A., Keane, W. M., Zhan, T., Tuluc, M., Bar-Ad, V., Martinez-Outschoorn, U., & Curry, J. M. (2015). Prognostic Indications of Elevated MCT4 and CD147 across Cancer Types: A Meta-Analysis. *Biomed Res Int, 2015*, 242437. doi: 10.1155/2015/242437

Broyl, A., Kuiper, R., van Duin, M., van der Holt, B., el Jarari, L., Bertsch, U., Zweegman, S., Buijs, A., Hose, D., Lokhorst, H. M., Goldschmidt, H., & Sonneveld, P. (2013). High cereblon expression is associated with better survival in patients with newly diagnosed multiple myeloma treated with thalidomide maintenance. *Blood, 121*(4), 624-627. doi: 10.1182/blood-2012-06-438101

Cavo, M., Tacchetti, P., Patriarca, F., Petrucci, M. T., Pantani, L., Galli, M., Di Raimondo, F., Crippa, C., Zamagni, E., Palumbo, A., Offidani, M., Corradini, P., Narni, F., Spadano, A., Pescosta, N., Deliliers, G. L., Ledda, A., Cellini, C., Caravita, T., Tosi, P., & Baccarani, M. (2010). Bortezomib with thalidomide plus dexamethasone compared with thalidomide plus dexamethasone as induction therapy before, and consolidation therapy after, double autologous stem-cell transplantation in newly diagnosed multiple myeloma: a randomised phase 3 study. *Lancet, 376*(9758), 2075-2085. doi: 10.1016/S0140-6736(10)61424-9

Chamberlain, P. P., Lopez-Girona, A., Miller, K., Carmel, G., Pagarigan, B., Chie-Leon, B., Rychak, E., Corral, L. G., Ren, Y. J., Wang, M., Riley, M., Delker, S. L., Ito, T., Ando, H., Mori, T., Hirano, Y., Handa, H., Hakoshima, T., Daniel, T. O., & Cathers, B. E. (2014). Structure of the human Cereblon-DDB1-lenalidomide complex reveals basis for responsiveness to thalidomide analogs. *Nat Struct Mol Biol, 21*(9), 803-809. doi: 10.1038/nsmb.2874

Chen, C., & Okayama, H. (1987). High-efficiency transformation of mammalian cells by plasmid DNA. *Mol Cell Biol, 7*(8), 2745-2752.

Chen, Y., Gou, X., Ke, X., Cui, H., & Chen, Z. (2012). Human tumor cells induce angiogenesis through positive feedback between CD147 and insulin-like growth factor-I. *PLoS One, 7*(7), e40965. doi: 10.1371/journal.pone.0040965

Colla, S., Storti, P., Donofrio, G., Todoerti, K., Bolzoni, M., Lazzaretti, M., Abeltino, M., Ippolito, L., Neri, A., Ribatti, D., Rizzoli, V., Martella, E., & Giuliani, N. (2010). Low bone marrow oxygen tension and hypoxia-inducible factor-1alpha overexpression characterize patients with multiple myeloma: role on the transcriptional and proangiogenic profiles of CD138(+) cells. *Leukemia, 24*(11), 1967-1970. doi: 10.1038/leu.2010.193

Cortes, M., & Georgopoulos, K. (2004). Aiolos is required for the generation of high affinity bone marrow plasma cells responsible for long-term immunity. *J Exp Med, 199*(2), 209-219. doi: 10.1084/jem.20031571

Cortes, M., Wong, E., Koipally, J., & Georgopoulos, K. (1999). Control of lymphocyte development by the Ikaros gene family. *Curr Opin Immunol, 11*(2), 167-171.

Costa, L. J., Zhang, M. J., Zhong, X., Dispenzieri, A., Lonial, S., Krishnan, A., Freytes, C., Vesole, D., Gale, R. P., Anderson, K., Wirk, B., Savani, B. N., Waller, E. K., Schouten, H., Lazarus, H., Meehan, K., Sharma, M., Kamble, R., Vij, R., Kumar, S., Nishihori, T., Kindwall-Keller, T., Saber, W., & Hari, P. N. (2013). Trends in utilization and outcomes of autologous transplantation as early therapy for multiple myeloma. *Biol Blood Marrow Transplant, 19*(11), 1615-1624. doi: 10.1016/j.bbmt.2013.08.002

D'Amato, R. J., Loughnan, M. S., Flynn, E., & Folkman, J. (1994). Thalidomide is an inhibitor of angiogenesis. *Proc Natl Acad Sci U S A, 91*(9), 4082-4085.

Dankbar, B., Padro, T., Leo, R., Feldmann, B., Kropff, M., Mesters, R. M., Serve, H., Berdel, W. E., & Kienast, J. (2000). Vascular endothelial growth factor and interleukin-6 in paracrine tumor-stromal cell interactions in multiple myeloma. *Blood, 95*(8), 2630-2636.

Das, D. S., Ray, A., Song, Y., Richardson, P., Trikha, M., Chauhan, D., & Anderson, K. C. (2015). Synergistic anti-myeloma activity of the proteasome inhibitor marizomib and the IMiD((R)) immunomodulatory drug pomalidomide. *Br J Haematol, 171*(5), 798-812. doi: 10.1111/bjh.13780

Davis, H. E., Morgan, J. R., & Yarmush, M. L. (2002). Polybrene increases retrovirus gene transfer efficiency by enhancing receptor-independent virus adsorption on target cell membranes. *Biophys Chem, 97*(2-3), 159-172.

Deora, A. A., Philp, N., Hu, J., Bok, D., & Rodriguez-Boulan, E. (2005). Mechanisms regulating tissue-specific polarity of monocarboxylate transporters and their chaperone CD147 in kidney and retinal epithelia. *Proc Natl Acad Sci U S A, 102*(45), 16245-16250. doi: 10.1073/pnas.0504419102

Dimopoulos, M., Spencer, A., Attal, M., Prince, H. M., Harousseau, J. L., Dmoszynska, A., San Miguel, J., Hellmann, A., Facon, T., Foa, R., Corso, A., Masliak, Z., Olesnyckyj, M., Yu, Z., Patin, J., Zeldis, J. B., & Knight, R. D. (2007). Lenalidomide plus dexamethasone for relapsed or refractory multiple myeloma. *N Engl J Med, 357*(21), 2123-2132. doi: 10.1056/NEJMoa070594

Doherty, J. R., & Cleveland, J. L. (2013). Targeting lactate metabolism for cancer therapeutics. *J Clin Invest, 123*(9), 3685-3692. doi: 10.1172/JCI69741

Dredge, K., Horsfall, R., Robinson, S. P., Zhang, L. H., Lu, L., Tang, Y., Shirley, M. A., Muller, G., Schafer, P., Stirling, D., Dalgleish, A. G., & Bartlett, J. B. (2005). Orally administered lenalidomide (CC-5013) is anti-angiogenic in vivo and inhibits endothelial cell migration and Akt phosphorylation in vitro. *Microvasc Res, 69*(1-2), 56-63. doi: 10.1016/j.mvr.2005.01.002

Dredge, K., Marriott, J. B., Macdonald, C. D., Man, H. W., Chen, R., Muller, G. W., Stirling, D., & Dalgleish, A. G. (2002). Novel thalidomide analogues display anti-angiogenic activity independently of immunomodulatory effects. *Br J Cancer, 87*(10), 1166-1172. doi: 10.1038/sj.bjc.6600607

Durie, B. G., & Salmon, S. E. (1975). A clinical staging system for multiple myeloma. Correlation of measured myeloma cell mass with presenting clinical features, response to treatment, and survival. *Cancer, 36*(3), 842-854.

Eichner, R., Heider, M., Fernandez-Saiz, V., van Bebber, F., Garz, A. K., Lemeer, S., Rudelius, M., Targosz, B. S., Jacobs, L., Knorn, A. M., Slawska, J., Platzbecker, U., Germing, U., Langer, C., Knop, S., Einsele, H., Peschel, C., Haass, C., Keller, U., Schmid, B., Gotze, K. S., Kuster, B., & Bassermann, F. (2016). Immunomodulatory drugs disrupt the cereblon-CD147-MCT1 axis to exert antitumor activity and teratogenicity. *Nat Med, 22*(7), 735-743. doi: 10.1038/nm.4128

Engelhardt, M., Terpos, E., Kleber, M., Gay, F., Wasch, R., Morgan, G., Cavo, M., van de Donk, N., Beilhack, A., Bruno, B., Johnsen, H. E., Hajek, R., Driessen, C., Ludwig, H., Beksac, M., Boccadoro, M., Straka, C., Brighen, S., Gramatzki, M., Larocca, A., Lokhorst, H., Magarotto, V., Morabito, F., Dimopoulos, M. A., Einsele, H., Sonneveld, P., & Palumbo, A. (2014). European Myeloma Network recommendations on the evaluation and treatment of newly diagnosed patients with multiple myeloma. *Haematologica, 99*(2), 232-242. doi: 10.3324/haematol.2013.099358

Estrella, V., Chen, T., Lloyd, M., Wojtkowiak, J., Cornnell, H. H., Ibrahim-Hashim, A., Bailey, K., Balagurunathan, Y., Rothberg, J. M., Sloane, B. F., Johnson, J., Gatenby, R. A., & Gillies, R. J. (2013). Acidity generated by the tumor microenvironment drives local invasion. *Cancer Res, 73*(5), 1524-1535. doi: 10.1158/0008-5472.CAN-12-2796

Fernandez-Saiz, V., Targosz, B. S., Lemeer, S., Eichner, R., Langer, C., Bullinger, L., Reiter, C., Slotta-Huspenina, J., Schroeder, S., Knorn, A. M., Kurutz, J.,

Peschel, C., Pagano, M., Kuster, B., & Bassermann, F. (2013). SCFFbxo9 and CK2 direct the cellular response to growth factor withdrawal via Tel2/Tti1 degradation and promote survival in multiple myeloma. *Nat Cell Biol, 15*(1), 72-81. doi: 10.1038/ncb2651

Fischer, E. S., Bohm, K., Lydeard, J. R., Yang, H., Stadler, M. B., Cavadini, S., Nagel, J., Serluca, F., Acker, V., Lingaraju, G. M., Tichkule, R. B., Schebesta, M., Forrester, W. C., Schirle, M., Hassiepen, U., Ottl, J., Hild, M., Beckwith, R. E., Harper, J. W., Jenkins, J. L., & Thoma, N. H. (2014). Structure of the DDB1-CRBN E3 ubiquitin ligase in complex with thalidomide. *Nature, 512*(7512), 49-53. doi: 10.1038/nature13527

Folkman, J. (1971). Tumor angiogenesis: therapeutic implications. *N Engl J Med, 285*(21), 1182-1186. doi: 10.1056/NEJM197111182852108

Fonseca, R., Barlogie, B., Bataille, R., Bastard, C., Bergsagel, P. L., Chesi, M., Davies, F. E., Drach, J., Greipp, P. R., Kirsch, I. R., Kuehl, W. M., Hernandez, J. M., Minvielle, S., Pilarski, L. M., Shaughnessy, J. D., Jr., Stewart, A. K., & Avet-Loiseau, H. (2004). Genetics and cytogenetics of multiple myeloma: a workshop report. *Cancer Res, 64*(4), 1546-1558.

Franks, M. E., Macpherson, G. R., & Figg, W. D. (2004). Thalidomide. *Lancet, 363*(9423), 1802-1811. doi: 10.1016/S0140-6736(04)16308-3

Fujiwara, S., Kawano, Y., Yuki, H., Okuno, Y., Nosaka, K., Mitsuya, H., & Hata, H. (2013). PDK1 inhibition is a novel therapeutic target in multiple myeloma. *Br J Cancer, 108*(1), 170-178. doi: 10.1038/bjc.2012.527

Fujiwara, S., Wada, N., Kawano, Y., Okuno, Y., Kikukawa, Y., Endo, S., Nishimura, N., Ueno, N., Mitsuya, H., & Hata, H. (2015). Lactate, a putative survival factor for myeloma cells, is incorporated by myeloma cells through monocarboxylate transporters 1. *Exp Hematol Oncol, 4*, 12. doi: 10.1186/s40164-015-0008-z

Gandhi, A. K., Kang, J., Havens, C. G., Conklin, T., Ning, Y., Wu, L., Ito, T., Ando, H., Waldman, M. F., Thakurta, A., Klippel, A., Handa, H., Daniel, T. O., Schafer, P. H., & Chopra, R. (2014a). Immunomodulatory agents lenalidomide and pomalidomide co-stimulate T cells by inducing degradation of T cell repressors Ikaros and Aiolos via modulation of the E3 ubiquitin ligase complex CRL4(CRBN.). *Br J Haematol, 164*(6), 811-821. doi: 10.1111/bjh.12708

Gandhi, A. K., Mendy, D., Waldman, M., Chen, G., Rychak, E., Miller, K., Gaidarova, S., Ren, Y., Wang, M., Breider, M., Carmel, G., Mahmoudi, A., Jackson, P., Abbasian, M., Cathers, B. E., Schafer, P. H., Daniel, T. O., Lopez-Girona, A., Thakurta, A., & Chopra, R. (2014b). Measuring cereblon as a biomarker of response or resistance to lenalidomide and pomalidomide requires use of standardized reagents and understanding of gene complexity. *Br J Haematol, 164*(2), 233-244. doi: 10.1111/bjh.12622

Gandhi, R., Kumar, D., Burns, E. J., Nadeau, M., Dake, B., Laroni, A., Kozoriz, D., Weiner, H. L., & Quintana, F. J. (2010). Activation of the aryl hydrocarbon receptor induces human type 1 regulatory T cell-like and Foxp3(+) regulatory T cells. *Nat Immunol, 11*(9), 846-853. doi: 10.1038/ni.1915

Greenberg, A. J., Walters, D. K., Kumar, S. K., Vincent Rajkumar, S., & Jelinek, D. F. (2013). Responsiveness of cytogenetically discrete human myeloma cell lines to lenalidomide: lack of correlation with cereblon and interferon regulatory factor 4 expression levels. *Eur J Haematol, 91*(6), 504-513. doi: 10.1111/ejh.12192

Greipp, P. R., San Miguel, J., Durie, B. G., Crowley, J. J., Barlogie, B., Blade, J., Boccadoro, M., Child, J. A., Avet-Loiseau, H., Kyle, R. A., Lahuerta, J. J., Ludwig, H., Morgan, G., Powles, R., Shimizu, K., Shustik, C., Sonneveld, P., Tosi, P., Turesson, I., & Westin, J. (2005). International staging system for multiple myeloma. *J Clin Oncol, 23*(15), 3412-3420. doi: 10.1200/JCO.2005.04.242

Gu, J., Zhang, C., Chen, R., Pan, J., Wang, Y., Ming, M., Gui, W., & Wang, D. (2009). Clinical implications and prognostic value of EMMPRIN/CD147 and MMP2 expression in pediatric gliomas. *Eur J Pediatr, 168*(6), 705-710. doi: 10.1007/s00431-008-0828-5

Gupta, D., Treon, S. P., Shima, Y., Hideshima, T., Podar, K., Tai, Y. T., Lin, B., Lentzsch, S., Davies, F. E., Chauhan, D., Schlossman, R. L., Richardson, P., Ralph, P., Wu, L., Payvandi, F., Muller, G., Stirling, D. I., & Anderson, K. C. (2001). Adherence of multiple myeloma cells to bone marrow stromal cells upregulates vascular endothelial growth factor secretion: therapeutic applications. *Leukemia, 15*(12), 1950-1961.

Halestrap, A. P. (2013). Monocarboxylic acid transport. *Compr Physiol, 3*(4), 1611-1643. doi: 10.1002/cphy.c130008

Halestrap, A. P., & Denton, R. M. (1974). Specific inhibition of pyruvate transport in rat liver mitochondria and human erythrocytes by alpha-cyano-4-hydroxycinnamate. *Biochem J, 138*(2), 313-316.

Halestrap, A. P., & Meredith, D. (2004). The SLC16 gene family-from monocarboxylate transporters (MCTs) to aromatic amino acid transporters and beyond. *Pflugers Arch, 447*(5), 619-628. doi: 10.1007/s00424-003-1067-2

Halestrap, A. P., & Wilson, M. C. (2012). The monocarboxylate transporter family--role and regulation. *IUBMB Life, 64*(2), 109-119. doi: 10.1002/iub.572

Hanahan, D., & Weinberg, R. A. (2000). The hallmarks of cancer. *Cell, 100*(1), 57-70.

Hanahan, D., & Weinberg, R. A. (2011). Hallmarks of cancer: the next generation. *Cell, 144*(5), 646-674. doi: 10.1016/j.cell.2011.02.013

Hanson, D. J., Nakamura, S., Amachi, R., Hiasa, M., Oda, A., Tsuji, D., Itoh, K., Harada, T., Horikawa, K., Teramachi, J., Miki, H., Matsumoto, T., & Abe, M. (2015). Effective impairment of myeloma cells and their progenitors by blockade of monocarboxylate transportation. *Oncotarget, 6*(32), 33568-33586. doi: 10.18632/oncotarget.5598

Heintel, D., Rocci, A., Ludwig, H., Bolomsky, A., Caltagirone, S., Schreder, M., Pfeifer, S., Gisslinger, H., Zojer, N., Jager, U., & Palumbo, A. (2013). High expression of cereblon (CRBN) is associated with improved clinical response in patients with multiple myeloma treated with lenalidomide and dexamethasone. *Br J Haematol, 161*(5), 695-700. doi: 10.1111/bjh.12338

Heintel, D., Zojer, N., Schreder, M., Strasser-Weippl, K., Kainz, B., Vesely, M., Gisslinger, H., Drach, J., Gaiger, A., Jager, U., & Ludwig, H. (2008). Expression of MUM1/IRF4 mRNA as a prognostic marker in patients with multiple myeloma. *Leukemia, 22*(2), 441-445. doi: 10.1038/sj.leu.2404895

Higgins, J. J., Pucilowska, J., Lombardi, R. Q., & Rooney, J. P. (2004). A mutation in a novel ATP-dependent Lon protease gene in a kindred with mild mental retardation. *Neurology, 63*(10), 1927-1931.

Higgins, J. J., Rosen, D. R., Loveless, J. M., Clyman, J. C., & Grau, M. J. (2000). A gene for nonsyndromic mental retardation maps to chromosome 3p25-pter. *Neurology, 55*(3), 335-340.

Hohberger, B., & Enz, R. (2009). Cereblon is expressed in the retina and binds to voltage-gated chloride channels. *FEBS Lett, 583*(4), 633-637. doi: 10.1016/j.febslet.2009.01.018

Hu, J., Handisides, D. R., Van Valckenborgh, E., De Raeve, H., Menu, E., Vande Broek, I., Liu, Q., Sun, J. D., Van Camp, B., Hart, C. P., & Vanderkerken, K. (2010). Targeting the multiple myeloma hypoxic niche with TH-302, a hypoxia-activated prodrug. *Blood, 116*(9), 1524-1527. doi: 10.1182/blood-2010-02-269126

Huang, S. Y., Lin, C. W., Lin, H. H., Yao, M., Tang, J. L., Wu, S. J., Chen, Y. C., Lu, H. Y., Hou, H. A., Chen, C. Y., Chou, W. C., Tsay, W., Chou, S. J., & Tien, H. F. (2014). Expression of cereblon protein assessed by immunohistochemicalstaining in myeloma cells is associated with superior response of thalidomide- and lenalidomide-based treatment, but not bortezomib-based treatment, in patients with multiple myeloma. *Ann Hematol, 93*(8), 1371-1380. doi: 10.1007/s00277-014-2063-7

Iacono, K. T., Brown, A. L., Greene, M. I., & Saouaf, S. J. (2007). CD147 immunoglobulin superfamily receptor function and role in pathology. *Exp Mol Pathol, 83*(3), 283-295. doi: 10.1016/j.yexmp.2007.08.014

Ito, T., Ando, H., Suzuki, T., Ogura, T., Hotta, K., Imamura, Y., Yamaguchi, Y., & Handa, H. (2010). Identification of a primary target of thalidomide teratogenicity. *Science, 327*(5971), 1345-1350. doi: 327/5971/1345 [pii]

10.1126/science.1177319

Jo, S., Lee, K. H., Song, S., Jung, Y. K., & Park, C. S. (2005). Identification and functional characterization of cereblon as a binding protein for large-conductance calcium-activated potassium channel in rat brain. *J Neurochem, 94*(5), 1212-1224. doi: 10.1111/j.1471-4159.2005.03344.x

Jonasova, A., Bokorova, R., Polak, J., Vostry, M., Kostecka, A., Hajkova, H., Neuwirtova, R., Siskova, M., Sponerova, D., Cermak, J., Mikulenkova, D., Cervinek, L., Brezinova, J., Michalova, K., & Fuchs, O. (2015). High level of full-length cereblon mRNA in lower risk myelodysplastic syndrome with isolated 5q deletion is implicated in the efficacy of lenalidomide. *Eur J Haematol, 95*(1), 27-34. doi: 10.1111/ejh.12457

Kaushal, G. P., Xiong, X., Athota, A. B., Rozypal, T. L., Sanderson, R. D., & Kelly, T. (1999). Syndecan-1 expression suppresses the level of myeloma matrix metalloproteinase-9. *Br J Haematol, 104*(2), 365-373.

Kelly, T., Borset, M., Abe, E., Gaddy-Kurten, D., & Sanderson, R. D. (2000). Matrix metalloproteinases in multiple myeloma. *Leuk Lymphoma, 37*(3-4), 273-281. doi: 10.3109/10428190009089428

Kennedy, K. M., & Dewhirst, M. W. (2010). Tumor metabolism of lactate: the influence and therapeutic potential for MCT and CD147 regulation. *Future Oncol, 6*(1), 127-148. doi: 10.2217/fon.09.145

Kenyon, B. M., Browne, F., & D'Amato, R. J. (1997). Effects of thalidomide and related metabolites in a mouse corneal model of neovascularization. *Exp Eye Res, 64*(6), 971-978. doi: 10.1006/exer.1997.0292

Khayati, F., Perez-Cano, L., Maouche, K., Sadoux, A., Boutalbi, Z., Podgorniak, M. P., Maskos, U., Setterblad, N., Janin, A., Calvo, F., Lebbe, C., Menashi, S., Fernandez-Recio, J., & Mourah, S. (2015). EMMPRIN/CD147 is a novel coreceptor of VEGFR-2 mediating its activation by VEGF. *Oncotarget, 6*(12), 9766-9780. doi: 10.18632/oncotarget.2870

Kingston, R. E., Chen, C. A., & Rose, J. K. (2003). Calcium phosphate transfection. *Curr Protoc Mol Biol, Chapter 9*, Unit 9 1. doi: 10.1002/0471142727.mb0901s63

Kirk, P., Wilson, M. C., Heddle, C., Brown, M. H., Barclay, A. N., & Halestrap, A. P. (2000). CD147 is tightly associated with lactate transporters MCT1 and MCT4 and facilitates their cell surface expression. *EMBO J, 19*(15), 3896-3904. doi: 10.1093/emboj/19.15.3896

Kovacs, M. J., Reece, D. E., Marcellus, D., Meyer, R. M., Mathews, S., Dong, R. P., & Eisenhauer, E. (2006). A phase II study of ZD6474 (Zactima, a selective inhibitor of VEGFR and EGFR tyrosine kinase in patients with relapsed multiple myeloma--NCIC CTG IND.145. *Invest New Drugs, 24*(6), 529-535. doi: 10.1007/s10637-006-9022-7

Kroger, N., Badbaran, A., Zabelina, T., Ayuk, F., Wolschke, C., Alchalby, H., Klyuchnikov, E., Atanackovic, D., Schilling, G., Hansen, T., Schwarz, S., Heinzelmann, M., Zeschke, S., Bacher, U., Stubig, T., Fehse, B., & Zander, A. R. (2013). Impact of high-risk cytogenetics and achievement of molecular remission on long-term freedom from disease after autologous-allogeneic tandem transplantation in patients with multiple myeloma. *Biol Blood Marrow Transplant, 19*(3), 398-404. doi: 10.1016/j.bbmt.2012.10.008

Kronke, J., Fink, E. C., Hollenbach, P. W., MacBeth, K. J., Hurst, S. N., Udeshi, N. D., Chamberlain, P. P., Mani, D. R., Man, H. W., Gandhi, A. K., Svinkina, T., Schneider, R. K., McConkey, M., Jaras, M., Griffiths, E., Wetzler, M., Bullinger, L., Cathers, B. E., Carr, S. A., Chopra, R., & Ebert, B. L. (2015). Lenalidomide induces ubiquitination and degradation of CK1alpha in del(5q) MDS. *Nature, 523*(7559), 183-188. doi: 10.1038/nature14610

Kronke, J., Udeshi, N. D., Narla, A., Grauman, P., Hurst, S. N., McConkey, M., Svinkina, T., Heckl, D., Comer, E., Li, X., Ciarlo, C., Hartman, E., Munshi, N., Schenone, M., Schreiber, S. L., Carr, S. A., & Ebert, B. L. (2014). Lenalidomide causes selective degradation of IKZF1 and IKZF3 in multiple myeloma cells. *Science, 343*(6168), 301-305. doi: 10.1126/science.1244851

Kumar, S., Witzig, T. E., Timm, M., Haug, J., Wellik, L., Fonseca, R., Greipp, P. R., & Rajkumar, S. V. (2003). Expression of VEGF and its receptors by myeloma cells. *Leukemia, 17*(10), 2025-2031. doi: 10.1038/sj.leu.2403084

Kumar, S. K., Berdeja, J. G., Niesvizky, R., Lonial, S., Laubach, J. P., Hamadani, M., Stewart, A. K., Hari, P., Roy, V., Vescio, R., Kaufman, J. L., Berg, D., Liao, E., Di Bacco, A., Estevam, J., Gupta, N., Hui, A. M., Rajkumar, V., & Richardson, P. G. (2014a). Safety and tolerability of ixazomib, an oral proteasome inhibitor, in combination with lenalidomide and dexamethasone in patients with previously untreated multiple myeloma: an open-label phase 1/2 study. *Lancet Oncol, 15*(13), 1503-1512. doi: 10.1016/S1470-2045(14)71125-8

Kumar, S. K., Dispenzieri, A., Lacy, M. Q., Gertz, M. A., Buadi, F. K., Pandey, S., Kapoor, P., Dingli, D., Hayman, S. R., Leung, N., Lust, J., McCurdy, A., Russell, S. J., Zeldenrust, S. R., Kyle, R. A., & Rajkumar, S. V. (2014b). Continued improvement in survival in multiple myeloma: changes in early mortality and outcomes in older patients. *Leukemia, 28*(5), 1122-1128. doi: 10.1038/leu.2013.313

Kumar, S. K., Rajkumar, S. V., Dispenzieri, A., Lacy, M. Q., Hayman, S. R., Buadi, F. K., Zeldenrust, S. R., Dingli, D., Russell, S. J., Lust, J. A., Greipp, P. R., Kyle, R. A., & Gertz, M. A. (2008). Improved survival in multiple myeloma and the impact of novel therapies. *Blood, 111*(5), 2516-2520. doi: 10.1182/blood-2007-10-116129

Kyle, R. A., & al. (2003). Criteria for the classification of monoclonal gammopathies, multiple myeloma and related disorders: a report of the International Myeloma Working Group. *Br J Haematol, 121*(5), 749-757.

Lacy, M. Q. (2013). "IM iD"eally treating multiple myeloma. *Blood, 121*(11), 1926-1928. doi: 10.1182/blood-2013-01-476267

Le Floch, R., Chiche, J., Marchiq, I., Naiken, T., Ilc, K., Murray, C. M., Critchlow, S. E., Roux, D., Simon, M. P., & Pouyssegur, J. (2011). CD147 subunit of lactate/H+ symporters MCT1 and hypoxia-inducible MCT4 is critical for energetics and growth of glycolytic tumors. *Proc Natl Acad Sci U S A, 108*(40), 16663-16668. doi: 10.1073/pnas.1106123108

Lenz, W., Pfeiffer, R. A., Kosenow, W., & Hayman, D. (1962). Thalidomide and congenital abnormalities. *The Lancet, 279*(7219), 45-46.

Liberti, M. V., & Locasale, J. W. (2016). The Warburg Effect: How Does it Benefit Cancer Cells? *Trends Biochem Sci*. doi: 10.1016/j.tibs.2015.12.001

Lopez-Girona, A., Heintel, D., Zhang, L. H., Mendy, D., Gaidarova, S., Brady, H., Bartlett, J. B., Schafer, P. H., Schreder, M., Bolomsky, A., Hilgarth, B., Zojer, N., Gisslinger, H., Ludwig, H., Daniel, T., Jager, U., & Chopra, R. (2011). Lenalidomide downregulates the cell survival factor, interferon regulatory factor-4, providing a potential mechanistic link for predicting response. *Br J Haematol, 154*(3), 325-336. doi: 10.1111/j.1365-2141.2011.08689.x

Lopez-Girona, A., Mendy, D., Ito, T., Miller, K., Gandhi, A. K., Kang, J., Karasawa, S., Carmel, G., Jackson, P., Abbasian, M., Mahmoudi, A., Cathers, B., Rychak, E., Gaidarova, S., Chen, R., Schafer, P. H., Handa, H., Daniel, T. O., Evans, J. F., & Chopra, R. (2012). Cereblon is a direct protein target for immunomodulatory and antiproliferative activities of lenalidomide and pomalidomide. *Leukemia, 26*(11), 2445. doi: 10.1038/leu.2012.235
leu2012235 [pii]

Lu, G., Middleton, R. E., Sun, H., Naniong, M., Ott, C. J., Mitsiades, C. S., Wong, K. K., Bradner, J. E., & Kaelin, W. G., Jr. (2014). The myeloma drug lenalidomide promotes the cereblon-dependent destruction of Ikaros proteins. *Science, 343*(6168), 305-309. doi: 10.1126/science.1244917

Ludwig, H., Sonneveld, P., Davies, F., Blade, J., Boccadoro, M., Cavo, M., Morgan, G., de la Rubia, J., Delforge, M., Dimopoulos, M., Einsele, H., Facon, T., Goldschmidt, H., Moreau, P., Nahi, H., Plesner, T., San-Miguel, J., Hajek, R., Sondergeld, P., & Palumbo, A. (2014). European perspective on multiple myeloma treatment strategies in 2014. *Oncologist, 19*(8), 829-844. doi: 10.1634/theoncologist.2014-0042

Majumdar, S., Lamothe, B., & Aggarwal, B. B. (2002). Thalidomide suppresses NF-kappa B activation induced by TNF and H2O2, but not that activated by ceramide, lipopolysaccharides, or phorbol ester. *J Immunol, 168*(6), 2644-2651.

Marchiq, I., Albrengues, J., Granja, S., Gaggioli, C., Pouyssegur, J., & Simon, M. P. (2015). Knock out of the BASIGIN/CD147 chaperone of lactate/H+ symporters

disproves its pro-tumour action via extracellular matrix metalloproteases (MMPs) induction. *Oncotarget, 6*(28), 24636-24648. doi: 10.18632/oncotarget.4323

Martin, S. K., Diamond, P., Gronthos, S., Peet, D. J., & Zannettino, A. C. (2011). The emerging role of hypoxia, HIF-1 and HIF-2 in multiple myeloma. *Leukemia, 25*(10), 1533-1542. doi: 10.1038/leu.2011.122

McBride, W. G. (1961). Thalidomide and congenital abnormalities. *The Lancet, 278*(7216), 1358.

Moffat, J., Grueneberg, D. A., Yang, X., Kim, S. Y., Kloepfer, A. M., Hinkle, G., Piqani, B., Eisenhaure, T. M., Luo, B., Grenier, J. K., Carpenter, A. E., Foo, S. Y., Stewart, S. A., Stockwell, B. R., Hacohen, N., Hahn, W. C., Lander, E. S., Sabatini, D. M., & Root, D. E. (2006). A lentiviral RNAi library for human and mouse genes applied to an arrayed viral high-content screen. *Cell, 124*(6), 1283-1298. doi: 10.1016/j.cell.2006.01.040

Moreau, P., Attal, M., & Facon, T. (2015). Frontline therapy of multiple myeloma. *Blood, 125*(20), 3076-3084. doi: 10.1182/blood-2014-09-568915

Munshi, N. C., & Wilson, C. (2001). Increased bone marrow microvessel density in newly diagnosed multiple myeloma carries a poor prognosis. *Semin Oncol, 28*(6), 565-569.

Ocio, E. M., Fernandez-Lazaro, D., San-Segundo, L., Lopez-Corral, L., Corchete, L. A., Gutierrez, N. C., Garayoa, M., Paino, T., Garcia-Gomez, A., Delgado, M., Montero, J. C., Diaz-Rodriguez, E., Mateos, M. V., Pandiella, A., Couto, S., Wang, M., Bjorklund, C. C., & San-Miguel, J. F. (2015). In vivo murine model of acquired resistance in myeloma reveals differential mechanisms for lenalidomide and pomalidomide in combination with dexamethasone. *Leukemia, 29*(3), 705-714. doi: 10.1038/leu.2014.238

Oranger, A., Carbone, C., Izzo, M., & Grano, M. (2013). Cellular mechanisms of multiple myeloma bone disease. *Clin Dev Immunol, 2013*, 289458. doi: 10.1155/2013/289458

Palumbo, A., & Anderson, K. (2011). Multiple myeloma. *N Engl J Med, 364*(11), 1046-1060. doi: 10.1056/NEJMra1011442

Palumbo, A., Avet-Loiseau, H., Oliva, S., Lokhorst, H. M., Goldschmidt, H., Rosinol, L., Richardson, P., Caltagirone, S., Lahuerta, J. J., Facon, T., Bringhen, S., Gay, F., Attal, M., Passera, R., Spencer, A., Offidani, M., Kumar, S., Musto, P., Lonial, S., Petrucci, M. T., Orlowski, R. Z., Zamagni, E., Morgan, G., Dimopoulos, M. A., Durie, B. G., Anderson, K. C., Sonneveld, P., San Miguel, J., Cavo, M., Rajkumar, S. V., & Moreau, P. (2015). Revised International Staging System for Multiple Myeloma: A Report From International Myeloma Working Group. *J Clin Oncol, 33*(26), 2863-2869. doi: 10.1200/JCO.2015.61.2267

Palumbo, A., Cavallo, F., Gay, F., Di Raimondo, F., Ben Yehuda, D., Petrucci, M. T., Pezzatti, S., Caravita, T., Cerrato, C., Ribakovsky, E., Genuardi, M., Cafro, A., Marcatti, M., Catalano, L., Offidani, M., Carella, A. M., Zamagni, E., Patriarca, F., Musto, P., Evangelista, A., Ciccone, G., Omedé, P., Crippa, C., Corradini, P., Nagler, A., Boccadoro, M., & Cavo, M. (2014). Autologous Transplantation and Maintenance Therapy in Multiple Myeloma. *New England Journal of Medicine, 371*(10), 895-905. doi: doi:10.1056/NEJMoa1402888

Parmar, K., Mauch, P., Vergilio, J. A., Sackstein, R., & Down, J. D. (2007). Distribution of hematopoietic stem cells in the bone marrow according to regional hypoxia. *Proc Natl Acad Sci U S A, 104*(13), 5431-5436. doi: 10.1073/pnas.0701152104

Payvandi, F., Wu, L., Haley, M., Schafer, P. H., Zhang, L. H., Chen, R. S., Muller, G. W., & Stirling, D. I. (2004). Immunomodulatory drugs inhibit expression of cyclooxygenase-2 from TNF-alpha, IL-1beta, and LPS-stimulated human PBMC in a partially IL-10-dependent manner. *Cell Immunol, 230*(2), 81-88. doi: 10.1016/j.cellimm.2004.09.003

Podar, K., Catley, L. P., Tai, Y. T., Shringarpure, R., Carvalho, P., Hayashi, T., Burger, R., Schlossman, R. L., Richardson, P. G., Pandite, L. N., Kumar, R., Hideshima, T., Chauhan, D., & Anderson, K. C. (2004). GW654652, the pan-inhibitor of VEGF receptors, blocks the growth and migration of multiple myeloma cells in the bone marrow microenvironment. *Blood, 103*(9), 3474-3479. doi: 10.1182/blood-2003-10-3527

Podar, K., Tai, Y. T., Davies, F. E., Lentzsch, S., Sattler, M., Hideshima, T., Lin, B. K., Gupta, D., Shima, Y., Chauhan, D., Mitsiades, C., Raje, N., Richardson, P., & Anderson, K. C. (2001). Vascular endothelial growth factor triggers signaling cascades mediating multiple myeloma cell growth and migration. *Blood, 98*(2), 428-435.

Polanski, R., Hodgkinson, C. L., Fusi, A., Nonaka, D., Priest, L., Kelly, P., Trapani, F., Bishop, P. W., White, A., Critchlow, S. E., Smith, P. D., Blackhall, F., Dive, C., & Morrow, C. J. (2014). Activity of the monocarboxylate transporter 1 inhibitor AZD3965 in small cell lung cancer. *Clin Cancer Res, 20*(4), 926-937. doi: 10.1158/1078-0432.CCR-13-2270

Possinger, K., & Dieing, A. (2015). *Facharztwissen Hämatologie Onkologie* (3rd ed.). Munich, Germany: Elsevier, Urban & Fischer.

Prince, H. M., Honemann, D., Spencer, A., Rizzieri, D. A., Stadtmauer, E. A., Roberts, A. W., Bahlis, N., Tricot, G., Bell, B., Demarini, D. J., Benjamin Suttle, A., Baker, K. L., & Pandite, L. N. (2009). Vascular endothelial growth factor inhibition is not an effective therapeutic strategy for relapsed or refractory multiple myeloma: a phase 2 study of pazopanib (GW786034). *Blood, 113*(19), 4819-4820. doi: 10.1182/blood-2009-02-207209

Raab, M. S., Podar, K., Breitkreutz, I., Richardson, P. G., & Anderson, K. C. (2009). Multiple myeloma. *Lancet, 374*(9686), 324-339. doi: 10.1016/S0140-6736(09)60221-X

Rajadhyaksha, A. M., Ra, S., Kishinevsky, S., Lee, A. S., Romanienko, P., DuBoff, M., Yang, C., Zupan, B., Byrne, M., Daruwalla, Z. R., Mark, W., Kosofsky, B. E., Toth, M., & Higgins, J. J. (2012). Behavioral characterization of cereblon forebrain-specific conditional null mice: a model for human non-syndromic intellectual disability. *Behav Brain Res, 226*(2), 428-434. doi: 10.1016/j.bbr.2011.09.039

Rehman, W., Arfons, L. M., & Lazarus, H. M. (2011). The rise, fall and subsequent triumph of thalidomide: lessons learned in drug development. *Ther Adv Hematol, 2*(5), 291-308. doi: 10.1177/2040620711413165

Ren, Y., Wang, M., Couto, S., Hansel, D. E., Miller, K., Lopez-Girona, A., Bjorklund, C. C., Gandhi, A. K., Thakurta, A., Chopra, R., & Breider, M. (2015). A Dual Color Immunohistochemistry Assay for Measurement of Cereblon in Multiple Myeloma Patient Samples. *Appl Immunohistochem Mol Morphol*. doi: 10.1097/PAI.0000000000000246

Richardson, P. G., Weller, E., Lonial, S., Jakubowiak, A. J., Jagannath, S., Raje, N. S., Avigan, D. E., Xie, W., Ghobrial, I. M., Schlossman, R. L., Mazumder, A., Munshi, N. C., Vesole, D. H., Joyce, R., Kaufman, J. L., Doss, D., Warren, D. L., Lunde, L. E., Kaster, S., Delaney, C., Hideshima, T., Mitsiades, C. S., Knight, R., Esseltine, D. L., & Anderson, K. C. (2010). Lenalidomide, bortezomib, and dexamethasone combination therapy in patients with newly diagnosed multiple myeloma. *Blood, 116*(5), 679-686. doi: 10.1182/blood-2010-02-268862

Riethdorf, S., Reimers, N., Assmann, V., Kornfeld, J. W., Terracciano, L., Sauter, G., & Pantel, K. (2006). High incidence of EMMPRIN expression in human tumors. *Int J Cancer, 119*(8), 1800-1810. doi: 10.1002/ijc.22062

Robert-Koch-Institut. (2015). *Krebs in Deutschland 2011/2012*. Robert Koch-Institut, Gesellschaft der epidemiologischen Krebsregister in Deutschland eV.

Roussel, M., Lauwers-Cances, V., Robillard, N., Hulin, C., Leleu, X., Benboubker, L., Marit, G., Moreau, P., Pegourie, B., Caillot, D., Fruchart, C., Stoppa, A. M., Gentil, C., Wuilleme, S., Huynh, A., Hebraud, B., Corre, J., Chretien, M. L., Facon, T., Avet-Loiseau, H., & Attal, M. (2014). Front-line transplantation program with lenalidomide, bortezomib, and dexamethasone combination as induction and consolidation followed by lenalidomide maintenance in patients with multiple myeloma: a phase II study by the Intergroupe Francophone du Myelome. *J Clin Oncol, 32*(25), 2712-2717. doi: 10.1200/JCO.2013.54.8164

Sampaio, E. P., Sarno, E. N., Galilly, R., Cohn, Z. A., & Kaplan, G. (1991). Thalidomide selectively inhibits tumor necrosis factor alpha production by stimulated human monocytes. *J Exp Med, 173*(3), 699-703.

San Miguel, J., Weisel, K., Moreau, P., Lacy, M., Song, K., Delforge, M., Karlin, L., Goldschmidt, H., Banos, A., Oriol, A., Alegre, A., Chen, C., Cavo, M., Garderet, L., Ivanova, V., Martinez-Lopez, J., Belch, A., Palumbo, A., Schey, S., Sonneveld, P., Yu, X., Sternas, L., Jacques, C., Zaki, M., & Dimopoulos, M. (2013). Pomalidomide plus low-dose dexamethasone versus high-dose dexamethasone alone for patients with relapsed and refractory multiple myeloma (MM-003): a randomised, open-label, phase 3 trial. *Lancet Oncol, 14*(11), 1055-1066. doi: 10.1016/S1470-2045(13)70380-2

Sanchez, W. Y., McGee, S. L., Connor, T., Mottram, B., Wilkinson, A., Whitehead, J. P., Vuckovic, S., & Catley, L. (2013). Dichloroacetate inhibits aerobic glycolysis in multiple myeloma cells and increases sensitivity to bortezomib. *Br J Cancer, 108*(8), 1624-1633. doi: 10.1038/bjc.2013.120

Schuster, S. R., Kortuem, K. M., Zhu, Y. X., Braggio, E., Shi, C. X., Bruins, L. A., Schmidt, J. E., Ahmann, G., Kumar, S., Rajkumar, S. V., Mikhael, J., Laplant, B., Champion, M. D., Laumann, K., Barlogie, B., Fonseca, R., Bergsagel, P. L., Lacy, M., & Stewart, A. K. (2014). The clinical significance of cereblon expression in multiple myeloma. *Leuk Res, 38*(1), 23-28. doi: 10.1016/j.leukres.2013.08.015

Segarra, M., Lozano, E., Corbera-Bellalta, M., Vilardell, C., Cibeira, M. T., Esparza, J., Izco, N., Blade, J., & Cid, M. C. (2010). Thalidomide decreases gelatinase production by malignant B lymphoid cell lines through disruption of multiple integrin-mediated signaling pathways. *Haematologica, 95*(3), 456-463. doi: 10.3324/haematol.2009.006395

Sheskin, J. (1965). Thalidomide in the Treatment of Lepra Reactions. *Clin Pharmacol Ther, 6*, 303-306.

Shortt, J., Hsu, A. K., & Johnstone, R. W. (2013). Thalidomide-analogue biology: immunological, molecular and epigenetic targets in cancer therapy. *Oncogene, 32*(36), 4191-4202. doi: 10.1038/onc.2012.599

Shou, Z. X., Jin, X., & Zhao, Z. S. (2012). Upregulated expression of ADAM17 is a prognostic marker for patients with gastric cancer. *Ann Surg, 256*(6), 1014-1022. doi: 10.1097/SLA.0b013e3182592f56

Singhal, S., Mehta, J., Desikan, R., Ayers, D., Roberson, P., Eddlemon, P., Munshi, N., Anaissie, E., Wilson, C., Dhodapkar, M., Zeddis, J., & Barlogie, B. (1999). Antitumor activity of thalidomide in refractory multiple myeloma. *N Engl J Med, 341*(21), 1565-1571. doi: 10.1056/NEJM199911183412102

Smith, C. K., Baker, T. A., & Sauer, R. T. (1999). Lon and Clp family proteases and chaperones share homologous substrate-recognition domains. *Proc Natl Acad Sci U S A, 96*(12), 6678-6682.

Smith, D., & Yong, K. (2013). Multiple myeloma. *BMJ, 346*, f3863. doi: 10.1136/bmj.f3863

Smithells, R. W., & Newman, C. G. (1992). Recognition of thalidomide defects. *J Med Genet, 29*(10), 716-723.

Somlo, G., Lashkari, A., Bellamy, W., Zimmerman, T. M., Tuscano, J. M., O'Donnell, M. R., Mohrbacher, A. F., Forman, S. J., Frankel, P., Chen, H. X., Doroshow, J. H., & Gandara, D. R. (2011). Phase II randomized trial of bevacizumab versus bevacizumab and thalidomide for relapsed/refractory multiple myeloma: a California Cancer Consortium trial. *Br J Haematol, 154*(4), 533-535. doi: 10.1111/j.1365-2141.2011.08623.x

Sonveaux, P., Vegran, F., Schroeder, T., Wergin, M. C., Verrax, J., Rabbani, Z. N., De Saedeleer, C. J., Kennedy, K. M., Diepart, C., Jordan, B. F., Kelley, M. J., Gallez, B., Wahl, M. L., Feron, O., & Dewhirst, M. W. (2008). Targeting lactate-fueled respiration selectively kills hypoxic tumor cells in mice. *J Clin Invest, 118*(12), 3930-3942. doi: 10.1172/JCI36843

Stella, F., Pedrazzini, E., Agazzoni, M., Ballester, O., & Slavutsky, I. (2015). Cytogenetic Alterations in Multiple Myeloma: Prognostic Significance and the Choice of Frontline Therapy. *Cancer Invest, 33*(10), 496-504. doi: 10.3109/07357907.2015.1080833

Stewart, A. K. (2014). How Thalidomide Works Against Cancer. *Science (New York, N.Y.), 343*(6168), 256-257. doi: 10.1126/science.1249543

Stewart, A. K., Rajkumar, S. V., Dimopoulos, M. A., Masszi, T., Spicka, I., Oriol, A., Hajek, R., Rosinol, L., Siegel, D. S., Mihaylov, G. G., Goranova-Marinova, V., Rajnics, P., Suvorov, A., Niesvizky, R., Jakubowiak, A. J., San-Miguel, J. F., Ludwig, H., Wang, M., Maisnar, V., Minarik, J., Bensinger, W. I., Mateos, M. V., Ben-Yehuda, D., Kukreti, V., Zojwalla, N., Tonda, M. E., Yang, X., Xing, B., Moreau, P., Palumbo, A., & Investigators, A. (2015). Carfilzomib, lenalidomide, and dexamethasone for relapsed multiple myeloma. *N Engl J Med, 372*(2), 142-152. doi: 10.1056/NEJMoa1411321

Stolberg, S. (1999, November 18, 1999). Thalidomide Found to Slow a Bone Cancer, *The New York Times*. Retrieved from http://www.nytimes.com/1999/11/18/us/thalidomide-found-to-slow-a-bone-cancer.html

Storti, P., Bolzoni, M., Donofrio, G., Airoldi, I., Guasco, D., Toscani, D., Martella, E., Lazzaretti, M., Mancini, C., Agnelli, L., Patrene, K., Maiga, S., Franceschi, V., Colla, S., Anderson, J., Neri, A., Amiot, M., Aversa, F., Roodman, G. D., & Giuliani, N. (2013). Hypoxia-inducible factor (HIF)-1alpha suppression in myeloma cells blocks tumoral growth in vivo inhibiting angiogenesis and bone destruction. *Leukemia, 27*(8), 1697-1706. doi: 10.1038/leu.2013.24

Tang, Y., Nakada, M. T., Kesavan, P., McCabe, F., Millar, H., Rafferty, P., Bugelski, P., & Yan, L. (2005). Extracellular matrix metalloproteinase inducer stimulates tumor angiogenesis by elevating vascular endothelial cell growth factor and matrix

metalloproteinases. *Cancer Res, 65*(8), 3193-3199. doi: 10.1158/0008-5472.CAN-04-3605

Ullah, M. S., Davies, A. J., & Halestrap, A. P. (2006). The plasma membrane lactate transporter MCT4, but not MCT1, is up-regulated by hypoxia through a HIF-1alpha-dependent mechanism. *J Biol Chem, 281*(14), 9030-9037. doi: 10.1074/jbc.M511397200

Urbaniak-Kujda, D., Kapelko-Slowik, K., Prajs, I., Dybko, J., Wolowiec, D., Biernat, M., Slowik, M., & Kuliczkowski, K. (2016). Increased expression of metalloproteinase-2 and -9 (MMP-2, MMP-9), tissue inhibitor of metalloproteinase-1 and -2 (TIMP-1, TIMP-2), and EMMPRIN (CD147) in multiple myeloma. *Hematology, 21*(1), 26-33. doi: 10.1179/1607845415Y.0000000043

Vacca, A., Ribatti, D., Presta, M., Minischetti, M., Iurlaro, M., Ria, R., Albini, A., Bussolino, F., & Dammacco, F. (1999). Bone marrow neovascularization, plasma cell angiogenic potential, and matrix metalloproteinase-2 secretion parallel progression of human multiple myeloma. *Blood, 93*(9), 3064-3073.

Vacca, A., Ribatti, D., Roncali, L., Ranieri, G., Serio, G., Silvestris, F., & Dammacco, F. (1994). Bone marrow angiogenesis and progression in multiple myeloma. *Br J Haematol, 87*(3), 503-508.

Vander Heiden, M. G., Cantley, L. C., & Thompson, C. B. (2009). Understanding the Warburg effect: the metabolic requirements of cell proliferation. *Science, 324*(5930), 1029-1033. doi: 10.1126/science.1160809

Vargesson, N. (2015). Thalidomide-induced teratogenesis: history and mechanisms. *Birth Defects Res C Embryo Today, 105*(2), 140-156. doi: 10.1002/bdrc.21096

von Lilienfeld-Toal, M., Hahn-Ast, C., Furkert, K., Hoffmann, F., Naumann, R., Bargou, R., Cook, G., & Glasmacher, A. (2008). A systematic review of phase II trials of thalidomide/dexamethasone combination therapy in patients with relapsed or refractory multiple myeloma. *Eur J Haematol, 81*(4), 247-252. doi: 10.1111/j.1600-0609.2008.01121.x

Walters, D. K., Arendt, B. K., & Jelinek, D. F. (2013). CD147 regulates the expression of MCT1 and lactate export in multiple myeloma cells. *Cell Cycle, 12*(19), 3175-3183. doi: 10.4161/cc.26193

Warburg, O. (1925). The Metabolism of Carcinoma Cells. *The Journal of Cancer Research, 9*(1), 148-163. doi: 10.1158/jcr.1925.148

Watanabe, Y., Terashima, Y., Takenaka, N., Kobayashi, M., & Matsushita, T. (2007). Prediction of avascular necrosis of the femoral head by measuring intramedullary oxygen tension after femoral neck fracture. *J Orthop Trauma, 21*(7), 456-461. doi: 10.1097/BOT.0b013e318126bb56

Weber, D. M., Chen, C., Niesvizky, R., Wang, M., Belch, A., Stadtmauer, E. A., Siegel, D., Borrello, I., Rajkumar, S. V., Chanan-Khan, A. A., Lonial, S., Yu, Z., Patin, J., Olesnyckyj, M., Zeldis, J. B., & Knight, R. D. (2007). Lenalidomide plus dexamethasone for relapsed multiple myeloma in North America. *N Engl J Med, 357*(21), 2133-2142. doi: 10.1056/NEJMoa070596

Weidle, U. H., Scheuer, W., Eggle, D., Klostermann, S., & Stockinger, H. (2010). Cancer-related issues of CD147. *Cancer Genomics Proteomics, 7*(3), 157-169.

White, D., Kassim, A., Bhaskar, B., Yi, J., Wamstad, K., & Paton, V. E. (2013). Results from AMBER, a randomized phase 2 study of bevacizumab and bortezomib versus bortezomib in relapsed or refractory multiple myeloma. *Cancer, 119*(2), 339-347. doi: 10.1002/cncr.27745

Winter, G. E., Buckley, D. L., Paulk, J., Roberts, J. M., Souza, A., Dhe-Paganon, S., & Bradner, J. E. (2015). DRUG DEVELOPMENT. Phthalimide conjugation as a strategy for in vivo target protein degradation. *Science, 348*(6241), 1376-1381. doi: 10.1126/science.aab1433

Xin, W., Xiaohua, N., Peilin, C., Xin, C., Yaqiong, S., & Qihan, W. (2008). Primary function analysis of human mental retardation related gene CRBN. *Mol Biol Rep, 35*(2), 251-256. doi: 10.1007/s11033-007-9077-3

Xiong, L., Edwards, C. K., 3rd, & Zhou, L. (2014). The biological function and clinical utilization of CD147 in human diseases: a review of the current scientific literature. *Int J Mol Sci, 15*(10), 17411-17441. doi: 10.3390/ijms151017411

Yang, M., Yuan, Y., Zhang, H., Yan, M., Wang, S., Feng, F., Ji, P., Li, Y., Li, B., Gao, G., Zhao, J., & Wang, L. (2013). Prognostic significance of CD147 in patients with glioblastoma. *J Neurooncol, 115*(1), 19-26. doi: 10.1007/s11060-013-1207-2

Zangari, M., Anaissie, E., Stopeck, A., Morimoto, A., Tan, N., Lancet, J., Cooper, M., Hannah, A., Garcia-Manero, G., Faderl, S., Kantarjian, H., Cherrington, J., Albitar, M., & Giles, F. J. (2004). Phase II study of SU5416, a small molecule vascular endothelial growth factor tyrosine kinase receptor inhibitor, in patients with refractory multiple myeloma. *Clin Cancer Res, 10*(1 Pt 1), 88-95.

Zdzisinska, B., Walter-Croneck, A., & Kandefer-Szerszen, M. (2008). Matrix metalloproteinases-1 and -2, and tissue inhibitor of metalloproteinase-2 production is abnormal in bone marrow stromal cells of multiple myeloma patients. *Leuk Res, 32*(11), 1763-1769. doi: 10.1016/j.leukres.2008.04.001

Zeldis, J. B., Knight, R., Hussein, M., Chopra, R., & Muller, G. (2011). A review of the history, properties, and use of the immunomodulatory compound lenalidomide. *Ann N Y Acad Sci, 1222*, 76-82. doi: 10.1111/j.1749-6632.2011.05974.x

Zhang, L. H., Kosek, J., Wang, M., Heise, C., Schafer, P. H., & Chopra, R. (2013). Lenalidomide efficacy in activated B-cell-like subtype diffuse large B-cell

lymphoma is dependent upon IRF4 and cereblon expression. *Br J Haematol, 160*(4), 487-502. doi: 10.1111/bjh.12172

Zhu, D., Wang, Z., Zhao, J. J., Calimeri, T., Meng, J., Hideshima, T., Fulciniti, M., Kang, Y., Ficarro, S. B., Tai, Y. T., Hunter, Z., McMilin, D., Tong, H., Mitsiades, C. S., Wu, C. J., Treon, S. P., Dorfman, D. M., Pinkus, G., Munshi, N. C., Tassone, P., Marto, J. A., Anderson, K. C., & Carrasco, R. D. (2015). The Cyclophilin A-CD147 complex promotes the proliferation and homing of multiple myeloma cells. *Nat Med, 21*(6), 572-580. doi: 10.1038/nm.3867

Zhu, S., Li, Y., Zhang, Y., Wang, X., Gong, L., Han, X., Yao, L., Lan, M., & Zhang, W. (2015). Expression and clinical implications of HAb18G/CD147 in hepatocellular carcinoma. *Hepatol Res, 45*(1), 97-106. doi: 10.1111/hepr.12320

Zhu, Y. X., Braggio, E., Shi, C. X., Bruins, L. A., Schmidt, J. E., Van Wier, S., Chang, X. B., Bjorklund, C. C., Fonseca, R., Bergsagel, P. L., Orlowski, R. Z., & Stewart, A. K. (2011). Cereblon expression is required for the antimyeloma activity of lenalidomide and pomalidomide. *Blood, 118*(18), 4771-4779. doi: blood-2011-05-356063 [pii]
10.1182/blood-2011-05-356063

Zhu, Y. X., Braggio, E., Shi, C. X., Kortuem, K. M., Bruins, L. A., Schmidt, J. E., Chang, X. B., Langlais, P., Luo, M., Jedlowski, P., LaPlant, B., Laumann, K., Fonseca, R., Bergsagel, P. L., Mikhael, J., Lacy, M., Champion, M. D., & Stewart, A. K. (2014). Identification of cereblon-binding proteins and relationship with response and survival after IMiDs in multiple myeloma. *Blood, 124*(4), 536-545. doi: 10.1182/blood-2014-02-557819

8 List of figures and tables

8.1 List of figures

8.2 List of tables

9 Publications

Parts of this study have been published in advance:

Ruth Eichner, Vanesa Fernández-Sáiz, Michael Heider, Simone Lemeer, Frauke van Bebber, Bianca-Sabrina Targosz, Christian Peschel, Bettina Schmid, Bernhard Kuster and Florian Bassermann: *Immunomodulatory drugs attenuate CRBN-dependent activation of the CD147- MCT1 complex to promote anti-myeloma activity* and teratogenicity.

EMBO Conference Ubiquitin and ubiquitin-like proteins. 19–24 October 2014, Buenos Aires, Argentina (Poster)

Ruth Eichner, Michael Heider, Vanesa Fernández-Sáiz, Frauke van Bebber, Anne-Kathrin Garz, Simone Lemeer, Martina Rudelius, Bianca-Sabrina Targosz, Laura Jacobs, Anna-Maria Knorn, Jolanta Slawska, Uwe Platzbecker, Ulrich Germing, Christian Langer, Stefan Knop, Herrmann Einsele, Christian Peschel, Christian Haas, Ulrich Keller, Bettina Schmid, Katharina S. Götze, Bernhard Kuster and Florian Bassermann: *Immunomodulatory drugs disrupt the cereblon–CD147–MCT1 axis to exert antitumor activity and teratogenicity.*

European Mantle Cell Lymphoma Network Annual Meeting, Vicenza, 2015. (Talk)

Ruth Eichner, Michael Heider, Vanesa Fernández-Sáiz, Frauke van Bebber, Anne-Kathrin Garz, Simone Lemeer, Bianca-Sabrina Targosz, Anna-Maria Knorn, Uwe Platzbecker, Ulrich Germing, Christian Peschel, Christian Haas, Ulrich Keller, Bettina Schmid, Katharina S. Götze, Bernhard Kuster and Florian Bassermann: *Immunomodulatory drugs restrain the CD147/MCT1 complex to exert antitumor activity and teratogenicity.*

DKTK 2nd Munich Cancer Retreat, Herrsching, 2015. (Poster)

Ruth Eichner, Michael Heider*, Vanesa Fernández-Sáiz*, Frauke van Bebber, Anne-Kathrin Garz, Simone Lemeer, Martina Rudelius, Bianca-Sabrina Targosz, Laura Jacobs, Anna-Maria Knorn, Jolanta Slawska, Uwe Platzbecker, Ulrich Germing, Christian Langer, Stefan Knop, Herrmann Einsele, Christian Peschel, Christian Haas, Ulrich Keller, Bettina Schmid, Katharina S. Götze, Bernhard Kuster and Florian Bassermann: *Immunomodulatory drugs disrupt the CRBN-CD147/MCT1 axis to exert anti-tumor activity and teratogenicity.* Nature Medicine 2016 Jul;22(7):735-43. doi: 10.1038/nm.4128. Epub 2016 Jun 13.

*equal contribution

10 Acknowledgements

First of all, I would like to express my gratitude to Prof. Florian Bassermann, who took me into his lab and gave me the opportunity to work on this particularly thrilling and clinically relevant project in his dynamic lab. I hope I was able to overcome the initial skepticism, with which most group leaders approach medical students with their limited laboratory expertise. I highly value his constant feedback, great ideas and thriving motivation for the project.

My biggest thanks go to Dr. Ruth Eichner, who could not have been a better supervisor, mentor and friend at the same time. Thank you for initially introducing me to the various techniques after long days in the clinic and your never-ending support during all my time in the lab. Thank you for inviting me to join you at the conference in Buenos Aires and for the following holiday in Brazil. Thanks a lot for always keeping me involved, even when I was away studying for exams or spending university time abroad.

Thank you also to my official mentor Dr. Vanesa Fernández-Sáiz for your honest and straightforward advice, creative ideas and even more, for fun times and stories about Bilbao. Thanks for the great time in Argentina and for trying to make our lab a bit less German.

My sincere thanks also go to Prof. Peschel for providing me with the opportunity to join the lab within the III. Department of Medicine at the Klinikum Rechts der Isar.

I would like to acknowledge the Department of Clinical Chemistry, especially Prof. P. Luppa and his team of technicians around Ms. Gloß for measuring my endless number of lactate samples.

Thanks to all the other lab members, particularly technicians and fellow students, for your assistance, encouragement, great lunches and fun times in the lab. I am happy to have found many new good friends.

I am deeply indepted to my parents and the rest of my family for their continuous support and motivation throughout all of my studies and my life in general. Thank you for believing in me and making everything possible!

Of course I would like to thank my friends and especially my girlfriend Isabella for her incredible patience and understanding at all times, in particular when hearing her least favorite phrase “we’ll get this out there as soon as possible”.

Last but not least, it would not have been possible to conduct this study without the generous financial support from the Germany Cancer Aid.